

For Reference

NOT TO BE TAKEN FROM THIS ROOM

Ex libris
UNIVERSITATIS
ALBERTAENSIS





Digitized by the Internet Archive
in 2024 with funding from
University of Alberta Library

https://archive.org/details/Cooper1977_0

THE UNIVERSITY OF ALBERTA

RELEASE FORM

NAME OF AUTHOR Edward David Cooper
TITLE OF THESIS A Study of the Glauber Eikonal
..... Approximation at Intermediate
..... Energies
DEGREE FOR WHICH THESIS WAS PRESENTED MSc
YEAR THIS DEGREE GRANTED 1977

Permission is hereby granted to THE UNIVERSITY OF
ALBERTA LIBRARY to reproduce single copies of this
thesis and to lend or sell such copies for private,
scholarly or scientific research purposes only.

The author reserves other publication rights, and
neither the thesis nor extensive extracts from it may
be printed or otherwise reproduced without the author's
written permission.

THE UNIVERSITY OF ALBERTA
A STUDY OF THE GLAUBER EIKONAL
APPROXIMATION AT INTERMEDIATE ENERGIES

by



Edward David Cooper

A THESIS
SUBMITTED TO THE FACULTY OF GRADUATE STUDIES
AND RESEARCH IN PARTIAL FULFILMENT
OF THE REQUIREMENTS FOR THE DEGREE
OF MASTER OF SCIENCE

DEPARTMENT OF PHYSICS

EDMONTON, ALBERTA

FALL, 1977

THE UNIVERSITY OF ALBERTA
FACULTY OF GRADUATE STUDIES AND RESEARCH

The undersigned certify that they have read, and recommend to the Faculty of Graduate Studies and Research, for acceptance, a thesis entitled A STUDY OF THE GLAUBER EIKONAL APPROXIMATION AT INTERMEDIATE ENERGIES submitted by Edward David Cooper in partial fulfilment of the requirements for the Degree of Master of Science.

DEDICATION

This thesis is dedicated to all those who
never find what they are seeking

ABSTRACT

The validity of the Glauber eikonal approximation has been assessed for elastic scattering of nucleons using optical potentials for lead, calcium and helium at various energies from 100 MeV to 1 GeV.

Since the above nuclei are even-even, the possible interactions are only central and spin-orbit, therefore an optical potential in the form of a complex central and complex spin-orbit modified Gaussian was used, the parameters of which were chosen so as to reproduce experimental data as closely as possible. There are three possible observables from such a system, and so three are studied here -- cross-section, polarisation and a polarisation transfer coefficient.

This is the first study of its kind to consider all possible independant observables, most others stopping short at just considering the cross-section.

An extra multiplicative factor has been found for the spin-flip amplitude whose presence is required formally, but whose effect upon the approximation is not found to be significant.

The results are presented graphically since each reader will have his (or her) own interpretation of when the approximation "fails". An interestig trend which emerged from the study is that at 0.5 GeV the approximation fairs almost as well as at 1 GeV, and that the expected result of decreasing angular range with increasing atomic weight was found to be less severe than expected.

ACKNOWLEDGEMENTS

I would like to take this opportunity to heartily thank my supervisor Helmy Sherif for not only suggesting this project and being a guiding light whenever I lost track of the overall purpose of the thesis in some dark details of the calculations, but also for the use of one of his computer programmes to do the exact calculations.

Thanks to Jim Easton for sharing with me much time, patience and knowledge on how to get the upper hand in the never ending struggle with computer systems and computer programming.

I would like to express my gratitude to Stephen Leung, who, through casual conversation, taught me almost all I know on the Optical Model. Thanks also to my fellow graduate students, especially Larry Antonuk, Dave Henty, Rick Hooper, Tom Newton, Dave Noakes, Gordon Semenoff and Ron Sloboda for many interesting and clarifying discussions on physics (and other topics).

Last, but by no means least, I would like to express thanks to Bruce Russell for undertaking the typing of this manuscript.

TABLE OF CONTENTS

CHAPTER	PAGE
I. INTRODUCTION	1
II. THE MATHEMATICAL BACKGROUND	11
The Born Approximation	16
The Glauber Eikonal Approximation	19
The Glauber Eikonal Approximation for Spin-half Projectiles	28
The Exact Calculation	38
III. THE RESULTS FOR GAUSSIAN POTENTIALS	44
The Results for a Gaussian Potential	46
The Results for a Modified Gaussian Potential	52
Observables	54
IV. PRESENTATION AND DISCUSSION OF RESULTS	60
Choice of the Potential Parameters	61
Comparison of Glauber and Exact Calculations	64
Comment on Amplitudes	110
The Effect of the $\cos \theta/2$ factor	110
V. CONCLUSION	121
REFERENCES	125
APPENDICES	
A. CROSS-SECTIONS	128
B. MATCHING POTENTIALS	138
C. SUMMARY OF TESTS	144

LIST OF TABLES

Table I	Experimental Data	62
Table II	Parameters of the Optical Potential	63
Table III	The Points of failure of the Approx- imation	76
Table IV	The Non-spin-flip Amplitudes for elastic scattering on Helium at 100 MeV	112
Table V	The Spin-flip Amplitudes for elastic scattering on Helium at 100 MeV	114
Table VI	The Non-spin-flip amplitudes for elastic scattering on Calcium at 500 MeV	116
Table VII	The Spin-flip Amplitudes for elastic scattering on Calcium at 500 MeV	118

LIST OF FIGURES

Figure	Page
1. Axes Convention	15
2. Impact Parameter	25
3. Axes Convention for Glauber Eikonal Approximation	28
4. p - ^4He Fit at 580 MeV	67
5. p - ^{40}Ca Fit at 1044 MeV	69
6. p - ^{208}Pb Fit at 155 MeV	71
7. p - ^{208}Pb Fit at 1044 MeV	73
8. Cross-section for Helium at 100 MeV and 380 MeV	78
9. Cross-section for Helium at 580 MeV and 1050 MeV	80
10. Polarisation for Helium at 100 MeV and 380 MeV	82
11. Polarisation for Helium at 580 MeV and 1050 MeV	84
12. P.T.C. for Helium at 100 MeV and 380 MeV	86
13. P.T.C. for Helium at 580 MeV and 1050 MeV	88
14. Cross-section for Calcium at 155 MeV	91
15. Cross-section for Calcium at 500 MeV	93
16. Cross-section for Calcium at 1044 MeV	95
17. Polarisation for Calcium	97
18. P.T.C. for Calcium	99
19. Cross-section for Lead at 155 MeV	101
20. Cross-section for Lead at 500 MeV	103

Figure	Page
21. Cross-section for Lead at 1044 MeV	105
22. Polarisation for Lead	107
23. Polarisation Transfer for Lead	109
24. Effect of the $\cos \theta/2$ Factor	120
25. Potential Matching	143

CHAPTER I
INTRODUCTION

In 1958 R.J. Glauber gave a lecture on an eikonal approximation for high energy collisions at the theoretical physics summer conference in Colorado (GL59). The approximation, now named after him, started to take shape a few years before; the earliest relevant papers appearing in 1947, one by Molière, (MO47), the other by Serber (SE47). The paper by Molière seems to be the first to clearly relate the eikonal phase to the classical action integral of the particle's trajectory, and the paper also gives a discussion of the related Born and W.K.B. approximations.

In 1954 J.B. Malenka (MA54) gave the expression for the amplitudes for scattering by spin- $\frac{1}{2}$ particles, the non-spin-flip amplitude agreeing with Molière's result.

Watson (WA53) put forward a multiple scattering formalism in 1953 in which scattering and absorption of particles were treated using the one and two particle nuclear densities, obtaining a formal solution for the scattering amplitude. By employing the impulse approximation, a solution is found which is of the form of a multiple scattering solution, and by considering only on-shell scattering for a large number of nucleons, he relates the formalism to the optical model.

Glauber did a lot of work in the field during the 1950's in particular showing (GL55) the additive property of the eikonal phases paving the way for the multiple scattering formalism, and by the end of the decade brought all the separate results together to form what is now called "Glauber Theory." The term Glauber Theory in the literature has a double meaning, the eikonal approximation or the multiple scattering theory, in this study the concern is with the former.

The eikonal approximation may be thought of as the result obtained by converting the sum over phase-shifts into an integral over an impact parameter, as shown by Razavy et al (RA74), and is therefore sometimes referred to as an impact parameter representation for the scattering amplitude. Other equivalent ways of obtaining the result are linearising the Hamiltonian, as is used in Chapter II of this thesis, or making the Schroedinger equation into a first order equation by means of the approximations

$$\frac{V}{E} \ll 1 \quad k a \ll 1 \quad k d \theta^2 \ll 1$$

as is done by Glauber (GL59). In the above θ is the scattering angle, V is the potential strength, E is the energy of the incident particle, k is the wavevector of the incident particle, a is a length of order of the spatial extent of the potential, d is the typical minimum distance over which the potential varies significantly. To satisfy these three inequalities, the potential must be smooth in some sense. A clear exposition of the relationship between the last two methods of derivation may be found in a paper by Kamal (KA72).

The linearised Hamiltonian approach is dealt with in quite some depth by Osborn (OS70), where off-shell effects are studied systematically and the linearised theory is shown to be exactly unitary (a consequence of the hermitian nature of the linearised Hamiltonian).

Another way of looking at the eikonal approximation

is to expand the exponential in the expression for the scattering amplitude

$$f(\theta) = ik \int_0^{\infty} J_0(qb)(1 - e^{i\chi(b)}) b db$$

to obtain a series in powers of χ , which corresponds term for term with the Born Series. The first order terms in each series turn out to be identical, and Byron et al. (BY73) have investigated relationships between higher order terms.

There are several other high energy approximations, and it is interesting to compare the accuracy of each to that of the Glauber eikonal approximation.

From the above it is apparent that the Glauber eikonal approximation is more accurate than the Born approximation, although Byron et al. (BY73) have pointed out that for a linear combination of Yukawa potentials, the second Born approximation is the most accurate at higher energies.

Razavy et al. (RA76) have looked at an alternative way of linearising the Hamiltonian, obtaining an expression for the amplitudes which, upon numerical testing, is more accurate than Glauber's result, although the expression is complicated.

Blankenbecler and Goldberger (BL61) have developed an impact parameter approximation. The expression they have obtained for the amplitude, which agrees with the Glauber eikonal amplitude to order χ^2 , is discussed and the formalism extended to spin- $\frac{1}{2}$ scattering by Kamal (KA72).

T. Adachi et al. (AD65) have developed an impact

parameter formalism without approximation, but it yields a rather less manageable expression for the scattering amplitude.

R. Sugar and R. Blankenbecler (SU69), Schiff (SC56) and Saxon and Schiff (SA57) have also developed eikonal formalisms, although to date no one has found expressions for the amplitudes of comparable simplicity to those of the Glauber eikonal, which gives significantly better results.

Y. Hahn (HA69)(HA70)(HA73) has carried out a survey of impact parameter formalisms, and comes to the conclusion that all fail beyond a certain value of momentum transfer. The approximation of Schiff (SC56) turned out to be the most accurate numerically, but the differences were slight and the survey was taken at only one energy and one geometry for the potential.

There have been several attempts in the past to give corrections to the Glauber eikonal approximation, the most systematic and successful approach seems to be that of Wallace (WA70)(WA71), who writes the amplitude in an expansion in powers of the difference between the exact and eikonal propagators, thereby obtaining a series with the Glauber eikonal approximation as the first term, which converges reasonably rapidly to the exact amplitude. Wallace points out the convergence of the series is worse for a Gaussian potential than for a Woods-Saxon potential. Gillespie et al. (GI75) have since examined numerically the Wallace corrections as applied to $p - {}^4\text{He}$ scattering at 0.1 GeV,

0.5 GeV and 1.0 GeV using a central Gaussian optical potential and find the convergence of the series to be excellent.

In this thesis the concern is not with the relative merits of impact parameter formalisms, but rather in establishing the accuracy of the Glauber eikonal approximation in reproducing observables from scattering by a nuclear optical potential. Several studies in the past have tested the validity of the approximation as regards potential scattering, and so some justification is needed for this one. First some of the previous studies are reviewed here.

Y. Hahn (HA70) has done Glauber eikonal and exact calculations on a non-singular Yukawa potential. Hahn considered only one energy (1 GeV) and concluded that the approximation is good for

$$0 < q < 3/4k .$$

S.J. Wallace (WA70) whilst testing the now called "Wallace corrections" to the Glauber eikonal approximation, tested the unmodified approximation on Woods-Saxon, Gaussian and Yukawa real central potentials.

F. W. Byron et al. (BY73) have examined the numerical accuracy of the Glauber eikonal approximation on potentials which are a linear combination of Yukawa potentials, and on a polarisation potential, and find Glauber's original criteria of validity unnecessarily restrictive.

With the exception of Gillespie's, the aforementioned studies have been performed on potentials which have not

resembled nuclear optical potentials in the property of having absorptive or polarising effects. Gillespie's potential had an imaginary term, but no spin-orbit term. A recent study by Brissaud et al. (BR75) rectifies these defects, by taking optical model parameters directly and also including the effects of the Coulomb interaction in the manner prescribed by Glauber (GL70). Brissaud et al find the interesting result that the approximation yields better results for the cross-section than for the polarisation. It will be seen later in this study that if one computes a polarisation transfer coefficient (P.T.C.) then this is reproduced less accurately still by the approximation. The P.T.C. used in this study is the first Wolfenstein parameter, commonly given the notation $K_x^{X'}$ (R067). Brissaud et al. also find the general rule of validity

$$q^2 \ll k/R$$

holds qualitatively, but is unnecessarily restrictive for heavier nuclei.

The main usage of Glauber theory is in the multiple scattering formalism, which is a combination of eikonal and phase additivity approximations. The eikonal phase from scattering off several centres of force turns out to be the sum of the single scattering phases from each centre, and so one can describe scattering from a nucleus using just the parameters of the nucleon-nucleon amplitude and the nuclear density. This is aesthetically pleasing since one can obtain

"macroscopic" results from microscopic input. To understand where the results from the multiple scattering are valid, it is necessary to understand the validity of the impulse and eikonal approximations. The latter, it is hoped, will be clarified in this thesis.

Tests have been performed in the past on the multiple scattering formalism; for example on $p - {}^4\text{He}$ at various energies Auger et al. (AU76) find excellent agreement with the experimental data.

Corrections to the multiple scattering formalism have been proposed and tested by Bleszynski et al. (BL76) who find a good fit, made excellent by their modifications, to the $p - {}^{58}\text{Ni}$ scattering data at 1 GeV.

The optical model can be tied in nicely with Glauber theory by means of inversion of the Bessel and Abel transforms in the expression

$$f(\theta) = ik \int_0^\infty \left(1 - e^{-i/\hbar v \int_{-\infty}^\infty V(b^2 + z^2) dz} \right) J_0(2kb \sin \theta/2) b db$$

to obtain an expression for $V(r)$ (not unique) from the observed scattering amplitude. Brissaud et al. (BR75) do a calculation for 155 MeV $p - {}^{208}\text{Pb}$ scattering where they use the multiple scattering formalism to compute the eikonal phases, and use these to obtain an optical potential. The potential so produced agrees well with the "best fit" Woods-Saxon potential, especially on the nuclear surface. A similar approach has been taken by Dymarz et al. (DY77), where multiple scattering formalism has been used to produce profile

functions for $p - {}^4\text{He}$ at 348 MeV, 650 MeV and 1050 MeV, and then instead of evaluating observables directly in the Glauber eikonal approximation, he evaluates an optical potential from which a phase shift calculation is performed to obtain the observables. The regular Glauber technique tends to produce rather sharp diffraction minima which are suppressed by Dymarz's method to give a better fit to the data.

In this thesis we take an optical potential of the form

$$V(r) = (v_0 + iw_0)(1 + \rho r^2) e^{-\alpha r^2} + (v_{\text{s.o.}} + iw_{\text{s.o.}})(1 + \rho r^2) e^{-\alpha r^2} \underline{\sigma} \cdot \underline{L} .$$

The six free parameters are varied as a function of energy to mimic the properties of the nuclear optical potential, in particular its strength, range and volume integral. This potential has the advantage of giving an analytic form for the amplitudes, but has the disadvantage of being unable to reproduce the scattering results from heavy nuclei; even for helium a Gaussian potential is not as good as a Woods-Saxon potential as shown by Frosh et al. (FR67), but nevertheless the results may be qualitatively fitted and so testing the approximation on these potentials is not entirely unrealistic.

The potential contains a spin-orbit part, which therefore compliments the earlier studies with central potentials, by having something to say about the spin-flip amplitude.

Most tests before have been in the 1 GeV range, we concern ourselves with the "intermediate energy" range, from

0.1 GeV to 1.0 GeV in this study, and hope to shed some light on the successes and failures of the multiple scattering in this energy region.

From spin- $\frac{1}{2}$ on spin-zero scattering one has four amplitudes. Accounting for an overall phase, one has three linearly independent quantities, this study appears to be the first to consider all three, taken here to be cross-section polarisation and a polarisation transfer coefficient.

The thesis starts with a recapitulation of the derivation of the scattering amplitudes and observables in Chapter II and a slight modification is found for the spin- $\frac{1}{2}$ spin-flip amplitude. The modification does not always improve the accuracy and does not have a large effect on the amplitudes, formally, from the theory its presence is required and therefore it is kept. In Chapter III the results for a modified Gaussian potential are derived and also the associated Born results. Chapter IV summarises the numerical results and draws conclusions. Various results for cross-sections are given in the appendices.

CHAPTER II

THE MATHEMATICAL BACKGROUND

TO THE GLAUBER APPROXIMATION

The Glauber approximation, like the W.K.B. approximation, is based on employing classical ideas into a quantum-mechanical framework. The Glauber approximation uses the classical concept of an impact parameter. The derivation of the approximation presented in this thesis unfortunately seems to mask this formalism. The essential point is that since we are using a semiclassical idea (i.e. we do not take just one impact parameter, we average over a probability distribution of them), we expect the approximation to be best when used under circumstances akin to classical.

The "akin to classical" circumstances are that the flux is not changed much by the presence of the scatterer. This means that the potential must be weak in some sense, in particular:

(a) The potential strength is weak compared to the incident energies.

(b) The potential varies little over one incoming particle wavelength.

This chapter starts off by deriving briefly the Born approximation results for the scattering amplitudes of spin $\frac{1}{2}$ particles. The spin zero results are well known (R067). The reason for these Born calculations is that one may see in action the correspondence between Glauber and Born approximations.

After these calculations the spin zero and spin $\frac{1}{2}$ Glauber approximation expressions are derived, and a version for the spin-flip amplitude is obtained, which is slightly different from that in the literature - - in particular (GL59).

Before performing any calculations, however, a recapitulation on scattering theory may be in order, especially for spin $\frac{1}{2}$ scattering which is rarely touched on in simple terms in the standard quantum mechanics texts.

Consider a particle of mass m and spin $\frac{1}{2}$ being scattered from a potential of the form

$$V(\underline{r}, \underline{\sigma})$$

where \underline{r} is the position vector from the scattering centre to the incident particle and $\underline{\sigma}$ is the spin operator. The essential problem is, of course, solving the Schroedinger equation

$$(\nabla^2 + k^2) \begin{pmatrix} \psi_1(\underline{r}) \\ \psi_2(\underline{r}) \end{pmatrix} = \frac{2m}{\hbar^2} V(\underline{r}, \underline{\sigma}) \begin{pmatrix} \psi_1(\underline{r}) \\ \psi_2(\underline{r}) \end{pmatrix}. \quad (1)$$

The wavefunction for a spin $\frac{1}{2}$ particle is represented by a 2×1 matrix.

At large distances the wavefunction looks like a linear superposition of the incident plane wave and an outgoing spherical wave,

$$\text{i.e.} \quad \begin{pmatrix} \psi_1(\underline{r}) \\ \psi_2(\underline{r}) \end{pmatrix}_{r \rightarrow \infty} \longrightarrow \begin{pmatrix} a \\ b \end{pmatrix} e^{i \underline{k}_i \cdot \underline{r}} + \frac{e^{i k r}}{r} M \begin{pmatrix} a \\ b \end{pmatrix} \quad (2)$$

Where M , a 2×2 matrix called the scattering operator, is a function of θ and ϕ and is an operator acting on spin.

a and b are two numbers satisfying $a^2 + b^2 = 1$ and describing the spin state of the particle. \underline{k}_i is the wavevector of the incident particle and $k = |\underline{k}_i|$ since we assume the scattering is elastic.

The differential equation (1) is best solved by turning it into an integral equation

$$\begin{pmatrix} \psi_1(\underline{r}) \\ \psi_2(\underline{r}) \end{pmatrix} = \begin{pmatrix} a \\ b \end{pmatrix} e^{i\underline{k}_i \cdot \underline{r}} + \int G(\underline{r}-\underline{r}') V(\underline{r}', \underline{\sigma}) \begin{pmatrix} \psi_1(\underline{r}') \\ \psi_2(\underline{r}') \end{pmatrix} d^3 r' . \quad (3)$$

where $G(\underline{r}-\underline{r}')$ is the free Green function which satisfies the equation

$$(\nabla^2 + k^2)G(\underline{r}-\underline{r}') = \frac{2m}{\hbar^2} \delta(\underline{r}-\underline{r}') . \quad (4)$$

The solution to (4), which, when used in (3) satisfies the boundary condition (2) is given as

$$G(\underline{r}-\underline{r}') = \frac{-m}{2\pi\hbar^2} \frac{e^{ik|\underline{r}-\underline{r}'|}}{|\underline{r}-\underline{r}'|} . \quad (5)$$

Thus, using this our equation (3) becomes

$$\begin{pmatrix} \psi_1(\underline{r}) \\ \psi_2(\underline{r}) \end{pmatrix} = \begin{pmatrix} a \\ b \end{pmatrix} e^{i\underline{k}_i \cdot \underline{r}} - \frac{m}{2\pi\hbar^2} \int \frac{e^{ik|\underline{r}-\underline{r}'|}}{|\underline{r}-\underline{r}'|} V(\underline{r}', \underline{\sigma}) \begin{pmatrix} \psi_1(\underline{r}') \\ \psi_2(\underline{r}') \end{pmatrix} d^3 r' . \quad (6)$$

Asymptotically we have the expansion

$$|\underline{r}-\underline{r}'| \xrightarrow{r \rightarrow \infty} r - \frac{\underline{r}' \cdot \underline{r}}{r} + o\left(\frac{1}{r}\right) . \quad (7)$$

Using this in (6) we have that at large distances from the scattering centre,

$$\begin{pmatrix} \psi_1(\underline{r}) \\ \psi_2(\underline{r}) \end{pmatrix} \xrightarrow{r \rightarrow \infty} \begin{pmatrix} a \\ b \end{pmatrix} e^{i\underline{k}_i \cdot \underline{r}} - \frac{m}{2\pi\hbar^2} \frac{e^{ikr}}{r} \int e^{-i\underline{k}_f \cdot \underline{r}'} V(\underline{r}', \underline{\sigma}) \begin{pmatrix} \psi_1(\underline{r}') \\ \psi_2(\underline{r}') \end{pmatrix} d^3r' , \quad (8)$$

where we have introduced the vector

$$\underline{k}_f = k\underline{r} .$$

Comparing equations (2) and (8) one then obtains

$$M \begin{pmatrix} a \\ b \end{pmatrix} = - \frac{m}{2\pi\hbar^2} \int e^{-i\underline{k}_f \cdot \underline{r}'} V(\underline{r}', \underline{\sigma}) \begin{pmatrix} \psi_1(\underline{r}') \\ \psi_2(\underline{r}') \end{pmatrix} d^3r' . \quad (9)$$

This is an exact expression for the scattering operator.

We see from it that in order to calculate the scattering operator, we must know the wavefunction at all points where the potential is non-zero.

Since any single particle scattering may be considered to take place in a plane, it is worth at this stage adopting the convention to be used throughout the thesis, of fixing the y-axis to be perpendicular to the scattering plane.

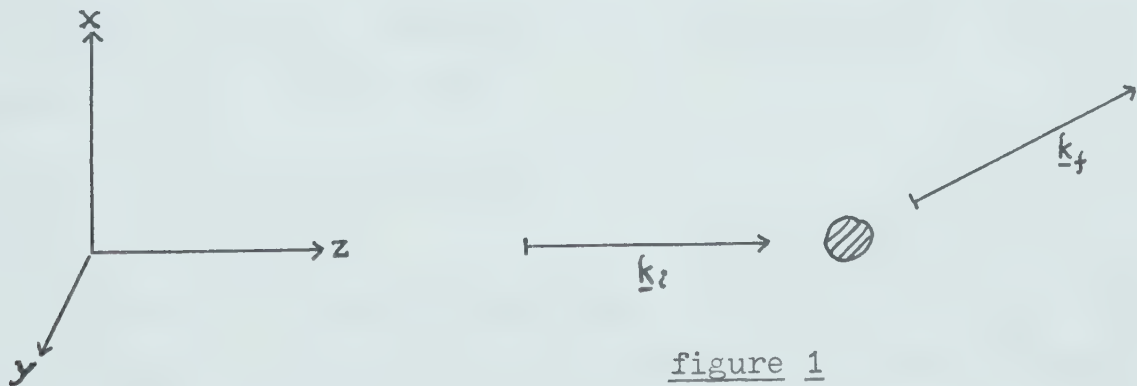


figure 1

In this picture we have indicated, too, the choice of the z-axis, that is to be parallel to \underline{k}_i . Later we shall choose it to be midway between \underline{k}_i and \underline{k}_f .

THE BORN APPROXIMATION

The Born approximation for the spin zero case is well known and well documented (R067), therefore the derivation is carried out here only for the spin $\frac{1}{2}$ case. The spin zero result may be obtained by considering only the diagonal elements of the scattering operator to be the spin zero scattering amplitude. The actual wavefunction may, in theory, be obtained by iterating equation (6) until it converges. The Born approximation essentially uses just one iteration of (6) starting from zero to get

$$\begin{pmatrix} \psi_1(\underline{r}) \\ \psi_2(\underline{r}) \end{pmatrix} = e^{i\mathbf{k}_i \cdot \underline{r}} \begin{pmatrix} a \\ b \end{pmatrix} . \quad (10)$$

Using this in equation (9) we obtain

$$M \begin{pmatrix} a \\ b \end{pmatrix} = - \frac{m}{2\pi\hbar^2} \int e^{-i\mathbf{k}_f \cdot \underline{r}} V(\underline{r}, \underline{\sigma}) e^{i\mathbf{k}_i \cdot \underline{r}} \begin{pmatrix} a \\ b \end{pmatrix} d^3r . \quad (11)$$

We now must specify something about the potential. Let us assume it to be of the form

$$V(\underline{r}, \underline{\sigma}) = V_c(r) + V_{s.o.}(r) \underline{\sigma} \cdot \underline{L} , \quad (12)$$

which is used in optical model type calculations for nuclear scattering, and therefore of interest. $M \begin{pmatrix} a \\ b \end{pmatrix}$ is then the sum of two terms

$$I_o = - \frac{m}{2\pi\hbar^2} \int e^{-i\mathbf{k}_f \cdot \underline{r}} V_c(r) e^{i\mathbf{k}_i \cdot \underline{r}} \begin{pmatrix} a \\ b \end{pmatrix} d^3r \quad (13)$$

and

$$I_1 = - \frac{m}{2\pi\hbar^2} \int e^{-i\mathbf{k}_f \cdot \mathbf{r}} V_{s.o.}(r) \underline{\sigma} \cdot \underline{L} e^{i\mathbf{k}_i \cdot \mathbf{r}} \begin{pmatrix} a \\ b \end{pmatrix} d^3r \quad (13)$$

The first term is the scattering amplitude in the familiar spin zero Born approximation. It may be simplified to give

$$I_0 = - \frac{2m}{\hbar^2} \begin{pmatrix} a \\ b \end{pmatrix} \int_0^\infty V_c(r) r^2 j_0(qr) dr$$

where $\hbar q = \hbar(\mathbf{k}_i - \mathbf{k}_f) \equiv$ momentum transfer, and $j_0(z)$ is the zeroth order spherical Bessel function (AB64). The second term is evaluated as follows

$$I_1 = - \frac{m}{2\pi\hbar^2} \int e^{-i\mathbf{k}_f \cdot \mathbf{r}} V_{s.o.}(r) \underline{\sigma} \cdot \underline{r} \times \mathbf{p} e^{i\mathbf{k}_i \cdot \mathbf{r}} \begin{pmatrix} a \\ b \end{pmatrix} d^3r \quad (14)$$

$$= \frac{m}{2\pi\hbar} \int e^{i\mathbf{q} \cdot \mathbf{r}} V_{s.o.}(r) \underline{\sigma} \cdot \mathbf{k}_i \times \mathbf{r} \begin{pmatrix} a \\ b \end{pmatrix} d^3r \quad (15)$$

$$= - \frac{mi}{2\pi\hbar} \underline{\sigma} \cdot \mathbf{k}_i \times \nabla_q \left\{ \int e^{i\mathbf{q} \cdot \mathbf{r}} V_{s.o.}(r) d^3r \right\} \begin{pmatrix} a \\ b \end{pmatrix} \quad (16)$$

Now using

$$\int e^{i\mathbf{q} \cdot \mathbf{r}} V_{s.o.}(r) d^3r = 4\pi \int_0^\infty j_0(qr) V_{s.o.}(r) r^2 dr \quad (17)$$

we get

$$I_1 = - \frac{4\pi mi}{2\pi\hbar} \underline{\sigma} \cdot \mathbf{k}_i \times \nabla_q \int j_0(qr) V_{s.o.}(r) r^2 \begin{pmatrix} a \\ b \end{pmatrix} dr \quad (18)$$

$$= - \frac{2mi}{\hbar} \underline{\sigma} \cdot \underline{k}_i \times \hat{q} \frac{\partial}{\partial q} \int_0^{\infty} j_0(qr) V_{s.o.}(r) r^2 \begin{pmatrix} a \\ b \end{pmatrix} dr , \quad (19)$$

which upon introducing $\underline{n} = \underline{k}_i \times \underline{k}_f$ and using $q = 2k \sin \theta/2$

$$= - \frac{2mi}{\hbar} k \cos \theta/2 \int_0^{\infty} j_1(qr) V_{s.o.}(r) r^3 \underline{\sigma} \cdot \underline{n} \begin{pmatrix} a \\ b \end{pmatrix} dr . \quad (20)$$

Collecting the terms we have the expression

$$\begin{aligned} M \begin{pmatrix} a \\ b \end{pmatrix} = & - \frac{2m}{\hbar^2} \int V_c(r) r^2 j_0(qr) \begin{pmatrix} a \\ b \end{pmatrix} dr \\ & - \frac{2mi}{\hbar} k \cos \theta/2 \int_0^{\infty} j_1(qr) V_{s.o.}(r) r^3 \underline{\sigma} \cdot \underline{n} \begin{pmatrix} a \\ b \end{pmatrix} dr . \end{aligned} \quad (21)$$

θ here is the angle between \underline{k}_i and \underline{k}_f . It is customary to write M in the following form:

$$M = f(\theta) + \underline{\sigma} \cdot \underline{n} g(\theta) = \begin{pmatrix} f(\theta) & 0 \\ 0 & f(\theta) \end{pmatrix} + \begin{pmatrix} 0 & -ig(\theta) \\ ig(\theta) & 0 \end{pmatrix} . \quad (22)$$

Since \underline{n} is normal to the scattering plane, it is parallel to the y-axis.

Equation (21) then tells us that

$$f(\theta) = - \frac{2m}{\hbar^2} \int_0^{\infty} V_c(r) r^2 j_0(qr) dr , \quad (23)$$

and

$$g(\theta) = - \frac{2mi}{\hbar} k \cos \theta/2 \int_0^{\infty} j_1(qr) V_{s.o.}(r) r^3 dr . \quad (24)$$

THE GLAUBER-EIKONAL APPROXIMATION

We study first the spin zero case, which is equivalent to ignoring the effects of spin, and then generalise afterwards. This derivation of the approximation follows that of Kamal (KA72). Starting from the Green function

$$G(\underline{r}, \underline{r}') = - \frac{m}{2\pi\hbar^2} \frac{e^{ik|\underline{r}-\underline{r}'|}}{|\underline{r}-\underline{r}'|}$$

$$= \lim_{\epsilon \rightarrow 0^+} \frac{2m}{\hbar^2} \frac{1}{(2\pi)^3} \int \frac{e^{i\underline{k}' \cdot (\underline{r}-\underline{r}')} d^3k'}{k_i^2 - k'^2 + i\epsilon} \quad (25)$$

and writing

$$\underline{k}' = \underline{k}_i + \underline{n} \quad ,$$

we obtain

$$G(\underline{r}, \underline{r}') = \frac{2m}{\hbar^2} \frac{1}{(2\pi)^3} \lim_{\epsilon \rightarrow 0^+} \int \frac{e^{i\underline{k}_i \cdot (\underline{r}-\underline{r}')} e^{i\underline{n} \cdot (\underline{r}-\underline{r}')} d^3n}{k_i^2 - (\underline{k}_i + \underline{n})^2 + i\epsilon} \quad (26)$$

$$= \frac{2m}{\hbar^2} \frac{1}{(2\pi)^3} \lim_{\epsilon \rightarrow 0^+} e^{i\underline{k}_i \cdot (\underline{r}-\underline{r}')} \int \frac{e^{i\underline{n} \cdot (\underline{r}-\underline{r}')} d^3n}{-n^2 - 2\underline{k}_i \cdot \underline{n} + i\epsilon} \quad (27)$$

In the integral if $|\underline{n}|$ is large, then the exponential will oscillate and therefore the integrand will contribute significantly only for small $|\underline{n}|$. So neglecting the $|\underline{n}|^2$ term in the denominator, we obtain

$$G_{G.L.}(\underline{r}, \underline{r}') = \frac{2m}{\hbar^2} \frac{1}{(2\pi)^3} \lim_{\epsilon \rightarrow 0^+} e^{i\underline{k}_i \cdot (\underline{r}-\underline{r}')} \int \frac{e^{i\underline{n} \cdot (\underline{r}-\underline{r}')} d^3n}{-2\underline{k}_i \cdot \underline{n} + i\epsilon} \quad (28)$$

Subsequently the subscript G.L. is dropped from the Green function. It is to be implicitly understood that the limit as 0^+ is to be taken wherever not explicitly stated.

$$G(\underline{r}, \underline{r}') = -\frac{2m}{\hbar^2} \frac{1}{(2\pi)^3} e^{i\mathbf{k}_i \cdot (\underline{r} - \underline{r}')} \int \frac{e^{i\mathbf{n} \cdot (\underline{r} - \underline{r}')} d^3n}{2\mathbf{k}_i \cdot \mathbf{n} - i\epsilon} . \quad (29)$$

At this stage it is worth a small digression to define a slightly different Green function. We have

$$G(\underline{r}, \underline{r}') = \frac{2m}{\hbar^2} \frac{1}{(2\pi)^3} \int \frac{e^{i\mathbf{k}' \cdot (\underline{r} - \underline{r}')} d^3k'}{k_i^2 - k'^2 + i\epsilon} . \quad (30)$$

Define two vectors

$$\underline{K} = \frac{1}{2}(\mathbf{k}_i + \mathbf{k}') , \quad \underline{n} = \mathbf{k}' - \mathbf{k}_i \quad (31)$$

$$\text{Then } \mathbf{k}' = \underline{K} + \frac{1}{2}\underline{n} \quad \text{and} \quad \mathbf{k}_i = \underline{K} - \frac{1}{2}\underline{n} . \quad (32)$$

Therefore

$$G(\underline{r}, \underline{r}') = \frac{2m}{\hbar^2} \frac{1}{(2\pi)^3} \int \frac{e^{i(\underline{K} + \frac{1}{2}\underline{n}) \cdot (\underline{r} - \underline{r}')} d^3k'}{(\underline{K}^2 - \underline{K} \cdot \underline{n} + \frac{1}{4}\underline{n}^2) - (\underline{K}^2 + \underline{K} \cdot \underline{n} + \frac{1}{4}\underline{n}^2) + i\epsilon} , \quad (33)$$

or changing the integration variable to \underline{n} ,

$$\begin{aligned} G(\underline{r}, \underline{r}') &= -\frac{2m}{\hbar^2} \frac{1}{(2\pi)^3} \int \frac{e^{i\mathbf{k}_i \cdot (\underline{r} - \underline{r}')} e^{i\mathbf{n} \cdot (\underline{r} - \underline{r}')} d^3n}{-2\underline{K} \cdot \underline{n} + i\epsilon} \\ &= -\frac{2m}{\hbar^2} \frac{1}{(2\pi)^3} e^{i\mathbf{k}_i \cdot (\underline{r} - \underline{r}')} \int \frac{e^{i\mathbf{n} \cdot (\underline{r} - \underline{r}')} d^3n}{-2\underline{K} \cdot \underline{n} + i\epsilon} . \end{aligned} \quad (35)$$

We now make the approximation that \underline{k} is independent of \underline{n} -- which is equivalent to neglecting the term in n^2 .

Since functionally these two Green functions are the same except for $\underline{k}_i \leftrightarrow \underline{k}$, we evaluate the integral for the first and the second will follow in an identical manner. Choose the n_z -axis parallel to \underline{k}_i . This incidentally fixes the z and z' axes also parallel to \underline{k}_i . Then

$$G(\underline{r}, \underline{r}') = - \frac{2m}{\hbar^2} \frac{1}{(2\pi)^3} e^{i\underline{k}_i \cdot (\underline{r} - \underline{r}')} \int_{-\infty}^{\infty} \int_{-\infty}^{\infty} \int_{-\infty}^{\infty} \frac{e^{in_z(z-z')} e^{in_x(x-x')} e^{in_y(y-y')} dn_x dn_y dn_z}{2|\underline{k}_i| n_z - i\epsilon} \quad (36)$$

$$= - \frac{2m}{\hbar^2} \frac{1}{(2\pi)^3} e^{i\underline{k}_i \cdot (\underline{r} - \underline{r}')} 2\pi\delta(x-x') 2\pi\delta(y-y') \frac{1}{2|\underline{k}_i|} \int_{-\infty}^{\infty} \frac{e^{in_z(z-z')} dn_z}{n_z - i\epsilon} \quad (37)$$

Upon doing a contour integration we see that the last term is

$$2\pi i \theta(z-z') \quad (38)$$

where θ is Heavyside's step function. Our Green function becomes

$$G(\underline{r}, \underline{r}') = - \frac{2m}{\hbar^2} \left(\frac{i}{2k} \right) e^{i\underline{k}_i \cdot (\underline{r} - \underline{r}')} \delta(x-x') \delta(y-y') \theta(z-z'). \quad (39)$$

With \underline{z} and \underline{z}' parallel to $(\underline{k}_i + \underline{k}_f)$ the other Green function is similarly

$$G(\underline{r}, \underline{r}') = - \frac{2m}{\hbar^2} \left(\frac{i}{2|\underline{k}|} \right) e^{i\underline{k}_i \cdot (\underline{r} - \underline{r}')} \delta(x-x') \delta(y-y') \theta(z-z') \quad (40)$$

We note however that

$$|\underline{k}| = \frac{1}{\sqrt{2}} \sqrt{k^2 + \underline{k} \cdot \underline{k}'} = \frac{1}{\sqrt{2}} k \sqrt{1 + \cos^2 \theta} \approx k \text{ for small } \theta. \quad (41)$$

The main difference between the first and second Green functions is in the way the z -axis is specified. This will have a bearing on the final result as we shall see later.

Using for now just the first Green function, we have the integral equation,

$$\psi(\underline{r}) = e^{i\underline{k}_i \cdot \underline{r}} - \frac{mi}{\hbar^2} \int e^{i\underline{k}_i \cdot (\underline{r} - \underline{r}')} \delta(x-x') \delta(y-y') \theta(z-z') V(\underline{r}') \psi(\underline{r}') d^3r'. \quad (42)$$

Define a function $\rho(\underline{r})$ by

$$\psi(\underline{r}) = \rho(\underline{r}) e^{i\underline{k}_i \cdot \underline{r}} \quad (43)$$

the equation for $\rho(\underline{r})$ is

$$(\rho(\underline{r}) - 1) = - \frac{mi}{\hbar^2} \int \delta(x-x') \delta(y-y') \theta(z-z') V(\underline{r}') \rho(\underline{r}') d^3r' \quad (44)$$

or

$$1 - \rho(x, y, z) = \frac{mi}{k\hbar^2} \int_{-\infty}^z V(x, y, z') \rho(x, y, z') dz' \quad (45)$$

To solve this integral equation, differentiate

$$- \frac{\partial \rho}{\partial z}(x, y, z) = \left(\frac{mi}{k\hbar^2} V(x, y, z) \right) \rho(x, y, z) \quad (46)$$

where

$$\frac{m}{k\hbar^2} = \frac{1}{\hbar v} \quad (47)$$

or,

$$\frac{\partial}{\partial z} \left(e^{i/\hbar v \int_{-\infty}^z V(x, y, z') dz'} \rho(x, y, z) \right) = 0 \quad (48)$$

Equation (48) implies

$$\rho(x, y, z) = A(x, y) e^{-i/\hbar v \int_{-\infty}^z V(x, y, z') dz'} \quad (49)$$

$A(x, y)$ is an arbitrary function of x and y .

Substituting this back into the integral equation we obtain

$$A(x, y) e^{-i/\hbar v \int_{-\infty}^z V(x, y, z') dz'} = 1 - \frac{i}{\hbar v} \int_{-\infty}^z V(x, y, z') A(x, y) e^{-i/\hbar v \int_{-\infty}^{z'} V(x, y, z'') dz''} dz' \quad (50)$$

$$= 1 + e^{-i/\hbar v \int_{-\infty}^z V(x, y, z') dz'} A(x, y) - A(x, y) \quad (51)$$

which shows

$$A(x,y) = 1 \quad (52)$$

$$\rho(x,y,z) = e^{-i/\hbar v \int_{-\infty}^z V(x,y,z') dz'} \quad (53)$$

Define the vector \underline{b} in the x-y plane as follows

$$\underline{r} = \underline{b} + z\hat{\underline{k}}_i \quad (54)$$

If the scattering takes place through small angles, then \underline{b} does not change appreciably and may be interpreted as an impact parameter. Thus, with

$$\psi(\underline{r}) = e^{i\hat{\underline{k}}_i \cdot \underline{r}} \rho(\underline{r}) = e^{i\hat{\underline{k}}_i \cdot \underline{r}} - i/\hbar v \int_{-\infty}^z V(x,y,z') dz' \quad (55)$$

we have the scattering amplitude (obtained by substituting into equation (9))

$$\begin{aligned} f(\theta) &= - \frac{m}{2\pi\hbar^2} \int e^{-i\hat{\underline{k}}_f \cdot \underline{r}} V(\underline{r}) e^{i\hat{\underline{k}}_i \cdot \underline{r}} - i/\hbar v \int_{-\infty}^z V(\underline{b} + \hat{\underline{k}}_i z') dz' d^2b \quad (56) \\ &= - \frac{m}{2\pi\hbar^2} \int e^{i\underline{q} \cdot (\underline{b} + \hat{\underline{k}}_i z)} V(\underline{b} + \hat{\underline{k}}_i z) e^{-i/\hbar v \int_{-\infty}^z V(\underline{b} + \hat{\underline{k}}_i z') dz'} dz' d^2b \end{aligned}$$

$$\text{where } \underline{q} = \hat{\underline{k}}_i - \hat{\underline{k}}_f \quad (58)$$

We have $z\hat{\underline{k}}_i \cdot \hat{\underline{k}}_i = zk(1-\cos\theta)$. The biggest contribution to the z-part of the integral is seen to come when $V(x,y,z)$ is a maximum, which occurs if $z \leq d$, the "distance over which the potential varies significantly" -- usually the same order of magnitude as its range. We make the approximation here of neglecting

$$dk(1 - \cos\theta) \approx \frac{dk\theta^2}{2} \ll 1, \quad (59)$$

which gives

$$f(\theta) = - \frac{m}{2\pi\hbar^2} \int e^{i\mathbf{q} \cdot \mathbf{b}} V(\mathbf{b} + \mathbf{k}_i z) e^{-i/\hbar v \int_{-\infty}^z V(\mathbf{b} + \mathbf{k}_i z') dz'} dz' dz d^2b \quad (60)$$

The z -integral may now be done exactly, yielding

$$f(\theta) = - \frac{m}{2\pi\hbar^2} \left(\frac{\hbar v}{-i} \right) \int e^{i\mathbf{q} \cdot \mathbf{b}} \left(e^{-i/\hbar v \int_{-\infty}^{\infty} V(\mathbf{b} + \mathbf{k}_i z) dz} - 1 \right) d^2b \quad (61)$$

Define the eikonal phase as

$$\chi(\mathbf{b}) = - \frac{1}{\hbar v} \int_{-\infty}^{\infty} V(\mathbf{b} + \mathbf{k}_i z) dz \quad (62)$$

To first order in the potential (i.e. if V is approximately constant) this is seen to be proportional to the classical action the particle encounters on its classical trajectory. From equations (61) and (62)

$$f(\theta) = - \frac{imv}{2\pi\hbar} \int e^{i\mathbf{q} \cdot \mathbf{b}} \left(e^{i\chi(\mathbf{b})} - 1 \right) d^2b \quad (63)$$

This expression simplifies if we assume the potential has axial symmetry about \mathbf{k}_i , in which case $\chi(\mathbf{b}) = \chi(b)$.

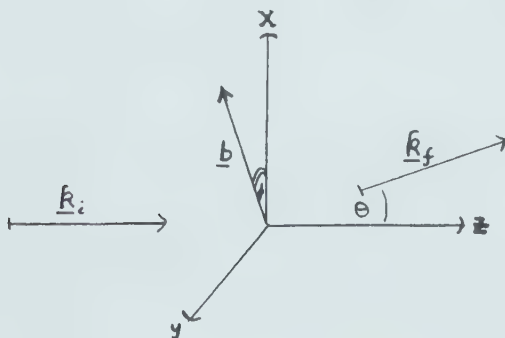


figure 2

$$\underline{k}_i = k \hat{z} , \quad \underline{k}_f = k \cos \theta \hat{z} + k \sin \theta \hat{x} , \quad \underline{b} = b \cos \phi \hat{x} + b \sin \phi \hat{y} \quad (64)$$

$$\text{Therefore } \underline{q} \cdot \underline{b} = (\underline{k}_i - \underline{k}_f) \cdot \underline{b} = -\underline{k}_f \cdot \underline{b} = -kb \sin \theta \cos \phi \quad (65)$$

and therefore

$$f(\theta) = -ik \int_0^\infty (e^{i\chi(b)} - 1) b db \frac{1}{2\pi} \int_0^{2\pi} e^{-i(kb \sin \theta) \cos \phi} d\phi \quad (66)$$

$$\text{Define } \Gamma(b) = 1 - e^{i\chi(b)} \quad (67)$$

$$\text{and using } \frac{1}{2\pi} \int_0^{2\pi} e^{i\lambda \cos \theta} d\theta = J_0(\lambda) \quad (68)$$

we get

$$f(\theta) = ik \int_0^\infty J_0(kb \sin \theta) \Gamma(b) b db . \quad (69)$$

This is just the result derived by Glauber in 1959 (GL59). The accuracy is improved by using the second Green function, which is where the propagator is expanded about the $\frac{1}{2}(\underline{k}_i + \underline{k}_f)$ direction. The derivation of the scattering amplitude is very much the same as above and is outlined here.

With $\underline{k} = \frac{1}{2}(\underline{k}_i + \underline{k}_f)$ equation (57) becomes

$$f(\theta) = -\frac{m}{2\pi\hbar^2} \int_0^\infty e^{i\underline{q} \cdot (\underline{b} + \hat{\underline{K}}z)} V(\underline{b} + \hat{\underline{K}}z) e^{-i/\hbar v \int_{-\infty}^\infty V(\underline{b} + \hat{\underline{K}}z') dz'} dz' dz d^2b . \quad (70)$$

Now using $\underline{q} \cdot \underline{k} = 0$ and performing the z -integral we get

$$f(\theta) = -\frac{ik}{2\pi} \int_0^\infty e^{i\underline{q} \cdot \underline{b}} (e^{i\chi(\underline{b})} - 1) d^2b . \quad (71)$$

Note that this step is exact now, whereas before it was an approximation.

For $\chi(\underline{b}) = \chi(b)$, we may do the angular integration, since $\underline{q} \cdot \underline{b} = (\underline{k}_i - \underline{k}_f) \cdot \underline{b}$, (72a)

$$\underline{k}_i = k \cos \theta / 2 \hat{\underline{z}} - k \sin \theta / 2 \hat{\underline{x}} , \quad (72b)$$

$$\underline{k}_f = k \cos \theta / 2 \hat{\underline{z}} + k \sin \theta / 2 \hat{\underline{x}} \quad \text{and} \quad (72c)$$

$$\underline{b} = b \cos \phi \hat{\underline{x}} + b \sin \phi \hat{\underline{y}} , \quad \text{then} \quad (72d)$$

$$\underline{q} \cdot \underline{b} = -2kb \sin \theta / 2 \cos \phi \quad \text{and} \quad (73)$$

$$f(\theta) = ik \int_0^\infty \Gamma(b) b db \frac{1}{2\pi} \int_0^{2\pi} e^{-i(2kb \sin \theta / 2) \cos \phi} d\phi . \quad (74)$$

Using the integral representation of J_0 ,

$$f(\theta) = ik \int_0^\infty J_0(2kb \sin \theta / 2) \Gamma(b) b db . \quad (75)$$

This form is in agreement with the Born approximation under $e^{i\chi(b)} \longrightarrow 1 + i\chi(b)$, and generally gives better agreement with the exact calculation. It is the form most used and is a manifestly time-reversal invariant result, since it treats \underline{k}_i and \underline{k}_f symmetrically.

We now go on to consider the case of particles with spin $\frac{1}{2}$.

THE GLAUBER-EIKONAL APPROXIMATION
FOR SPIN $\frac{1}{2}$ PROJECTILES

The derivation presented here is the one which follows from changing the axes in the manner that Glauber did originally, i.e.

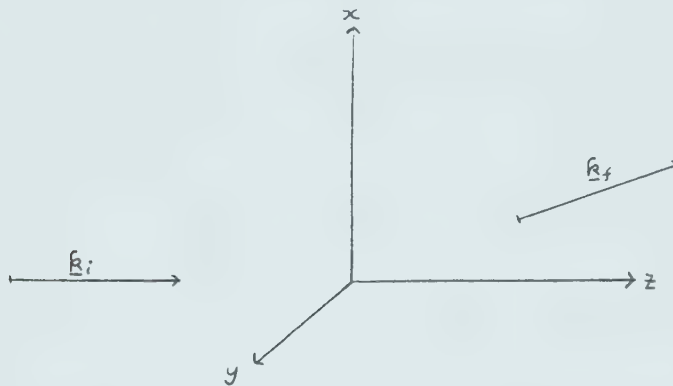


figure 3

As in the spin $\frac{1}{2}$ Born approximation we assume an interaction of the form

$$V(\underline{r}) = V_c(\underline{r}) + V_s(\underline{r}) \underline{\sigma} \cdot \underline{L} \quad (76)$$

Then

$$\begin{pmatrix} \psi_1(\underline{r}) \\ \psi_2(\underline{r}) \end{pmatrix} = \begin{pmatrix} a \\ b \end{pmatrix} e^{i\underline{k}_i \cdot \underline{r}} + \frac{2m}{\hbar^2} \int d^3r' G(\underline{r}-\underline{r}') V(\underline{r}', \underline{\sigma}) \begin{pmatrix} \psi_1(\underline{r}') \\ \psi_2(\underline{r}') \end{pmatrix} \quad (77)$$

with (see equation (39))

$$G(\underline{r}-\underline{r}') = -\frac{2m}{\hbar^2} \left(\frac{i}{2k} \right) e^{i\underline{k}_i \cdot (\underline{r}-\underline{r}')} \delta(x-x') \delta(y-y') (z-z') \quad (78)$$

Let us write

$$\begin{pmatrix} \psi \\ \psi_2(\underline{r}) \end{pmatrix} = e^{i\mathbf{k}_i \cdot \underline{r}} \rho(\underline{r}) \begin{pmatrix} a \\ b \end{pmatrix} . \quad (79)$$

$\rho(\underline{r})$ may be considered in this case to operate on the spin variables. The integral equation for $\rho(\underline{r})$ is

$$(\rho(\underline{r}) - 1) \begin{pmatrix} a \\ b \end{pmatrix} = \frac{2m}{\hbar^2} \int d^3r' G(\underline{r}, \underline{r}') e^{-i\mathbf{k}_i \cdot \underline{r}} V(\underline{r}', \underline{\sigma}) e^{i\mathbf{k}_i \cdot \underline{r}'} \rho(\underline{r}') \begin{pmatrix} a \\ b \end{pmatrix} \quad (80)$$

which upon substituting the approximated Green function from equation (78), takes the form

$$(\rho(\underline{r}) - 1) \begin{pmatrix} a \\ b \end{pmatrix} = - \frac{mi}{\hbar^2} \int d^3r' e^{-i\mathbf{k}_i \cdot \underline{r}} \delta(\underline{b} - \underline{b}') \theta(z - z') V(\underline{r}', \underline{\sigma}) e^{i\mathbf{k}_i \cdot \underline{r}'} \rho(\underline{r}') \begin{pmatrix} a \\ b \end{pmatrix} \quad (81)$$

We cannot commute the $V(\underline{r}', \underline{\sigma})$ with $e^{i\mathbf{k}_i \cdot \underline{r}'}$, since $V(\underline{r}', \underline{\sigma})$ contains a differential operator. We have

$$V(\underline{r}', \underline{\sigma}) e^{i\mathbf{k}_i \cdot \underline{r}'} = \{V_c(\underline{r}') + V_s(\underline{r}') \underline{\sigma} \cdot \underline{r}' \times (-i \underline{\nabla})\} e^{i\mathbf{k}_i \cdot \underline{r}'} \quad (82)$$

Now we assume the $\rho(\underline{r})$ is a slowly varying function of \underline{r} compared to $e^{i\mathbf{k}_i \cdot \underline{r}}$, thus

$$\underline{\nabla} e^{i\mathbf{k}_i \cdot \underline{r}} \rho(\underline{r}) \approx i\mathbf{k}_i e^{i\mathbf{k}_i \cdot \underline{r}} \rho(\underline{r}) . \quad (83)$$

Therefore

$$(\rho(\underline{r}) - 1) \begin{pmatrix} a \\ b \end{pmatrix} = - \frac{mi}{\hbar^2} \int (V_c(\underline{\tilde{r}}) + V_s(\underline{\tilde{r}}) \underline{\sigma} \cdot \underline{\tilde{r}} \times \underline{k}_i) \rho(\underline{\tilde{r}}) dz' \begin{pmatrix} a \\ b \end{pmatrix} \quad (84)$$

where for convenience we have introduced the "vector"

$$\underline{\tilde{r}}, \text{ where } \underline{\tilde{r}} = (x, y, z') . \quad (85)$$

As before in the spin zero case this integral equation may be solved by differentiation and the boundary conditions decided by substituting the solution back into the integral equation yielding

$$\rho(x, y, z) = \exp \left(- \frac{mi}{\hbar^2} \int_{-\infty}^z (V_c(x, y, z') + V_s(x, y, z') \underline{\sigma} \cdot (\tilde{\underline{r}} \times \underline{k}_i)) dz' \right) \quad (86)$$

We now substitute this into the equation for the scattering operator

$$M \begin{pmatrix} a \\ b \end{pmatrix} = - \frac{m}{2\pi\hbar^2} \int e^{-i\underline{k}_f \cdot \underline{r}} (V_c(\underline{r}) + V_s(\underline{r}) \underline{\sigma} \cdot \underline{r} \times (-i\nabla) e^{i\underline{k}_i \cdot \underline{r}} \rho(\underline{r}) \begin{pmatrix} a \\ b \end{pmatrix} d^3r \quad (87)$$

Again we assume $\rho(\underline{r})$ to be a slowly varying function of \underline{r} to get

$$M \begin{pmatrix} a \\ b \end{pmatrix} = - \frac{m}{2\pi\hbar^2} \int e^{i\underline{q} \cdot \underline{r}} (V_c(\underline{r}) + V_s(\underline{r}) \underline{\sigma} \cdot \underline{r} \times \underline{k}_i) e^{-i/\hbar v \int_{-\infty}^z V_c(x, y, z') + V_s(x, y, z') \underline{\sigma} \cdot \tilde{\underline{r}} \times \underline{k}_i) dz' \begin{pmatrix} a \\ b \end{pmatrix} d^3r \quad (88)$$

We now make an approximation that

$$i\underline{q} \cdot \underline{r} = i(\underline{k}_i - \underline{k}_f) \cdot (\underline{b} + \hat{\underline{k}}_i z) \approx i(\underline{k}_i - \underline{k}_f) \cdot \underline{b} \quad (89)$$

This is tantamount to saying that, since the integral has its maximum value within $z = d$, $dk(1 - \cos \theta)$ is small; and is of course the same approximation made in the corresponding spin zero case.

$$M \begin{pmatrix} a \\ b \end{pmatrix} = - \frac{m}{2\pi\hbar^2} \int e^{i\mathbf{q} \cdot \mathbf{b}} (V_c(\mathbf{r}) + V_s(\mathbf{r}) \mathbf{\sigma} \cdot \mathbf{r} \times \mathbf{k}_i) e^{-i/\hbar v \int_{-\infty}^z (V_c(x,y,z') + V_s(x,y,z') \mathbf{\sigma} \cdot \tilde{\mathbf{r}} \times \mathbf{k}_i) dz'} \begin{pmatrix} a \\ b \end{pmatrix} d^3r . \quad (90)$$

The z -integral may now be done exactly, to get

$$M \begin{pmatrix} a \\ b \end{pmatrix} = - \frac{m}{2\pi\hbar^2} \frac{\hbar v}{(-i)} \int e^{i\mathbf{q} \cdot \mathbf{b}} \left[e^{-i/\hbar v \int_{-\infty}^z (V_c(x,y,z') + V_s(x,y,z') \mathbf{\sigma} \cdot \tilde{\mathbf{r}} \times \mathbf{k}_i) dz'} - 1 \right] dx dy \begin{pmatrix} a \\ b \end{pmatrix} . \quad (91)$$

In the coordinates chosen we have:

$$(\tilde{\mathbf{r}} \times \mathbf{k}_i) = (\mathbf{b} + z' \hat{\mathbf{k}}_i) \times \mathbf{k}_i = \mathbf{b} \times \mathbf{k}_i . \quad (92)$$

Define our eikonal phases as

$$\chi_c(\mathbf{b}) = - \frac{1}{\hbar v} \int_{-\infty}^{\infty} V_c(x,y,z') dz' \quad (93a)$$

$$\chi_s(\mathbf{b}) = - \frac{1}{\hbar v} \int_{-\infty}^{\infty} V_s(x,y,z') dz' , \text{ getting} \quad (93b)$$

$$M \begin{pmatrix} a \\ b \end{pmatrix} = - \frac{m}{2\pi\hbar^2} \frac{\hbar v}{-i} \int e^{i\mathbf{q} \cdot \mathbf{b}} \left[e^{i\chi_c(\mathbf{b}) + \chi_s(\mathbf{b}) \mathbf{\sigma} \cdot \mathbf{b} \times \mathbf{k}_i} - 1 \right] \begin{pmatrix} a \\ b \end{pmatrix} d^2b . \quad (94)$$

We now expand the exponential in $\mathbf{\sigma}$,

$$e^{i\chi_s(\mathbf{b}) \mathbf{\sigma} \cdot \mathbf{b} \times \mathbf{k}_i} \equiv \sum_{n=0}^{\infty} \frac{(i\chi_s(\mathbf{b}))^n (\mathbf{\sigma} \cdot \mathbf{b} \times \mathbf{k}_i)^n}{n!} \quad (95)$$

$$= \sum_{n=0}^{\infty} \frac{(i\chi_s(\underline{b}))^{2n} (\underline{\sigma} \cdot \underline{b} \times \underline{k}_i)^{2n}}{(2n)!} + \sum_{n=0}^{\infty} \frac{(i\chi_s(\underline{b}))^{2n+1} (\underline{\sigma} \cdot \underline{b} \times \underline{k}_i)^{2n+1}}{(2n+1)!} \quad (96)$$

$(\underline{\sigma} \cdot \underline{A})^2 = A^2$ implies $(\underline{\sigma} \cdot \underline{A})^{2n+1} = \underline{\sigma} \cdot \underline{A} (A)^{2n}$ and
 $(\underline{\sigma} \cdot \underline{A})^{2n} = (A)^{2n}$. Using this, we get

$$e^{i\chi_s(\underline{b}) \underline{\sigma} \cdot \underline{b} \times \underline{k}_i} = \sum_{n=0}^{\infty} \frac{(-1)^n (|\underline{b} \times \underline{k}_i| \chi_s(\underline{b}))^{2n}}{(2n)!} \\ + \frac{i \underline{\sigma} \cdot \underline{b} \times \underline{k}_i}{|\underline{b} \times \underline{k}_i|} \sum_{n=0}^{\infty} \frac{(-1)^n (|\underline{b} \times \underline{k}_i| \chi_s(\underline{b}))^{2n+1}}{(2n+1)!} \quad (97)$$

Since \underline{b} is perpendicular to \underline{k}_i in this coordinate system,

$$|\underline{b} \times \underline{k}_i| = bk, \text{ giving} \quad (98)$$

$$e^{i\chi_s(\underline{b}) \underline{\sigma} \cdot \underline{b} \times \underline{k}_i} = \cos(bk\chi_s(\underline{b})) + (i\underline{\sigma} \cdot \underline{b} \times \underline{k}_i) \sin(bk\chi_s(\underline{b})) \quad (99)$$

and therefore

$$M\left(\frac{\underline{a}}{\underline{b}}\right) = \frac{mv}{2\pi\hbar i} \int e^{i\underline{q} \cdot \underline{b}} \left\{ e^{i\chi_c(\underline{b})} \right. \\ \left. (\cos(bk\chi_s(\underline{b})) + i\underline{\sigma} \cdot \underline{\hat{b}} \times \underline{\hat{k}}_i \sin(bk\chi_s(\underline{b})) - 1) \right\} \left(\frac{\underline{a}}{\underline{b}}\right) d^2b \quad (100)$$

$$M\left(\frac{\underline{a}}{\underline{b}}\right) = -\frac{k}{2\pi i} \int e^{i\underline{q} \cdot \underline{b}} \left\{ \Gamma_c(\underline{b}) + i\underline{\sigma} \cdot \underline{\hat{b}} \times \underline{\hat{k}}_i \Gamma_s(\underline{b}) \right\} \left(\frac{\underline{a}}{\underline{b}}\right) d^2b, \quad (101)$$

$$\text{where } \Gamma_c(\underline{b}) = 1 - e^{i\chi_c(\underline{b})} \cos(bk\chi_s(\underline{b})) \quad (102)$$

$$\text{and } \Gamma_s(\underline{b}) = -e^{i\chi_c(\underline{b})} \sin(bk\chi_s(\underline{b})) \quad (103)$$

We may go one step further if the potentials possess cylindrical symmetry, in which case $\chi(\underline{b}) = \chi(b)$. Using this

and $\underline{b} \cdot \underline{q} = -kb \sin \theta \cos \phi$

$$M \begin{pmatrix} a \\ b \end{pmatrix} = - \frac{k}{2\pi i} \int_0^\infty \int_0^{2\pi} e^{-i(kb \sin \theta) \cos \phi} \left\{ \Gamma_c(b) + i \underline{\sigma} \cdot \underline{\hat{b}} \times \underline{\hat{k}}_i \Gamma_s(b) \right\} \begin{pmatrix} a \\ b \end{pmatrix} d^2 b \quad (104)$$

$$\begin{aligned} &= ik \int_0^\infty \Gamma_c(b) b db \frac{1}{2\pi} \int_0^{2\pi} e^{-i(kb \sin \theta) \cos \phi} d\phi \begin{pmatrix} a \\ b \end{pmatrix} \\ &- k \int_0^\infty \Gamma_s(b) b db \frac{1}{2\pi} \int_0^{2\pi} \underline{\sigma} \cdot \underline{\hat{b}} \times \underline{\hat{k}}_i e^{-i(kb \sin \theta) \cos \phi} d\phi \begin{pmatrix} a \\ b \end{pmatrix} . \end{aligned} \quad (105)$$

In our coordinate system we have

$$\underline{\hat{b}} \times \underline{\hat{k}}_i = \underline{\hat{x}} \sin \phi - \underline{\hat{y}} \cos \phi . \quad (106)$$

Using the three integrals

$$\frac{1}{2\pi} \int_0^{2\pi} e^{i\lambda \cos \phi} d\phi = J_0(\lambda) , \quad (107a)$$

$$\frac{i}{2\pi} \int_0^{2\pi} e^{i\lambda \cos \phi} \cos \phi d\phi = J_1(\lambda) , \quad (107b)$$

$$\int_0^{2\pi} e^{i\lambda \cos \phi} \sin \phi d\phi = 0 , \quad (107c)$$

We see that only the \underline{y} term contributes to the second integral (a consequence of conservation of parity) yielding

$$\begin{aligned} M \begin{pmatrix} a \\ b \end{pmatrix} &= ik \int_0^\infty J_0(kb \sin \theta) \Gamma_c(b) b db \begin{pmatrix} a \\ b \end{pmatrix} \\ &- \frac{k}{i} \int_0^\infty J_1(kb \sin \theta) \Gamma_s(b) b db \sigma_y \begin{pmatrix} a \\ b \end{pmatrix} \\ &= ik \int_0^\infty J_0(kb \sin \theta) \Gamma_c(b) b db \begin{pmatrix} a \\ b \end{pmatrix} \end{aligned} \quad (108)$$

$$+ k \int_0^{\infty} J_0(kb \sin \theta) \Gamma_s(b) b db \begin{pmatrix} -b \\ a \end{pmatrix} \quad (109)$$

Now, using the relation between the scattering operator M and the scattering amplitudes, we obtain

$$f(\theta) = ik \int_0^{\infty} J_0(kb \sin \theta) \Gamma_c(b) b db \quad (110)$$

$$g(\theta) = -ik \int_0^{\infty} J_1(kb \sin \theta) \Gamma_s(b) b db \quad . \quad (111)$$

As Glauber points out in his 1959 lectures, the system of axes used earlier (\underline{k}_i parallel to \underline{z}) is not the best, since it

(i) treats \underline{k}_i and \underline{k}_f differently, therefore making the result not manifestly time reversible from the outset,

(ii) does not reduce to the Born approximation in the limit $e^{i\chi} \rightarrow 1 + i\chi$ and

(iii) does not lead to such a good approximation.

In his article Glauber considers these points with the following prescription.

Approximation (89) becomes exact in our \underline{z} parallel to $(\underline{k}_i + \underline{k}_f)$ system

$$\underline{q} \cdot \underline{r} = \underline{q} \cdot \underline{b} + \underline{q} \cdot \underline{z} = \underline{q} \cdot \underline{b} \quad . \quad (112)$$

Equation (92) is unfortunately no longer exact, but reference to (91) shows the difference is of order

$\int_{-\infty}^{\infty} V_S(x, y, z') z' dz' \quad ,$ which may be neglected either
 (i) since this ratio to the other term is $k a \theta^2 \ll 1$,

or (ii) since, if we assume an even parity potential along the z-axis, the integral vanishes.

Equation (98) is also no longer exact, but the correction term encountered by not making the approximation is of order $z d \theta^2$ relative to the remaining term, so we may neglect it to a good approximation.

Each coordinate system has its limitations. In the first we have to make the approximation $\underline{q} \cdot \underline{r} = \underline{q} \cdot \underline{b}$ which requires $k d \theta^2 \ll 1$. In the second we have to make $\underline{b} \times \underline{k}_i = b \underline{k}_i$ which requires $k d \theta^2 \ll 16$; and $\underline{r} \times \underline{k}_i = \underline{b} \times \underline{k}_i$ requiring $k d \theta^2 \ll 1$ only for even parity potentials. Since most potentials encountered are of even parity, then the second coordinate system appears to have the least restrictive approximations. (Both of course have the linearised Green function.)

Glauber points out the first improvement, which is that for equation (89) $\underline{q} \cdot \underline{r} = \underline{q} \cdot \underline{b}$ exactly in this coordinate system, and then appears to say, since

$$\underline{b} = \underline{x} \cos \phi + \underline{y} \sin \phi , \quad (113a)$$

$$\underline{k}_i = \underline{z} \cos \theta/2 - \underline{x} \sin \theta/2 , \quad (113b)$$

$$\underline{k}_f = \underline{z} \cos \theta/2 + \underline{x} \sin \theta/2 , \quad (113c)$$

$$\underline{q} \cdot \underline{b} = -2kb \sin \theta/2 \cos \phi . \quad (114)$$

This will make a difference only of replacing $\sin \theta$ by $2 \sin \theta/2$ in the arguments of the Bessel functions, yielding

$$f(\theta) = ik \int_0^\infty J_0(kb \sin \theta/2) \Gamma_c(b) b db \quad (115)$$

$$g(\theta) = -ik \int_0^{\infty} J_1(2kbs \sin \theta/2) \Gamma_s(b) b db . \quad (116)$$

This is adequate and it is true that the approximation so obtained is a better one than before, but inherent in the prescription is a small flaw.

If one were to start out in the \underline{z} parallel to $(\underline{k}_i + \underline{k}_f)$ system, then one should stay in it throughout the calculation. After modifying equations (104) and (105) with the prescription, Glauber seems to quietly slip back to the old coordinate system to obtain (115) and (116). It seems that to just change coordinate systems at any stage one merely makes the approximation $k d \theta^2 \ll 1$, which is satisfactory within the formalism, but in the above case there is no need for it. If one sticks rigorously to the second coordinate system, then (104) gives (115) in a straightforward manner, however the expression for $g(\theta)$ is modified. Consider the second term in (105)

$$-k \int_0^{\infty} \Gamma_s(b) b db \frac{1}{2\pi} \int (\underline{\sigma} \cdot \underline{\hat{b}} \times \underline{\hat{k}}_i) e^{-i(2kbs \sin \theta/2) \cos \phi} d\phi \begin{pmatrix} a \\ b \end{pmatrix} . \quad (117)$$

Equations (113) and (114) yield

$$\underline{\hat{b}} \times \underline{\hat{k}}_i = \sin \phi \cos \theta/2 \underline{\hat{x}} - \cos \phi \cos \theta/2 \underline{\hat{y}} + \sin \phi \sin \theta/2 \underline{\hat{z}} \quad (118)$$

Equation (107c) shows the $\underline{\hat{x}}$ and $\underline{\hat{z}}$ terms do not contribute (conservation of parity) and we obtain from the \underline{y} term

$$+ k \int_0^{\infty} \Gamma_s(b) b db \frac{1}{2\pi} \int \cos \theta/2 \cos \phi e^{-i(2kbs \sin \theta/2) \cos \phi} d\phi \sigma_y \begin{pmatrix} a \\ b \end{pmatrix} \quad (119)$$

which is as before, except for the presence of the extra factor $\cos \theta/2$. The scattering amplitudes resulting are

$$f(\theta) = ik \int_0^{\infty} J_0(2kb \sin \theta/2) \Gamma_c(b) b db \quad \text{and} \quad (120)$$

$$g(\theta) = -ik \cos \theta/2 \int_0^{\infty} J_1(2kb \sin \theta/2) \Gamma_s(b) b db \quad . \quad (121)$$

One may argue that the presence of the $\cos \theta/2$ is splitting hairs, since we have already assumed small angle scattering and this may be true. Nevertheless there are reasons for keeping it, namely

(i) it follows from the mathematics by starting with the second Green function and sticking to one coordinate system,

(ii) it is a simple modification which does not lead to any further difficulty in the calculations,

(iii) it is necessary to make the spin-flip amplitude reduce to that of the Born approximation as $e^{i\chi(b)} \rightarrow 1 + i\chi(b)$ exactly. Without the additional factor this is true only for small angles.

(iv) it ensures that the polarisation vanishes at 180° , even though one does not intend to press the validity of the approximation that far.

THE EXACT CALCULATION

This is essentially a phase-shift calculation. The wavefunction is expanded in partial waves and the contributions from each partial wave to each scattering amplitude are summed. This method of obtaining the scattering amplitudes is described rather well in (RO67), a summary of which is given here. The exact results for the observables are required, of course, to test the approximation.

We have to solve the Schroedinger equation

$$(p^2/2m + V_c(r) + V_{s.o.}(r) \underline{L} \cdot \underline{S})\Psi = E\Psi, \quad (122)$$

$$\text{where } \Psi = \begin{pmatrix} \gamma_1(\underline{r}) \\ \gamma_2(\underline{r}) \end{pmatrix} \quad (123)$$

The eigenfunctions will be in the "j" representation since the Hamiltonian contains a term coupling space and spin coordinates. The angular and spin parts of the eigenfunctions are the generalised spherical harmonics, defined as

$$Y_{l s j}^m(\theta, \phi) = \sum_{m_l m_s} (l m_l s m_s | j m) Y_{l m_l}(\theta, \phi) \chi_{\frac{1}{2} m_s}, \quad (124)$$

$$\text{where } \chi_{\frac{1}{2} \frac{1}{2}} = \begin{pmatrix} 1 \\ 0 \end{pmatrix} \text{ and } \chi_{\frac{1}{2} -\frac{1}{2}} = \begin{pmatrix} 0 \\ 1 \end{pmatrix}. \quad (125)$$

The boundary conditions require the wavefunction to be asymptotically a linear superposition of a plane wave and an outgoing spherical wave.

Using the plane wave expansion

$$e^{i\mathbf{k}\cdot\mathbf{r}} = \sum_{\ell=0}^{\infty} i^{\ell} (4\pi(2\ell+1))^{\frac{1}{2}} j_{\ell}(kr) Y_{\ell 0}(\theta, \phi) \quad (126)$$

and Clebsch-Gordan coupling coefficient obtained from (DE74)

we may write

$$e^{i\mathbf{k}\cdot\mathbf{r}} \begin{pmatrix} 1 \\ 0 \end{pmatrix} = \sum_{\ell=0}^{\infty} i^{\ell} (4\pi)^{\frac{1}{2}} j_{\ell}(kr) \left\{ (\ell+1)^{\frac{1}{2}} y_{\ell\frac{1}{2}}^{\frac{1}{2}}(\ell+\frac{1}{2})(\theta, \phi) + \ell^{\frac{1}{2}} y_{\ell\frac{1}{2}}^{\frac{1}{2}}(\ell-\frac{1}{2})(\theta, \phi) \right\} \quad (127)$$

which helps in the description of the boundary conditions later.

Going back to equation (122) and writing

$$\Psi_{\ell j m}(\mathbf{r}) = \frac{1}{r} R_{\ell j}(r) \mathcal{Y}_{\ell\frac{1}{2}j}^m(\theta, \phi) \quad , \quad \text{we obtain} \quad (128)$$

$$\left[\frac{p^2}{2m} + V_c(r) + V_{s.o.}(r) \frac{\mathbf{L}\cdot\mathbf{S}}{r} - \frac{R_{\ell j}(r)}{r} \right] \mathcal{Y}_{\ell\frac{1}{2}j}^m(\theta, \phi) = E \frac{R_{\ell j}(r)}{r} \mathcal{Y}_{\ell\frac{1}{2}j}^m(\theta, \phi) \quad (129)$$

$$\text{writing } p^2 = p_r^2 + \frac{L^2}{r^2} \quad \text{and} \quad (130)$$

noting that the generalised spherical harmonics are eigenfunctions of L^2 , S^2 and J^2 , we obtain

$$\left\{ \frac{p_r^2}{2m} + V_c(r) + \frac{\hbar^2(\ell(\ell+1))}{2mr^2} + \frac{V_{s.o.}(r)}{2} (j(j+1) - \ell(\ell+1) - 3/4) - E \right\} \frac{R_{\ell j}(r)}{r} = 0 \quad ,$$

which we can write as

$$\begin{aligned}
 -\frac{\hbar^2}{2m} \frac{d^2 R_{\ell j}(r)}{dr^2} + \left[V_c(r) + \frac{\hbar^2 \ell(\ell+1)}{2mr^2} + \right. \\
 \left. \frac{V_{s.o.}(r)}{2} (j(j+1) - \ell(\ell+1) - 3/4) - E \right] R_{\ell j}(r) = 0 \quad .
 \end{aligned} \quad (132)$$

We consider the two cases of $j = \ell \pm \frac{1}{2}$.

$$\begin{aligned}
 -\frac{\hbar^2}{2m} \frac{d^2}{dr^2} R_{\ell(\ell+\frac{1}{2})}(r) + \\
 \left(V_c(r) + \frac{\hbar^2 \ell(\ell+1)}{2mr^2} + \frac{1}{2} V_{s.o.}(r) - E \right) R_{\ell(\ell+\frac{1}{2})}(r) = 0
 \end{aligned} \quad (133)$$

$$\begin{aligned}
 -\frac{\hbar^2}{2m} \frac{d^2}{dr^2} R_{\ell(\ell-\frac{1}{2})}(r) + \\
 \left(V_c(r) + \frac{\hbar^2 \ell(\ell+1)}{2mr^2} - \frac{(\ell+1)}{2} V_{s.o.}(r) - E \right) R_{\ell(\ell-\frac{1}{2})}(r) = 0
 \end{aligned} \quad (134)$$

Clearly demonstrated here is the difference to potential made by the spin-orbit potential for aligned and unaligned spins.

These two equations may be integrated using the Numerov (SH68) method and we may write

$$\begin{aligned}
 \Psi(r) = \sum_{\ell=0}^{\infty} i^{\ell} (4\pi)^{\frac{1}{2}} \left(\frac{R_{\ell(\ell+\frac{1}{2})}(r)}{kr} Y_{\ell\frac{1}{2}(\ell+\frac{1}{2})}(\theta, \phi) (\ell+1)^{\frac{1}{2}} + \right. \\
 \left. \frac{R_{\ell(\ell-\frac{1}{2})}(r)}{kr} Y_{\ell\frac{1}{2}(\ell-\frac{1}{2})}(\theta, \phi) \ell^{\frac{1}{2}} \right) .
 \end{aligned} \quad (135)$$

The asymptotic solutions of the radial equation where the

potentials have vanished are the solutions of

$$\frac{d^2 R_{\ell j}}{dr^2} - \left(\frac{\ell(\ell+1)}{r^2} - k^2 \right) R_{\ell j} = 0 \quad (136)$$

which are the spherical Bessel and Neumann functions

$$kr j_{\ell}(kr) , \text{ and } kr n_{\ell}(kr) . \quad (137)$$

These functions have sinusoidal asymptotic forms.

Taking the general solutions to be linear combinations, we get

$$e^{i\delta_{\ell}^{\pm}} \sin \left(kr - \frac{1}{2} + \delta_{\ell}^{\pm} \right) \quad \pm \text{ refers to } j = \ell \pm \frac{1}{2} \quad (138)$$

δ_{ℓ}^{\pm} are called the phase-shifts.

The above expression is the same as for the incident plane wave expression, but for the presence of the phase-shifts δ_{ℓ}^{\pm} .

Using these solutions as the asymptotic solution to the Schrodinger equation we get

$$\begin{aligned} \Psi(r) \xrightarrow{r \rightarrow \infty} & \sqrt{4\pi} \sum_{\ell=0}^{\infty} i^{\ell} \frac{\sin \left(kr - \frac{\ell\pi}{2} \right)}{kr} \\ & \left\{ (\ell+1)^{\frac{1}{2}} y_{\ell+\frac{1}{2}}^m(\ell+\frac{1}{2})(\theta, \phi) + i^{\frac{1}{2}} y_{\ell-\frac{1}{2}}^m(\ell-\frac{1}{2})(\theta, \phi) \right\} + \\ & \sqrt{4\pi} \frac{e^{ikr}}{kr} \sum_{\ell=0}^{\infty} \left\{ (\ell+1)^{\frac{1}{2}} e^{i\delta_{\ell}^{+}} \sin \delta_{\ell}^{+} y_{\ell+\frac{1}{2}}^m(\ell+\frac{1}{2})(\theta, \phi) + \right. \\ & \left. e^{\frac{1}{2}} e^{i\delta_{\ell}^{-}} \sin \delta_{\ell}^{-} y_{\ell-\frac{1}{2}}^m(\ell-\frac{1}{2})(\theta, \phi) \right\} . \end{aligned} \quad (139)$$

Compare equation (128)

$$e^{i\mathbf{k} \cdot \mathbf{r}} \begin{pmatrix} 1 \\ 0 \end{pmatrix} \xrightarrow{r \rightarrow \infty} \sqrt{4\pi} \sum_{\ell=0}^{\infty} \frac{i^{\ell} \sin(kr - \frac{\ell\pi}{2})}{kr} \left\{ (\ell+1)^{\frac{1}{2}} Y_{\ell\frac{1}{2}}^{\frac{1}{2}}(\ell+\frac{1}{2})(\theta, \phi) + \ell^{\frac{1}{2}} Y_{\ell\frac{1}{2}}^{\frac{1}{2}}(\ell-\frac{1}{2})(\theta, \phi) \right\} \quad (140)$$

with the first term in (139). We have therefore

$$\Psi(\mathbf{r}) \xrightarrow{r \rightarrow \infty} e^{i\mathbf{k} \cdot \mathbf{r}} \begin{pmatrix} 1 \\ 0 \end{pmatrix} + \frac{e^{ikr}}{r} \left\{ \frac{\sqrt{4\pi}}{k} \sum_{\ell=0}^{\infty} (\ell+1)^{\frac{1}{2}} e^{i\delta_{\ell}^{+}} \sin \delta_{\ell}^{+} Y_{\ell\frac{1}{2}}^{\frac{1}{2}}(\ell+\frac{1}{2})(\theta, \phi) + \ell^{\frac{1}{2}} e^{i\delta_{\ell}^{-}} \sin \delta_{\ell}^{-} Y_{\ell\frac{1}{2}}^{\frac{1}{2}}(\ell-\frac{1}{2})(\theta, \phi) \right\}. \quad (141)$$

We may identify the scattering operator in here. Converting to the ℓ -s basis, we have

$$M \begin{pmatrix} 1 \\ 0 \end{pmatrix} = \left(\frac{\sqrt{4\pi}}{k} \sum_{\ell=0}^{\infty} \frac{1}{\sqrt{2\ell+1}} \left[(\ell+1) e^{i\delta_{\ell}^{+}} \sin \delta_{\ell}^{+} + e^{i\delta_{\ell}^{-}} \sin \delta_{\ell}^{-} \right] Y_{\ell 0}(\theta, \phi) \right) \begin{pmatrix} 1 \\ 0 \end{pmatrix} \quad (142)$$

$$+ \left(\frac{\sqrt{4\pi}}{2ik} \sum_{\ell=0}^{\infty} \left(\frac{\ell(\ell+1)}{2\ell+1} \right)^{\frac{1}{2}} \left[e^{2i\delta_{\ell}^{+}} - e^{2i\delta_{\ell}^{-}} \right] Y_{\ell 1}(\theta, \phi) \right) \begin{pmatrix} 0 \\ 1 \end{pmatrix}$$

We may derive a similar expression for the spinor $M \begin{pmatrix} 0 \\ 1 \end{pmatrix}$ in exactly the same way. Let the scattering take place in the $x - z$ plane ($\phi = 0$). We may now write

$$M = f(\theta) + \underline{\sigma} \cdot \underline{n} g(\theta) = \begin{pmatrix} f(\theta) & -ig(\theta) \\ ig(\theta) & f(\theta) \end{pmatrix}. \quad (143)$$

Obtaining finally

$$f(\theta) = -\frac{1}{k} \sum_{\ell=0}^{\infty} \left((\ell+1) e^{i\delta_{\ell}^{+}} \sin \delta_{\ell}^{+} + \ell e^{i\delta_{\ell}^{-}} \sin \delta_{\ell}^{-} \right) P_{\ell}(\cos \theta) \quad (144)$$

$$g(\theta) = \frac{1}{2k} \sum_{\ell=0}^{\infty} \left(e^{2i\delta_{\ell}^{+}} - e^{2i\delta_{\ell}^{-}} \right) P_{\ell}^1(\cos \theta) \quad . \quad (145)$$

The phase shifts may be found by matching the logarithmic derivatives of the numerically integrated radial wavefunctions to the logarithmic derivatives of the free particle wavefunctions at a sufficient distance from the scattering centre that the potentials have effectively vanished.

CHAPTER III
ELASTIC SCATTERING FROM
A GAUSSIAN POTENTIAL

In this chapter the expressions for the scattering amplitudes derived in Chapter II are evaluated for a Gaussian potential of the form

$$V(r) = (v_0 + iw_0)e^{-\alpha r^2} + (v_{s.o.} + iw_{s.o.})e^{-\alpha r^2} \underline{\sigma} \cdot \underline{L} \quad . \quad (146)$$

This form of the potential is used since it leads to a convenient expression for numerical calculation of scattering amplitudes, a series in fact which converges reasonably quickly.

The spin-orbit potential is chosen so as to have the same decay constant as the central potential. This is restrictive when it comes to fitting experimental data, but it is used since it is in line with the philosophy of the analytic form of the spin-orbit potential being $1/r \, d/dr$ of the central potential -- it also makes the calculations much easier! The spin-orbit potential has also been taken as complex since the optical model analyses have shown that this is the case for energies higher than 100 Mev.

This potential in the Glauber approximation has been studied by Wallace (WA70), and his results have been reproduced. Wallace, however, considered neither the spin-orbit term nor complex potentials

Also included in this chapter is the result for a modified Gaussian potential

$$\begin{aligned}
 V(r) = & (v_o + iw_o) (1 + \rho r^2) e^{-\alpha r^2} \\
 & + (v_{s.o.} + iw_{s.o.}) (1 + \rho r^2) e^{-\alpha r^2} \underline{\sigma} \cdot \underline{L} .
 \end{aligned}
 \tag{147}$$

The validity of the Glauber approximation as applied to just the central part of this potential has been reproduced numerically for the Glauber calculations. Included also in this chapter are the corresponding results for the scattering amplitudes evaluated in the Born approximation. The correspondence Glauber \longrightarrow Born as $e^{i\chi} \longrightarrow 1 + i\chi$ is noted.

GLAUBER AMPLITUDE FOR A GAUSSIAN POTENTIAL

We must first obtain expressions for the eikonal phases. The equations (93a) and (93b) give

$$\chi_c(b) = - \frac{1}{\hbar v} \int_{-\infty}^{\infty} V_c(\underline{b} + \underline{\hat{z}}z) dz \tag{148}$$

$$= - \frac{1}{\hbar v} \int_{-\infty}^{\infty} (v_o + iw_o) e^{-\alpha(b^2+z^2)} dz \tag{149}$$

$$= - \frac{(v_o + iw_o)}{\hbar v} \sqrt{\pi} e^{-\alpha b^2} . \tag{150}$$

Similarly

$$\chi_s(b) = - \frac{1}{\hbar v} \int_{-\infty}^{\infty} V_s(\underline{b} + \underline{\hat{z}}z) dz \tag{151}$$

$$= - \frac{(v_{s.o.} + iw_{s.o.})}{\hbar v} \sqrt{\pi} e^{-\alpha b^2} . \tag{152}$$

Equations (102) and (103) now read

$$\Gamma_c(b) = 1 - e^{-i\sqrt{\frac{\pi}{\alpha}} \frac{1}{\hbar v} (v_o + iw_o) e^{-\alpha b^2}} \cos \left(\frac{kb}{\hbar v} \sqrt{\frac{\pi}{\alpha}} (v_{s.o.} + iw_{s.o.}) e^{-\alpha b^2} \right) \quad (153)$$

$$\Gamma_s(b) = -e^{-i\sqrt{\frac{\pi}{\alpha}} \frac{1}{\hbar v} (v_{s.o.} + iw_{s.o.}) e^{-\alpha b^2}} \sin \left(-\frac{kb}{\hbar v} \sqrt{\frac{\pi}{\alpha}} (v_{s.o.} + iw_{s.o.}) e^{-\alpha b^2} \right) . \quad (154)$$

Introduce two constants

$$A_c \equiv -i\sqrt{\frac{\pi}{\alpha}} \frac{(v_o + iw_o)}{\hbar v} \quad (155a)$$

$$A_s \equiv -\frac{k}{\hbar v} \sqrt{\frac{\pi}{\alpha}} (v_{s.o.} + iw_{s.o.}) \quad (155b)$$

$$\Gamma_c(b) = 1 - e^{A_c e^{-\alpha b^2}} \cos (bA_s e^{-\alpha b^2}) \quad (156a)$$

$$\Gamma_s(b) = -e^{A_c e^{-\alpha b^2}} \sin (bA_s e^{-\alpha b^2}) \quad (156b)$$

For the non-spin-flip part of the scattering operator equation (120) gives

$$f(\theta) = ik \int_0^\infty J_0(qb) \Gamma_c(b) b db \quad (157)$$

$$= ik \int_0^\infty J_0(qb) \left(1 - \frac{1}{2} e^{A_c e^{-\alpha b^2}} (e^{ibA_s e^{-\alpha b^2}} + e^{-ibA_s e^{-\alpha b^2}}) \right) b db \quad (158)$$

$$= f(\theta, A_s) + f(\theta, -A_s) \quad (159)$$

where

$$f(\theta, A_s) = \frac{ik}{2} \int_0^\infty J_0(qb) \left(1 - e^{(A_c + ibA_s)} e^{-\alpha b^2} \right) b \, db \quad (160)$$

The integral involved cannot be evaluated analytically, we therefore expand the exponential

$$f(\theta, A_s) = - \frac{ik}{2} \int_0^\infty J_0(qb) \left(\sum_{r=1}^{\infty} \frac{(A_c + ibA_s)^r}{r!} e^{-\alpha r b^2} \right) b \, db \quad (161)$$

Using uniform convergence we may integrate term by term to obtain

$$f(\theta, A_s) = - \frac{ik}{2} \sum_{r=1}^{\infty} \int_0^\infty J_0(qb) \frac{(A_c + ibA_s)^r}{r!} e^{-\alpha r b^2} b \, db \quad (162)$$

This integral has no simple analytic expression, and so we must expand further, using the binomial theorem:

$$f(\theta, A_s) = - \frac{ik}{2} \sum_{r=1}^{\infty} \frac{J_0(qb)}{r!} \sum_{t=0}^r \binom{r}{t} A_c^{r-t} (ibA_s)^t e^{-\alpha r b^2} b \, db \quad (163)$$

where the symbol $\binom{r}{t}$ is the binomial coefficient

$$\frac{r!}{t!(r-t)!} \quad (164)$$

$$f(\theta, A_s) = - \frac{ik}{2} \sum_{r=1}^{\infty} \sum_{t=0}^r \binom{r}{t} \frac{1}{r!} A_c^{r-t} (ibA_s)^t \int_0^\infty J_0(qb) b^{t+1} e^{-\alpha r b^2} db \quad (165)$$

We may write

$$f(\theta) = -\frac{ik}{2} \sum_{r=1}^{\infty} \sum_{t=0}^r \frac{(A_c)^{r-t}}{t!(r-t)!} (iA_s)^t (1+(-1)^t) \int_0^{\infty} J_0(qb) b^{t+1} e^{-\alpha r b^2} db. \quad (166)$$

Since only even values of t contribute to the sum, we may define a new variable

$$t = 2t' \quad (167)$$

which runs from zero to $[r/2]$.

Therefore

$$f(\theta) = -ik \sum_{r=1}^{\infty} \sum_{t'=r(2t')!}^{[r/2]} \frac{(A_c)^{r-2t'} (iA_s)^{2t'}}{(2t')!(r-2t')!} \int_0^{\infty} J_0(qb) b^{2t'+1} e^{-\alpha r b^2} db. \quad (168)$$

This integral may be evaluated analytically (WH68), the general expression is

$$\int_0^{\infty} J_v(qx) x^{u-1} e^{-a^2 x^2} dx = \frac{q^v \Gamma\left(\frac{u+v}{2}\right) e^{-q^2/4a^2}}{2^{u+1} a^{u+v} \Gamma(v+1)} {}_1F_1\left(\frac{v-u}{2} + 1; v+1; q^2/4a^2\right) \quad (169)$$

where ${}_1F_1$ is the confluent hypergeometric function.

$$f(\theta) = -\frac{ik}{2} \sum_{r=1}^{\infty} \sum_{t'=0}^{[r/2]} \frac{(A_c)^{r-2t'} (iA_s)^{2t'}}{(2t')!(r-2t')! (\alpha r)^{t'+1}} \quad (170)$$

$$\frac{2t+2}{2} e^{-q^2/4\alpha r} {}_1F_1\left(1 - \frac{2t+2}{2}; 1; q^2/4\alpha r\right).$$

The confluent hypergeometric function may be expressed as
(AB64)

$${}_1F_1(-t; 1; q^2/4\alpha r) = L_t(q^2/4\alpha r) \quad (171)$$

where $L_n(x)$ is the n 'th Laguerre polynomial.

We arrive then at the result

$$f(\theta) = - \frac{ik}{2} \sum_{r=1}^{\infty} \sum_{t=0}^{[r/2]} \frac{(A_c)^{r-2t} (iA_s)^{2t} t! e^{-q^2/4\alpha r} L_t(q^2/4\alpha r)}{(2t)!(r-2t)!(\alpha r)^{t+1}} \quad (172)$$

The convergence of this series is best seen by taking the absolute convergence. The magnitude of the r 'th term is bounded above by

$$\frac{\left\{ |A_c| \left(1 + \frac{k(v_{s.o.} + iw_{s.o.})}{\sqrt{\alpha}(v_o + iw_o)} \right) \right\}^r}{r!} \quad (173)$$

which means the series is convergent providing α or

$v_o + iw_o$ do not vanish, and we must have the inequality

$$|f(\theta)| \leq \frac{k}{2} \exp \left\{ |A_c| \left(1 + \frac{k(v_{s.o.} + iw_{s.o.})}{\sqrt{\alpha}(v_o + iw_o)} \right) \right\} . \quad (174)$$

The same procedure may be followed for the spin-flip part of the scattering operator. Equation (121) gives

$$g(\theta) = -ik \int_0^{\infty} J_1(qb) \Gamma_s(b) b db . \quad (175)$$

using (156)

$$g(\theta) = ik \int_0^{\infty} J_1(qb) e^{A_c e^{-\alpha b^2}} \sin(b A_s e^{-\alpha b^2}) b db \quad (176)$$

$$= g(\theta, A_s) - g(\theta, -A_s) \quad (177)$$

$$g(\theta, A_s) = \frac{k}{2} \int_0^{\infty} J_1(qb) e^{A_c e^{-\alpha b^2}} e^{ib A_s e^{-\alpha b^2}} b db \quad (178)$$

$$= \frac{k}{2} \int_0^{\infty} J_1(qb) e^{(A_c + ib A_s) e^{-\alpha b^2}} b db \quad (179)$$

$$= \frac{k}{2} \sum_{r=0}^{\infty} \frac{1}{r!} \int_0^{\infty} J_1(qb) (A_c + ib A_s)^r e^{-\alpha r b^2} b db \quad (180)$$

$$= \frac{k}{2} \sum_{r=0}^{\infty} \frac{1}{r!} \int_0^{\infty} \sum_{t=0}^r \binom{r}{t} (A_c)^{r-t} (ib A_s)^t J_1(qb) e^{-\alpha r b^2} b db \quad (181)$$

Therefore

$$g(\theta) = \frac{k}{2} \sum_{r=0}^{\infty} \sum_{t=r}^{\infty} \binom{r}{t} \frac{1}{r!} (A_c)^{r-t} (i A_s)^t (1 - (-1)^t) \int_0^{\infty} J_1(qb) e^{-\alpha r b^2} b^{t+1} db \quad (182)$$

Only odd values of t now contribute to the sum so we define

$$\text{a new variable } t' = 2t + 1 \quad (183)$$

which runs from zero to $[(r-1)/2]$.

$$g(\theta) = k \sum_{r=0}^{\infty} \sum_{t'=0}^{[(r-1)/2]} \frac{(A_c)^{r-2t'-1} (i A_s)^{2t'+1}}{(2t'+1)!(r-2t'-1)!} \int_0^{\infty} J_1(qb) e^{-\alpha r b^2} b^{2t'+2} db \quad (184)$$

Using (166) and the result (AB64)

$${}_1F_1(-t; 2; q^2/4\alpha r) = \frac{L_t^1(q^2/4\alpha r)}{(t+1)} \quad (185)$$

(where $L_n^1(x)$ is an associated Laguerre polynomial) we obtain

$$g(\theta) = \frac{kq}{4} \sum_{r=1}^{\infty} \sum_{t=0}^{\left[\frac{r-1}{2}\right]} \frac{(A_c)^{r-2t-1} (iA_s)^{2t+1} t! e^{-q^2/4\alpha r} L_t^1(q^2/4\alpha r)}{(2t+1)!(r-2t-1)!(\alpha r)^{t+2}} \quad (186)$$

GLAUBER AMPLITUDES FOR A MODIFIED GAUSSIAN POTENTIAL

If instead of a Gaussian potential a modified Gaussian potential had been used,

$$V(r) = (v_0 + iw_0)e^{-\alpha r^2} (1 + \rho r^2) + (v_{s.o.} + iw_{s.o.})(1 + \rho r^2)e^{-\alpha r^2} \quad (187)$$

the calculation would have proceeded in a similar manner to arrive at the results

$$f(\theta) = -\frac{ik}{2} \sum_{r=1}^{\infty} \sum_{t=0}^{\left[\frac{r}{2}\right]} \frac{(A_c)^r \left(\frac{iA_s}{A_c}\right)^{2t} e^{-q^2/4\alpha r} t!}{(2t)!(r-2t)!(\alpha r)^{t+1}} \quad (188)$$

$$\sum_{s=0}^r \frac{r! \lambda^{r-s} \rho^s (t+s)! L_{(t+s)}(q^2/4\alpha r)}{s!(r-s)!(\alpha r)^s t!}$$

where $\lambda \equiv \frac{\rho}{2\alpha} + 1$.

$$g(\theta) = \frac{kq}{4} \sum_{r=1}^{\infty} \sum_{t=0}^{\left[\frac{r-1}{2}\right]} \frac{(A_c)^r \left(\frac{iA_s}{A_c}\right)^{2t+1} t! e^{-q^2/4\alpha r}}{(2t+1)!(r-2t-1)!(\alpha r)^{t+2}} \quad (189)$$

$$\left(r! \lambda^r \sum_{s=0}^r \frac{(s+t)! L_{(s+t)}^1(q^2/4\alpha r) (\rho/\lambda)^s}{s!(r-s)!(\alpha r)^s (t)!} \right)$$

If we let $\rho \rightarrow 0$, only the $s=0$ term contributes

$$f(\theta) \xrightarrow{\rho \rightarrow 0} -\frac{ik}{2} \sum_{r=1}^{\infty} \sum_{t=0}^{\left[\frac{r}{2}\right]} \frac{(A_c)^r \left(\frac{iA_s}{A_c}\right)^{2t} e^{-q^2/4\alpha r} t! L_t(q^2/4\alpha r)}{(2t)!(r-2t)!(\alpha r)^{t+1}} \quad (190)$$

$$g(\theta) \xrightarrow{\rho \rightarrow 0} \frac{kq}{4} \sum_{r=1}^{\infty} \sum_{t=0}^{\left[\frac{r-1}{2}\right]} \frac{(A_c)^r \left(\frac{iA_s}{A_c}\right)^{2t+1} t! e^{-q^2/4\alpha r} L_t^1(q^2/4\alpha r)}{(2t+1)!(r-2t-1)!(\alpha r)^{t+2}} \quad (191)$$

which are just the results obtained previously.

If we use the Born approximation to calculate the scattering amplitudes for a modified Gaussian potential, we obtain the results

$$f_B(\theta) = -\frac{m(v_o + iw_o)}{2\alpha\hbar^2} \sqrt{\frac{\pi}{\alpha}} e^{-q^2/4\alpha r} \left(1 + \frac{\rho}{2\alpha} \left(3 - \frac{q^2}{2\alpha} \right) \right) \quad (192)$$

$$g_B(\theta) = -\frac{im k^2 \sin \theta (v_{s.o.} + iw_{s.o.})}{4\alpha^2 \hbar^2} \sqrt{\frac{\pi}{\alpha}} e^{-q^2/4\alpha r} \left(1 + \frac{\rho}{2\alpha} \left(5 - \frac{q^2}{2\alpha} \right) \right) \quad (193)$$

If we take just the $r=1$ terms in (188) and (189) we get (using the definitions of A_c and A_s)

$$f(\theta)_{r=1} = -\frac{m(v_o + iw_o)}{2\alpha\hbar^2} \sqrt{\frac{\pi}{\alpha}} e^{-q^2/4\alpha} \left(1 + \frac{\rho}{2\alpha} \left(3 - \frac{q^2}{2\alpha} \right) \right) \quad (194)$$

$$g(\theta)_{r=1} = -\frac{im k^2 \sin \theta/2 (v_{s.o.} + iw_{s.o.})}{2\alpha^2 \hbar^2} \sqrt{\frac{\pi}{\alpha}} e^{-q^2/4\alpha} \left(1 + \frac{\rho}{2\alpha} \left(5 - \frac{q^2}{2\alpha} \right) \right) \quad (195)$$

which agree with the Born results, except for a factor of

$\cos \theta/2$ missing from the ' $g(\theta)$ ' term of equation (196).

The argument for the presence of the $\cos \theta/2$ factor multiplying the $g(\theta)$ term gains weight here since then the first term in the Born series is reproduced exactly.

Considering the unmodified Gaussian potential, the Born results are

$$f_B(\theta) = - \frac{m(v_o + iw_o)}{2\alpha\hbar^2} \sqrt{\frac{\pi}{\alpha}} e^{-q^2/4\alpha} \quad (196)$$

$$g_B(\theta) = - \frac{imk^2 \sin \theta (v_{s.o.} + iw_{s.o.})}{4\alpha^2 \hbar^2} \sqrt{\frac{\pi}{\alpha}} e^{-q^2/4\alpha} \quad (197)$$

(as in (192) and (193) with $\rho = 0$).

Equations (172) and (186) with just the $r=1$ term yield as expected the expressions for the left hand side

$$- \frac{m(v_o + iw_o)}{2\alpha\hbar^2} \sqrt{\frac{\pi}{\alpha}} e^{-q^2/4\alpha} \quad \text{and} \quad (198)$$

$$- \frac{imk^2 \sin \theta/2}{2\alpha^2 \hbar^2} (v_{s.o.} + iw_{s.o.}) \sqrt{\frac{\pi}{\alpha}} e^{-q^2/4\alpha} \quad (199)$$

Which again agree with the Born approximation except for the $\cos \theta/2$ factor in the ' $g(\theta)$ ' term.

OBSERVABLES

Whereas from our calculations we obtain amplitudes f and g , experimentally we cannot measure these. Instead, using an initially unpolarised beam, all that we can measure from a

single scattering experiment is the differential cross-section. With an initially polarised beam we may determine the polarisation from a single scattering experiment and the polarisation transfer coefficients may be determined from a double scattering experiment.

If the Glauber approximation were to have the effect of altering the amplitudes by an overall phase factor, then the observables would not be affected. We therefore study the observables to determine the region of validity of the approximation.

Differential Cross-Section

This is defined as the number of particles scattered into a given unit angle per unit time for a unit incident flux.

The wavefunction describing the system for large r is

$$= e^{i\mathbf{k}_i \cdot \mathbf{r}} \begin{pmatrix} a \\ b \end{pmatrix} + \frac{e^{ikr}}{r} M \begin{pmatrix} a \\ b \end{pmatrix} \quad (200)$$

The flux vector is given by

$$\mathbf{j} = \frac{\hbar}{2im} \left[\psi^\dagger \nabla \psi - (\nabla \psi^\dagger) \psi \right] \quad (201)$$

which, upon keeping terms of order $1/r^2$, discarding non-radial flux and using the Riemann-Lebesgue lemma

$$\lim_{r \rightarrow \infty} \int_{\Delta\Omega} e^{ikr} e^{-i\mathbf{k} \cdot \mathbf{r}} d\Omega = 0 \quad (202)$$

gives

$$\underline{j} = \frac{\hbar k}{m} \left[\underline{\hat{k}}_i + (a, b) M^\dagger M \begin{pmatrix} a \\ b \end{pmatrix} \frac{\hat{r}}{r^2} \right] \quad (203)$$

The first term corresponds to the number of incident particles per unit area, the second to the number of scattered particles per unit solid angle.

Thus, by definition, the differential cross-section is given by

$$\frac{d\sigma}{d\Omega} = (a, b) M^\dagger M \begin{pmatrix} a \\ b \end{pmatrix} = |f(\theta)|^2 + |g(\theta)|^2. \quad (204)$$

This can be seen to be the "normalisation" for the scattering operator M in that

$$|f(\theta)|^2 + |g(\theta)|^2 = \frac{1}{2} \text{tr} (M^\dagger M). \quad (205)$$

Polarisation

The polarisation of a beam of particles is defined as the expectation value of the spin operator divided by the amplitude of the spin ($\frac{1}{2}$ in our case). Therefore

$$\underline{P} = 2 \langle \underline{S} \rangle = \langle \underline{\sigma} \rangle \quad (206)$$

$$= \frac{\text{tr} (M^\dagger \underline{\sigma} M)}{\text{tr} (M^\dagger M)} \quad (207)$$

We have from the above

$$\text{tr} (M^\dagger M) = 2(|f(\theta)|^2 + |g(\theta)|^2). \quad (208)$$

From the form of M we can see that it can be written as

$$M = f(\theta) I_2 + g(\theta) \sigma_y \quad (209)$$

where I_2 is the unit 2×2 matrix and σ_y is a Pauli matrix. Treating each component separately, we have

$$\text{tr} (M^\dagger \sigma_x M) = \text{tr} [f^*(\theta) + \sigma_y g^*(\theta)] \sigma_x [f(\theta) + \sigma_y g(\theta)] \quad (210)$$

$$= \text{tr} [\sigma_x |f(\theta)|^2 + if^*(\theta)g(\theta)\sigma_z - ig^*(\theta)f(\theta)\sigma_z - |g(\theta)|^2 \sigma_x] \quad (211)$$

= 0 since all the Pauli matrices are traceless.

$$\text{Similarly } \text{tr} (M^\dagger \sigma_z M) = 0 \quad (212)$$

and

$$\text{tr}(M^\dagger \sigma_y M) = \text{tr} [\sigma_y |f(\theta)|^2 + f^*(\theta)g(\theta)I_2 + g^*(\theta)f(\theta)I_2 + \sigma_y |g(\theta)|^2] \quad (213)$$

$$= 4 \text{Re}(f^*(\theta)g(\theta)) \quad (214)$$

So collecting terms we have

$$\underline{P} = \langle \underline{\sigma} \rangle = \frac{2 \text{Re}(f^*(\theta)g(\theta))}{|f(\theta)|^2 + |g(\theta)|^2} \hat{y} \quad (215)$$

\hat{y} is a unit vector in the y-direction, which is normal to the scattering plane.

Polarisation Transfer Coefficient

The polarisation transfer coefficients (P.T.C.'s) give a measure of how the polarisation state of the incident beam contributes to the polarisation state of the outgoing beam.

The underlying formalism of P.T.C.'s is described in (OH72) and (RO69). We will consider only the $K_x^{x'}$ coefficient, commonly called the first Wolfenstein parameter. The expression for this observable is

$$K_x^{x'} = \frac{\text{tr}(M \sigma_x M^\dagger \sigma_{x'})}{\text{tr}(M M^\dagger)} \quad (216)$$

The primed system is related to the unprimed system by rota-

tion of θ , the scattering angle, about the $y = y'$ axis.

Therefore

$$x' = x \cos \theta - z \sin \theta \quad (217a)$$

$$y' = y \quad (217b)$$

$$z' = z \cos \theta + x \sin \theta \quad (217c)$$

Therefore

$$\sigma_{x'} = \sigma_x \cos \theta - \sigma_z \sin \theta, \quad (218)$$

where the $\sigma_{x'}$ refers to that component of the particle-spin after scattering and σ_x refers to the component before scattering.

We have

$$\text{tr}(\mathbf{M}\mathbf{M}^\dagger) = 2(|f(\theta)|^2 + |g(\theta)|^2) \quad (219)$$

and

$$\text{tr}(\mathbf{M}\sigma_x\mathbf{M}^\dagger\sigma_{x'}) = \text{tr}(\mathbf{M}\sigma_x\mathbf{M}^\dagger(\sigma_x \cos \theta - \sigma_z \sin \theta)) \quad (220)$$

$$\begin{aligned} &= \text{tr}((f(\theta) + \sigma_y g(\theta))\sigma_x(f^*(\theta) + \sigma_y g^*(\theta))\sigma_x \cos \theta) \\ &- \text{tr}((f(\theta) + \sigma_y g(\theta))\sigma_x(f^*(\theta) + \sigma_y g^*(\theta))\sigma_z \sin \theta) \end{aligned} \quad (221)$$

$$\begin{aligned} &= 2(|f(\theta)|^2 - |g(\theta)|^2)\cos \theta \\ &- 2i(f(\theta)g^*(\theta) - f^*(\theta)g(\theta))\sin \theta \end{aligned} \quad (222)$$

Now we may write

$$i(f(\theta)g^*(\theta) - g(\theta)f^*(\theta)) = 2 \text{Im}(f^*(\theta)g(\theta)) \quad (223)$$

$$\text{so we have} \quad (224)$$

$$\text{tr}(\mathbf{M}\sigma_x\mathbf{M}^\dagger\sigma_{z'}) = 2\cos \theta(|f(\theta)|^2 - |g(\theta)|^2) - 4 \text{Im}(f^*(\theta)g(\theta))\sin \theta$$

and

$$K_x^{x'} = \cos \theta \left(\frac{|f(\theta)|^2 - |g(\theta)|^2}{|f(\theta)|^2 + |g(\theta)|^2} \right) - \frac{2 \operatorname{Im}(f^*(\theta)g(\theta)) \sin \theta}{|f(\theta)|^2 + |g(\theta)|^2} \quad (225)$$

CHAPTER IV

RESULTS

This chapter is mainly concerned with a comparison of the results obtained using the eikonal approximation with those obtained from an exact calculation. As mentioned in Chapter I, the energy region above 1 GeV has, for central potentials, been studied exhaustively, therefore this study is limited to the energy range from 0.1 GeV to 1.0 GeV. This so called "intermediate energy" range is witnessing a great deal of activity these days, and often the Glauber multiple scattering theory is used to describe the collisions.

We choose here to study the elastic scattering of a neutral particle from a complex central and spin-orbit modified Gaussian potential. Instead of picking arbitrary parameters for the study, parameters are chosen to reproduce as closely as possible the scattering of protons by actual nuclei, and then the charges are set to zero to simulate neutron-nucleus scattering. The nuclei chosen in this study are helium, calcium and lead, representing light, medium and heavy nuclei respectively.

Choice of the potential parameters

The potential parameters are chosen by taking the parameters obtained from matching a modified Gaussian potential to the "best fit" Woods-Saxon potential using the formulae of Appendix B, then using these as a starting point of a search for a potential to reproduce as closely as possible the elastic scattering data taken from the references in Table I. The resulting parameters are shown in Table II.

TABLE I

The sources used for the experimental
proton-nucleus elastic scattering data

Target	Energy(MeV)	Observable	Reference
helium	100	cross-section	G070
	540	polarisation	G068
	580	cross-section	B072
	1050	cross-section	AL75
calcium	155	cross-section	WI68
	155	polarisation	WI68
	1044	cross-section	AL76
lead	155	cross-section	WI68
	155	polarisation	WI68
	1044	cross-section	BE73

TABLE II

The parameters used in the optical potential

The potential used is

$$V(\underline{r}, \underline{\sigma}) = (v_0 + iw_0)(1 + \rho r^2)e^{-\alpha r^2} + (v_{s.o.} + iw_{s.o.})(1 + \rho r^2)e^{-\alpha r^2} \underline{\sigma} \cdot \underline{L}$$

Nucleus and Energy (MeV)	v_0 (MeV)	w_0 (MeV)	$v_{s.o.}$ (MeV)	$w_{s.o.}$ (MeV)	α^{-2} (fm ⁻²)	ρ (fm ⁻²)
Helium						
100	10.0	35.0	15.0	5.0	1.01	2.0
380	1.0	80.0	10.0	0.0	1.01	1.34
580	-23.0	115.0	8.0	4.0	1.01	1.34
1000	-51.4	122.5	12.5	-24.5	1.01	1.34
Calcium						
155	9.0	14.0	1.1	-0.05	0.1	0.1
500	-18.0	30.0	1.3	-0.25	0.1	0.1
1044	-35.0	40.0	1.5	-0.4	0.1	0.1
Lead						
155	19.0	18.0	1.0	-0.2	0.0644	0.207
500	0.0	60.0	0.5	-0.15	0.0644	0.207
1044	-7.0	120.0	0.1	-0.1	0.0644	0.207
			(1.0)	(-0.5)		

Fits were made for all the potentials used except for helium at 380 MeV, calcium and lead at 500 MeV. The parameters for these potentials were obtained by considerations of the behavior of the optical model parameters as a function of energy, and interpolating between the regions where experimental data had been fitted. Five fits are shown here (figs (4-7)).

As expected from geometric considerations, the fits worsen as the ranges of the potentials increase, but in all cases the essential features of the curves, in particular the first diffraction minimum, are reproduced. Fits obtained with a more conventional Woods-Saxon potential would be more accurate (OE76), but would lead to rather complicated expressions for the scattering amplitudes, and so for the sake of simplicity are not used here.

Generally the geometry of the potential was kept fixed for each nucleus, the exception being helium at 100 MeV where an increased range was required to reproduce the scattering data well. At 1044 MeV the lead potential obtained by minimising the chi-squared between theory and experiment gave a spin-orbit strength which was rather too low to produce a realistic polarisation or P.T.C., the strength of the spin-orbit interaction was therefore increased slightly to the values shown in parentheses in Table II.

Comparison of Glauber and exact calculations

For spin- $\frac{1}{2}$ on spin-zero scattering one has two complex amplitudes which, considering an overall phase factor,

give rise to the three independent quantities. We therefore have to consider three observables in order to fully describe the system. We choose here the differential cross-section $\frac{d\sigma}{d\Omega}$, the polarisation P , and the first Wolfenstein parameter $K_X^{X'}(Z_X^{X'})$.

The three observables are calculated here for three different nuclei at various energies from 0.1 GeV to 1.0 GeV, and the graphs obtained giving exact and eikonal curves for them as a function of either the centre of mass scattering angle or the momentum transfer.

What exactly constitutes a failure of the approximation is a subjective matter. One may be trying to reproduce experimental data as in the multiple scattering use, in which case if the differences between exact and eikonal calculations are smaller than the error bars then one may say the approximation is valid. One may be wishing for a 5%, 10%, 20% or "general features" reproduction, and so one should not conclude with a table of angles, energies and ranges showing decisively where one can and cannot use the approximation.

Despite the pessimistic attitude projected by the previous paragraph, a cursory glance at the curves will reveal that there is often a point where the approximation fails drastically (for example 80° for helium at 380 MeV (fig 8)). One may therefore draw the following conclusions for the various nuclei.

fig 4

The fit to the experimental $p - {}^4\text{He}$ elastic scattering cross-section data at 580 MeV and the fit to the experimental polarisation taken from 540 MeV, both evaluated at 580 MeV.

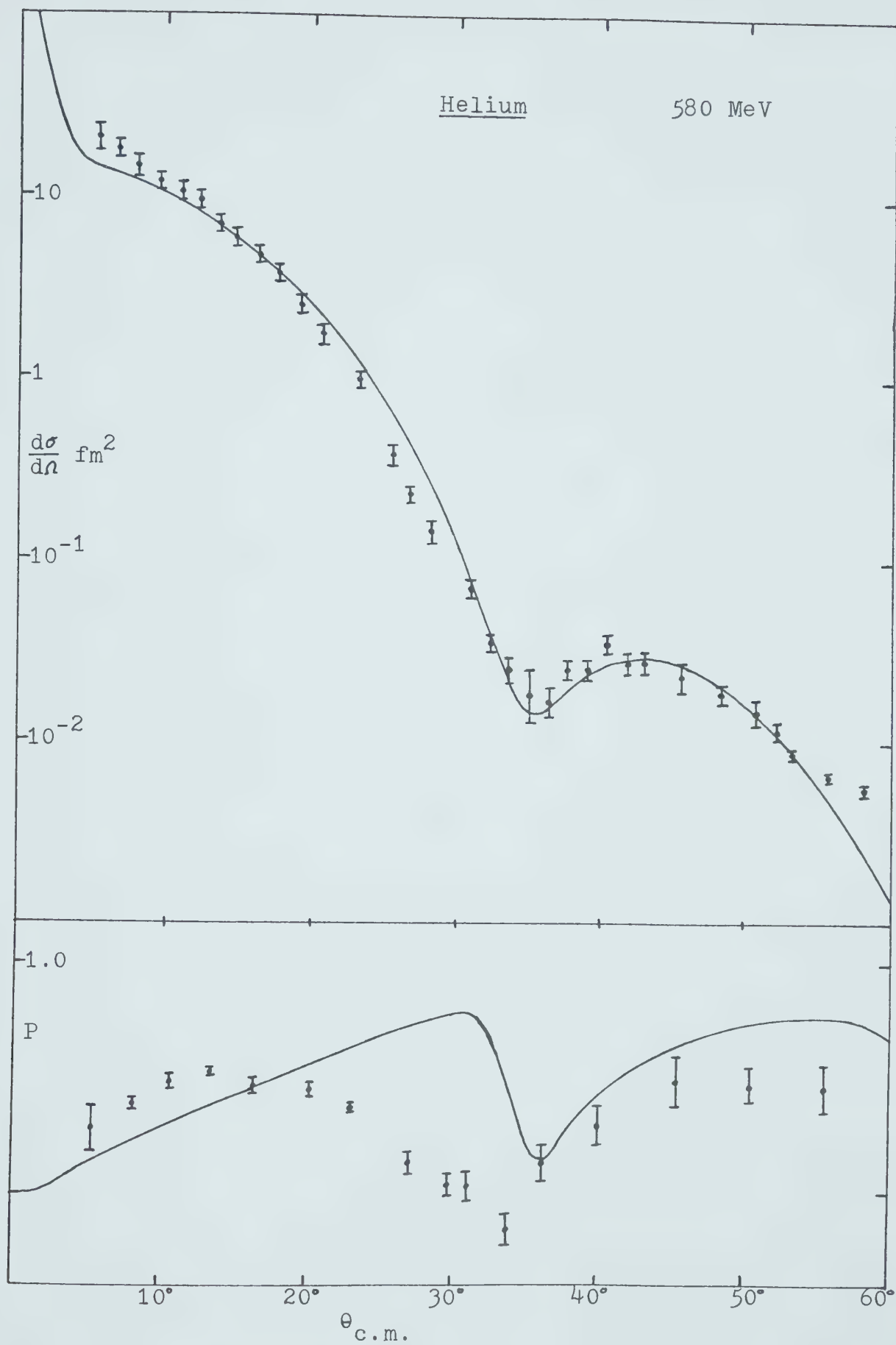


fig 5

The fit to the experimental $p - {}^{40}\text{Ca}$ elastic scattering cross-section at 1044 MeV.

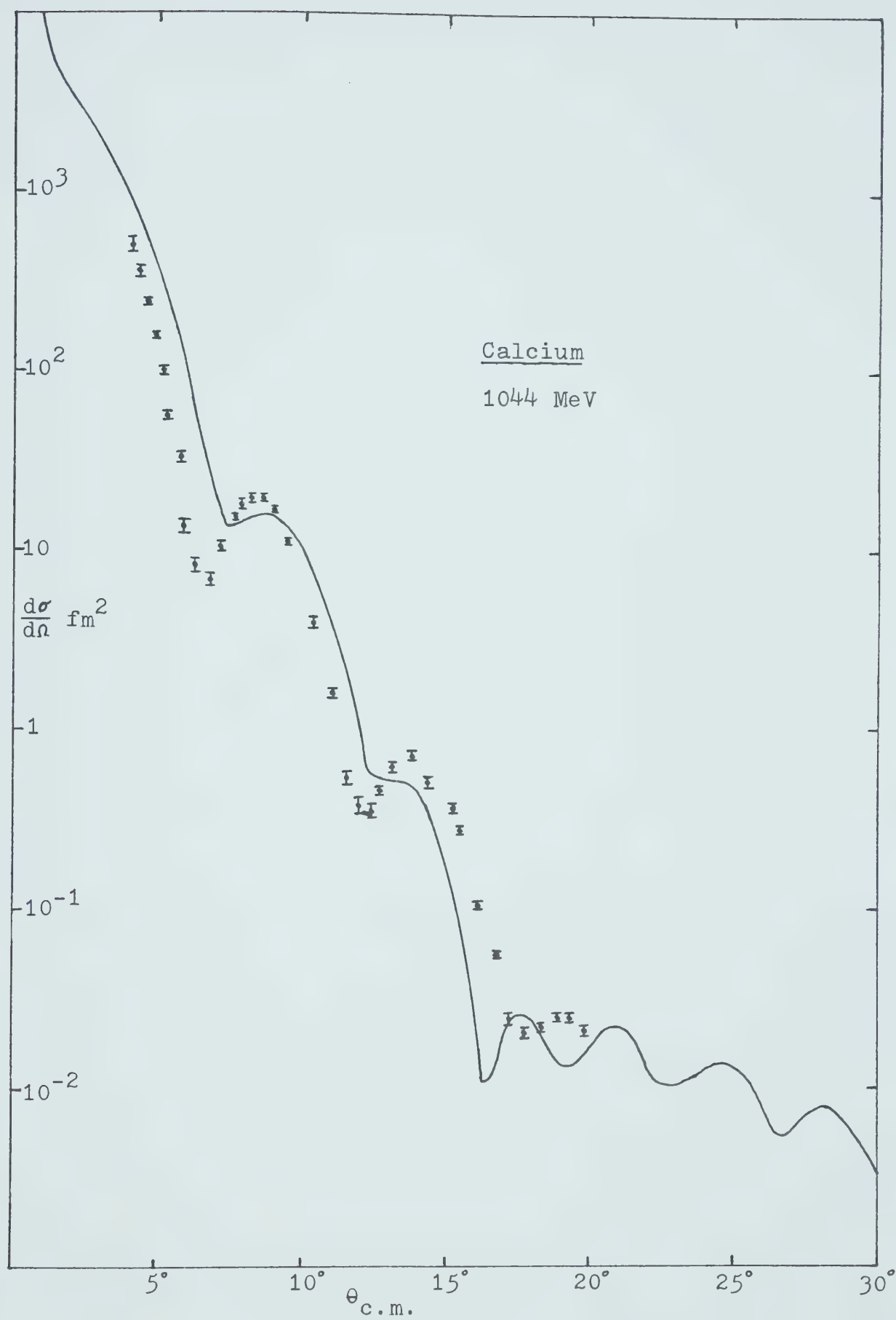


fig 6

The fit to the experimental $p - {}^{208}\text{Pb}$ elastic scattering cross-section data at 155 MeV.

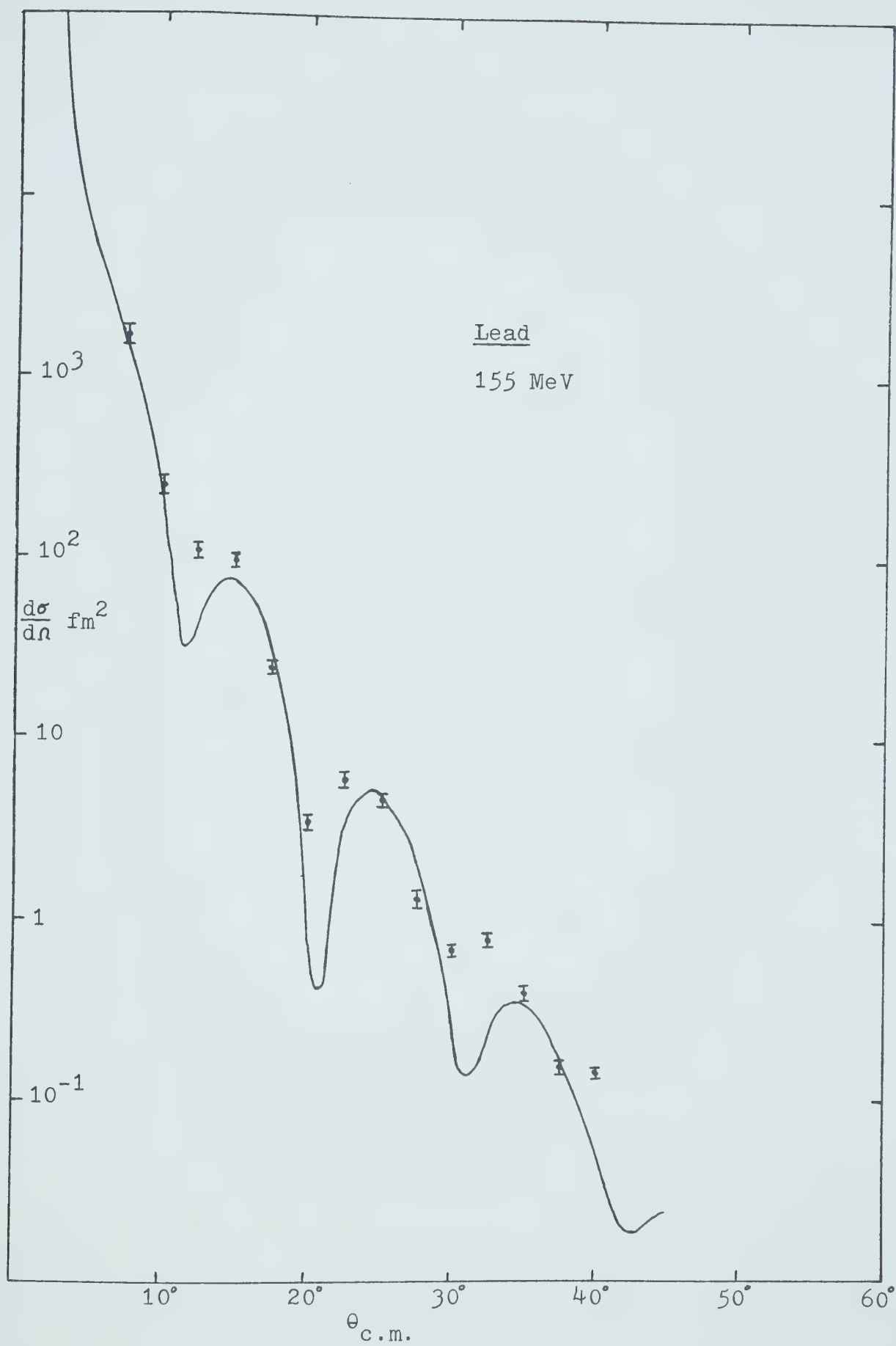
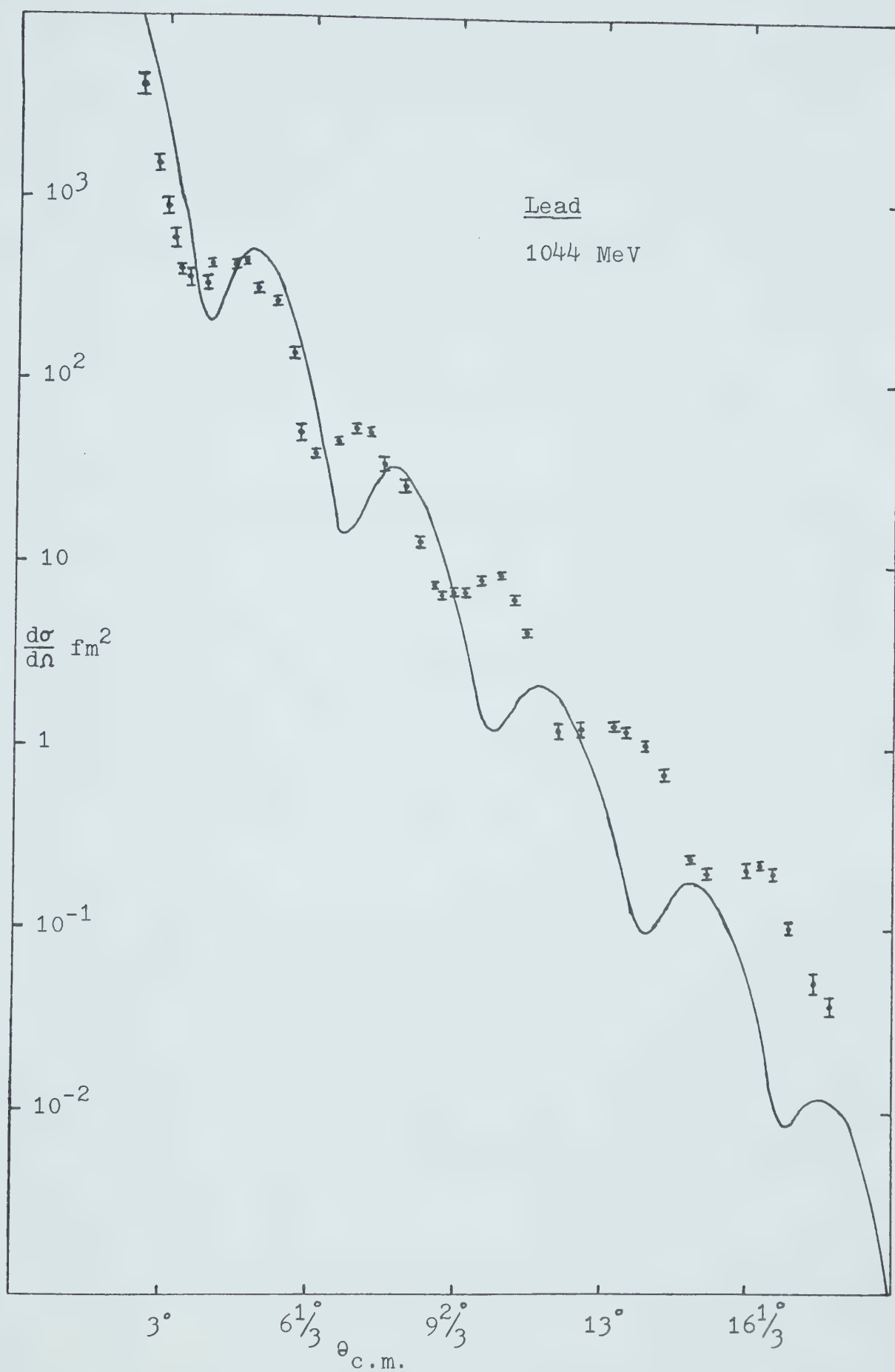


fig 7

The fit to the experimental $p - {}^{208}\text{Pb}$ elastic scattering cross-section data at 1044 MeV.



Helium

The cross-sections are reproduced rather well. At 1050 MeV (fig 9) the approximation reproduces the first two minima, beginning to go astray at the third (see insert). At 580 MeV the approximation may be said to fail at the first minimum, recovering to fail drastically at 64° . For the lower energies of 100 MeV and 380 MeV the approximation does well up to 80° on the cross-section. The polarisation and P.T.C. fail at or before the first minimum for all energies however.

Calcium

The cross-section consistently fails just before the second minimum regardless of energy. The polarisation fails badly at the first dip at 150 MeV, the P.T.C. failing at the top of the first rise; corresponding to the same value of momentum transfer. For the other two energies the first dip in the polarisation is obtained, but the reproduction of the P.T.C. is not appreciably improved.

Lead

Since experiments performed on lead, particularly at high energies are constrained to the forward angles, it is of interest to note that in the case of 1 GeV, the replication of the cross-section covers the entire angular range demanded of it. The approximation does rather well at 500 MeV, the polarisation and P.T.C. being reproduced significantly better than at 1 GeV.

As mentioned previously, to conclude with a table of angles, energies and ranges showing absolutely where one can use the approximation would be overambitious. However, if one decides upon a criterion of failure and then constructs a table, one may expound upon the relative performance of the approximation as regards these variables and hence no apologies need be offered for the presence of Table III from which one may draw the following general conclusions.

With increase of energy, the angular range goes down, but the momentum transfer increases. Since the momentum transfer is physically more meaningful than the scattering angle, the approximation may be said to be better at higher energies.

For lighter nuclei the angular range is greater than for the other two, however the difference between the angular ranges of lead and calcium is not large.

The cross-section is found to be reproduced to a greater angle than the polarisation. The reproductions of polarisation and P.T.C. are roughly the same, the P.T.C. being slightly worse.

Brissaud's (BR75) finding that the formula $q^2 \ll k/R$ is unnecessarily restrictive for heavier nuclei is confirmed: lead fairs hardly worse than calcium. It is found here that the formula is also rather too restrictive for very light nuclei -- i.e. helium.

Whilst increasing the energy from 500 MeV to 1044 MeV

TABLE III

The angles of failure of the approximation

Nucleus Energy (MeV)	Cross-section		Polarisation		P.T.C.	
	$\theta_{\text{c.m.}}$	$q \text{ fm}^{-1}$	$\theta_{\text{c.m.}}$	$q \text{ fm}^{-1}$	$\theta_{\text{c.m.}}$	$q \text{ fm}^{-1}$
Helium						
100	80	2.3	50	1.5	40	1.2
380	80	4.5	42	2.5	41	2.5
580	36	2.7	35	2.7	33	2.5
1050	80	7.8	40	4.2	42	4.3
Calcium						
155	32	1.5	17	0.8	20	0.9
500	20	1.9	17	1.6	12	1.1
1044	12	1.7	10	1.5	8	1.2
Lead						
155	30	1.4	10	0.5	8	0.4
500	28	2.6	12	2.1	23	2.2
1044	20	3.0	10	1.5	11	1.8

fig 8

The differential cross-section for helium at 100 MeV and at 380 MeV, calculated exactly and in the eikonal approximation. The solid line is the exact calculation, the dashed line is the eikonal approximation.

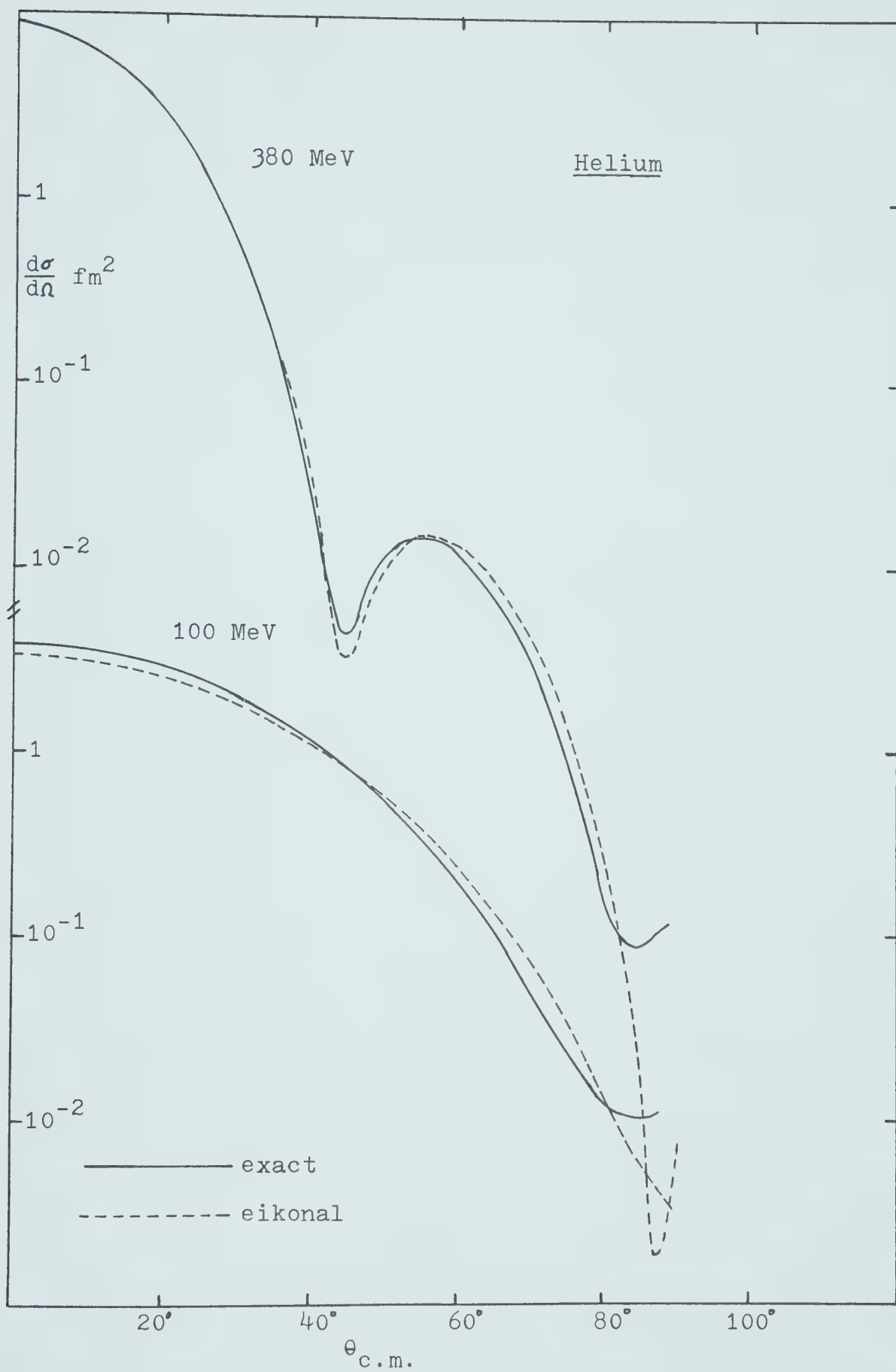


fig 9

The differential cross-section for helium at 580 MeV and at 1050 MeV, calculated exactly and in the eikonal approximation. The solid line is the exact calculation, the dashed line is the eikonal approximation.

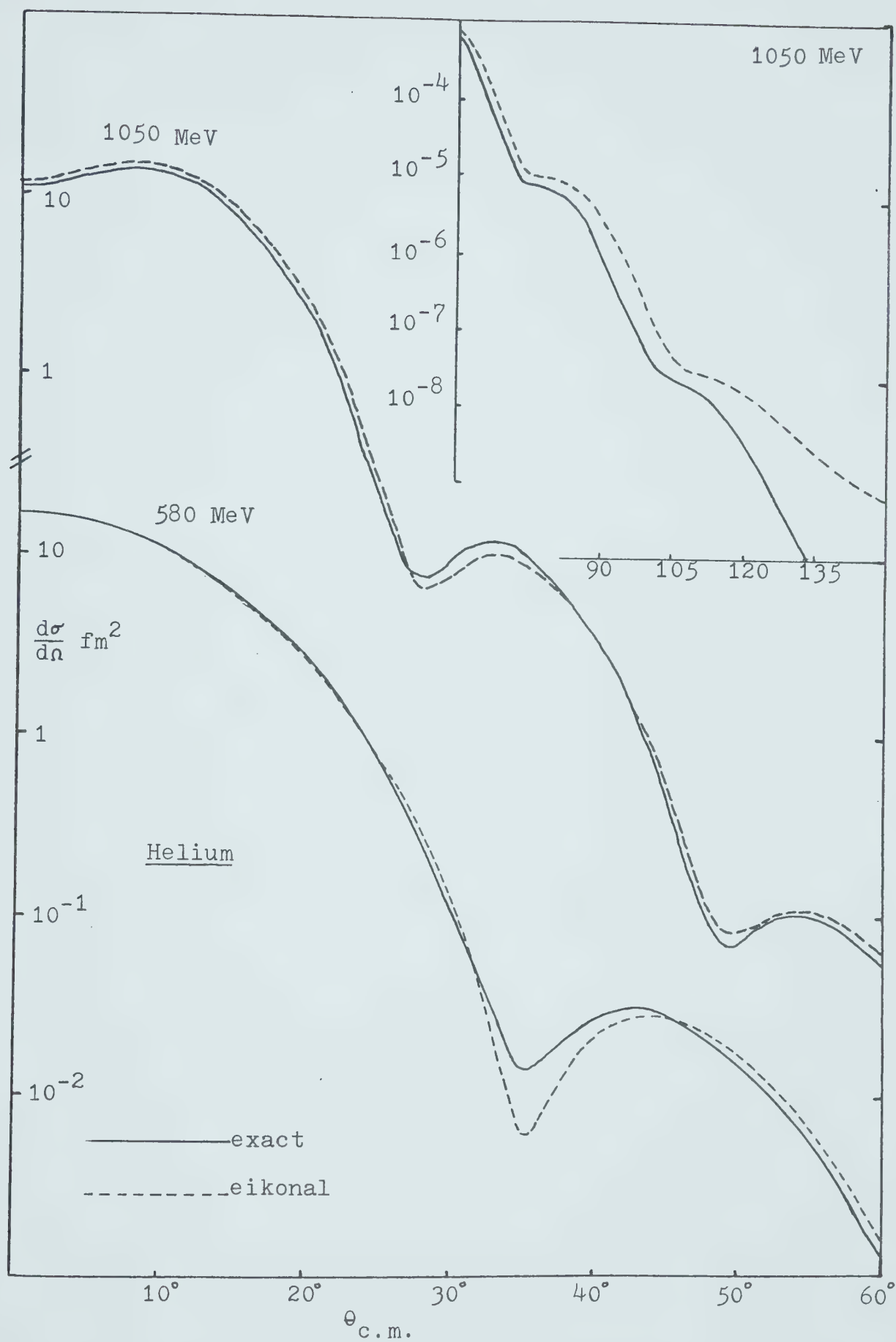


fig 10

The polarisation for helium at 100 MeV and 380 MeV, calculated exactly and in the eikonal approximation. The solid line is the exact calculation, the dashed line is the eikonal approximation. The graphs are plotted as functions of momentum transfer.

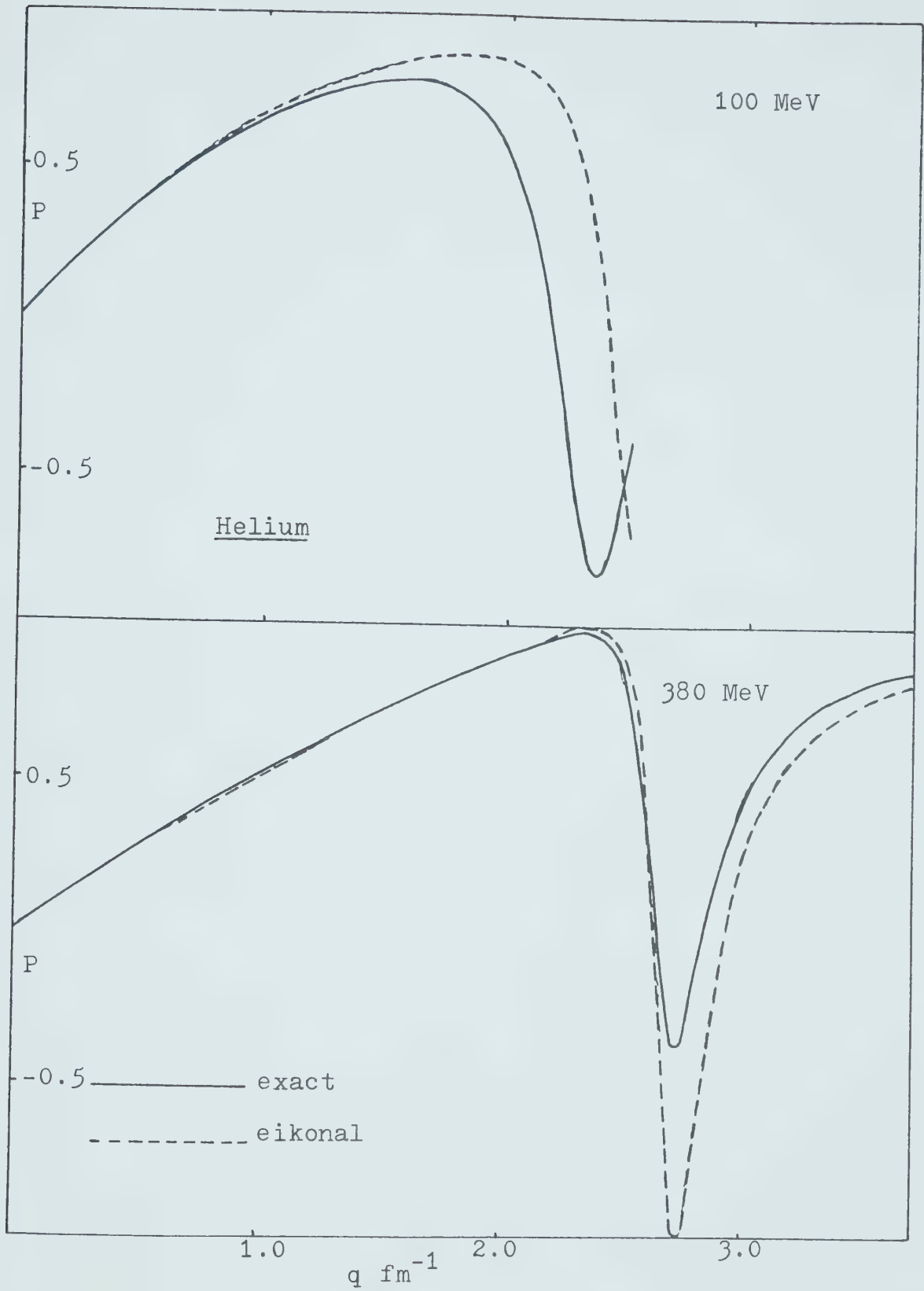


fig 11

The polarisation for helium at 580 MeV and 1050 MeV, calculated exactly and in the eikonal approximation. The solid line is the exact calculation, the dashed line is the eikonal approximation. The graphs are plotted as functions of momentum transfer.

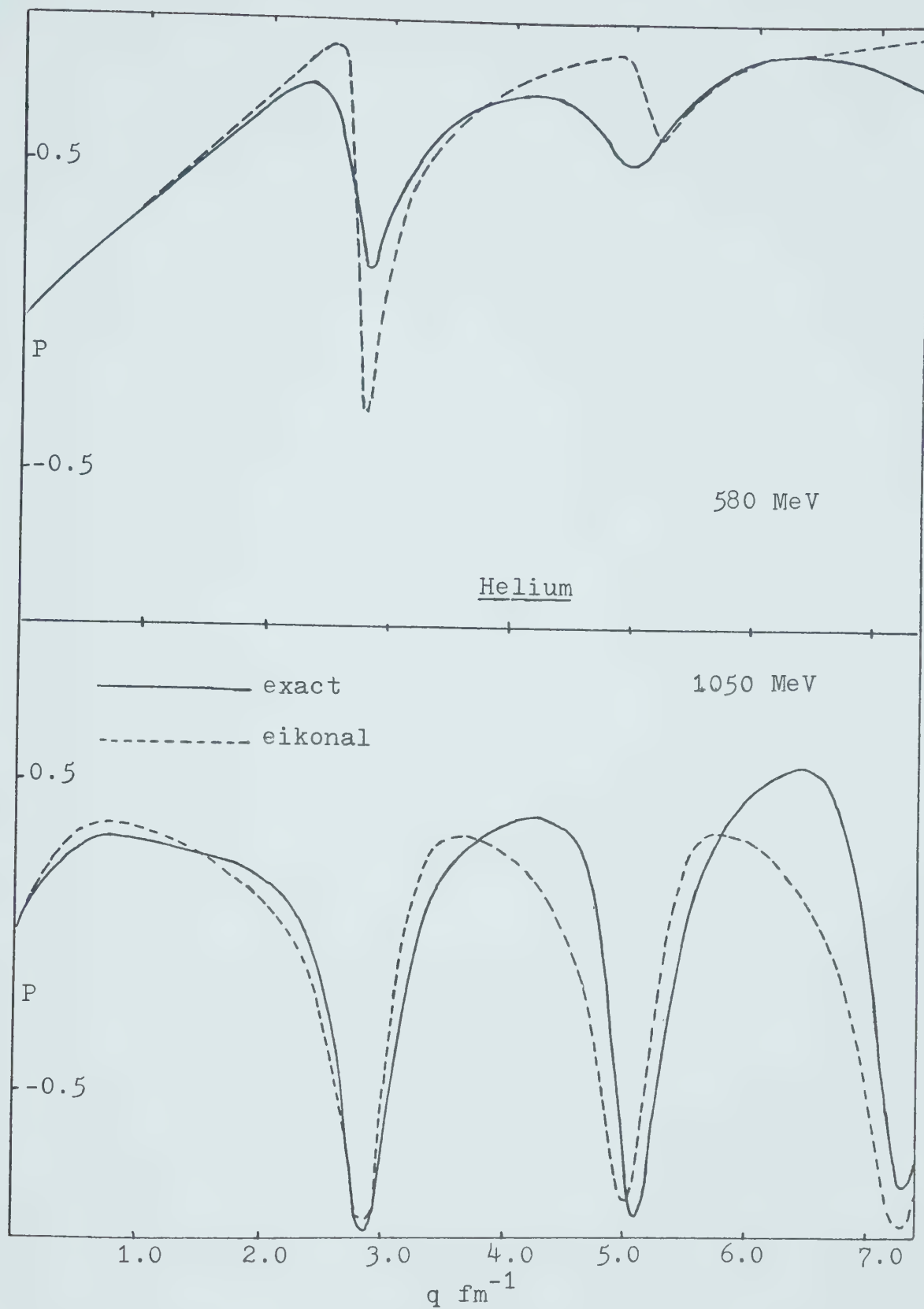


fig 12

The P.T.C. for helium at 100 MeV and 380 MeV, calculated exactly and in the eikonal approximation. The solid line is the exact calculation, the dashed line is the eikonal approximation. The graphs are plotted as functions of momentum transfer.

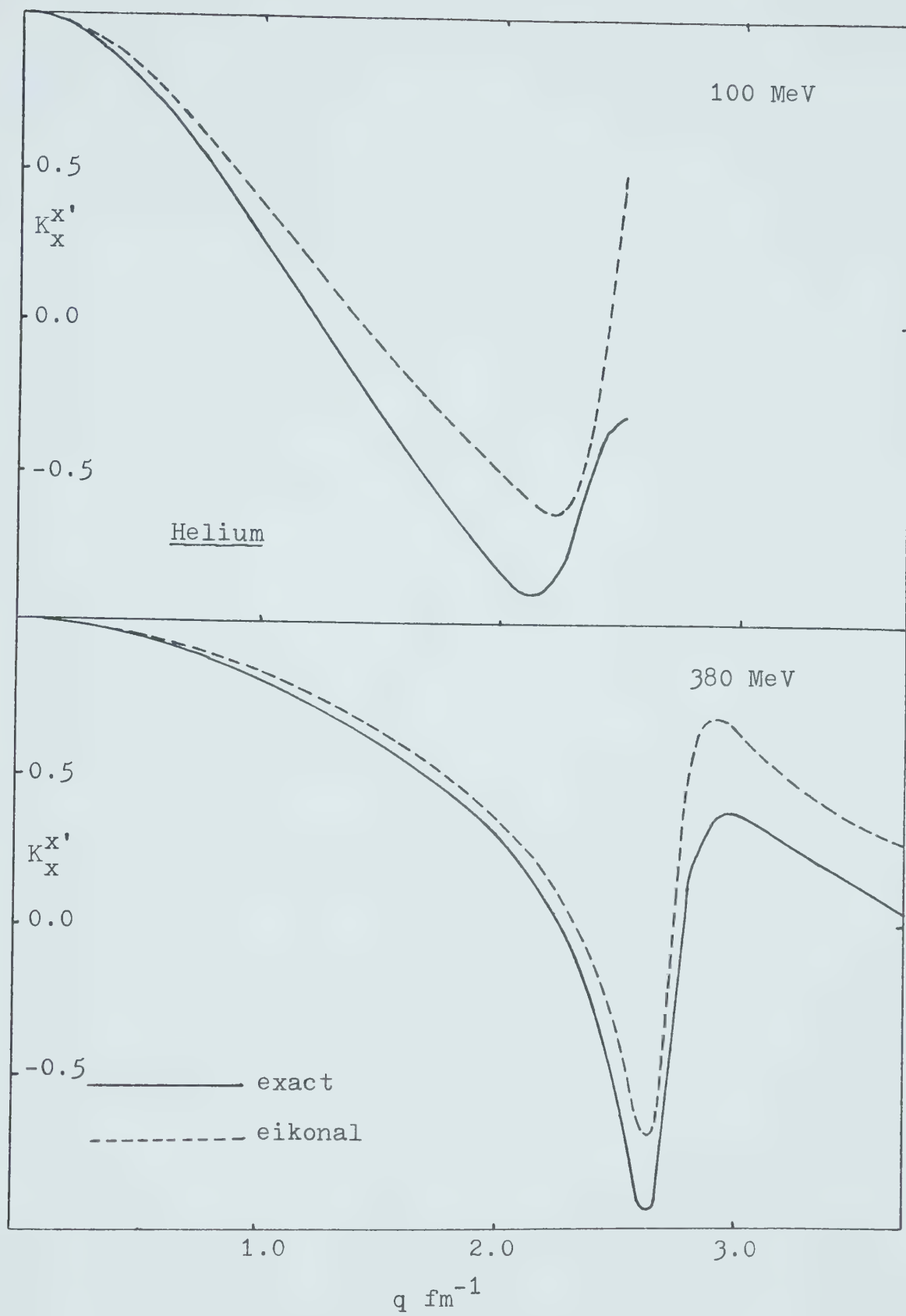
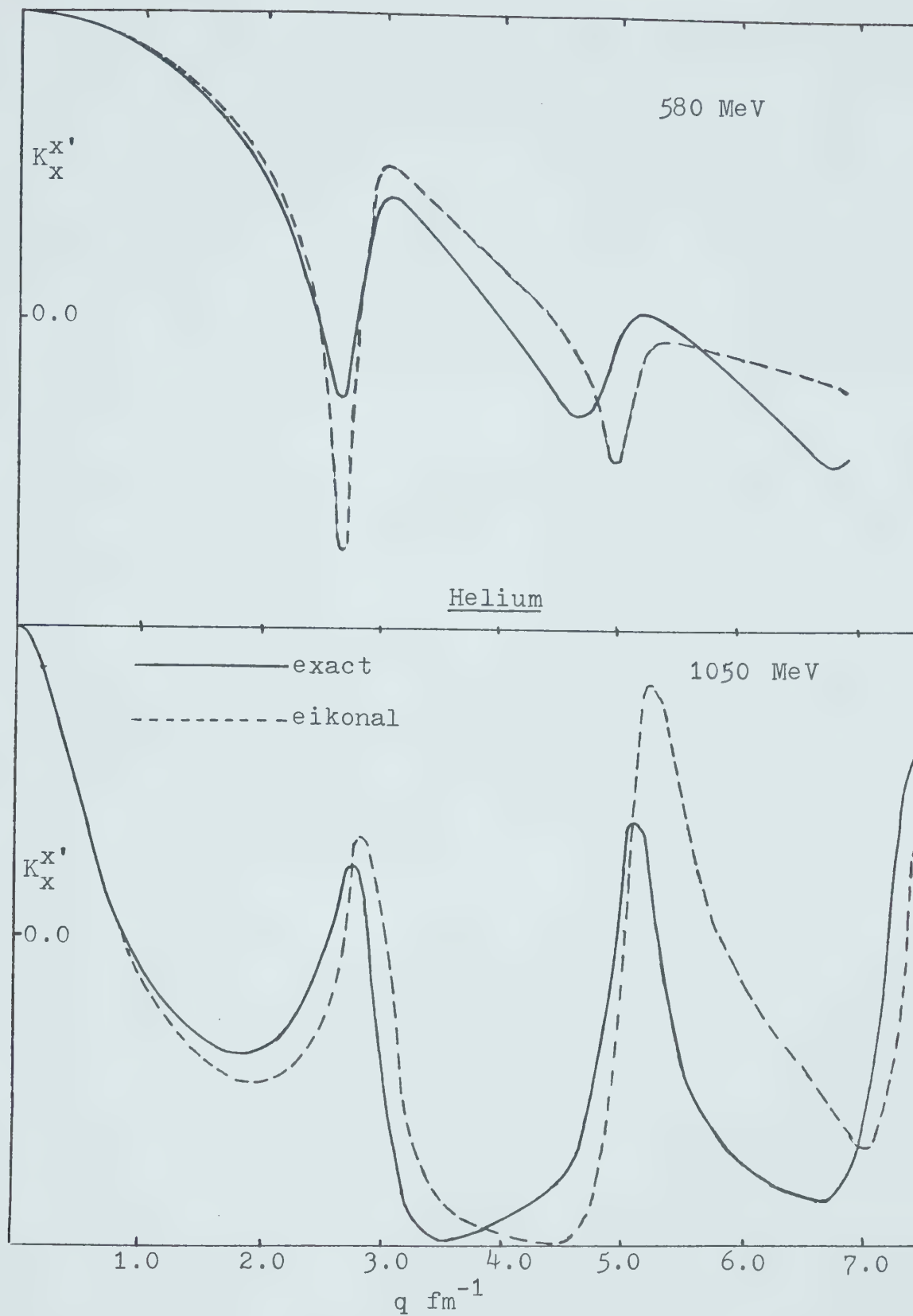


fig 13

The P.T.C. for helium at 580 MeV and 1050 MeV, calculated exactly and in the eikonal approximation. The solid line is the exact calculation, the dashed line is the eikonal approximation. The graphs are plotted as functions of momentum transfer.

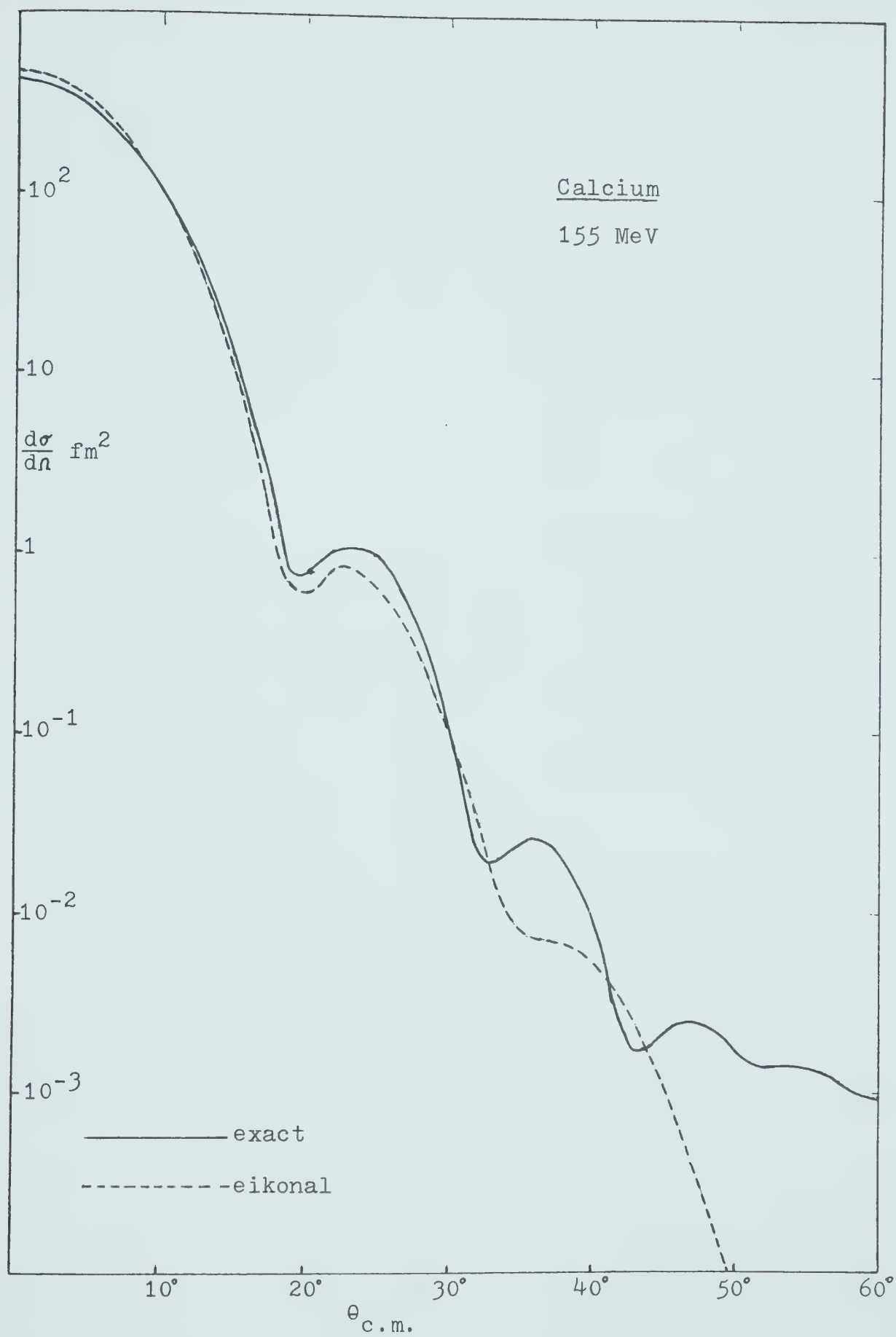


the accuracy does not vary significantly; in several cases a greater momentum transfer is reproduced at 500 MeV than at 1044 MeV (see for example figs 17, 18, 22, 23). This may be due to the fact that the potentials used try to mimic realistic optical potentials in which the real central potential changes sign somewhere below 500 MeV, also the reaction cross-section is smaller at 500 MeV, giving smaller imaginary potentials at the lower energy.

The apparent early failure for helium at 580 MeV (fig 9) occurs at the first diffraction minimum, however the approximation is awry for only a few degrees and then recovers, failing again at a higher angle. At 380 MeV, where the potentials, especially the real central, are smaller, the first minimum is reproduced more accurately (fig 8) and so the variance between exact and eikonal curves is not considered (by the author) a failure.

fig 14

The differential cross-section for calcium at 155 MeV, calculated exactly and in the eikonal approximation. The solid line is the exact calculation, the dashed line is the eikonal approximation.



1

fig 15

The differential cross-section for calcium at 500 Mev, calculated exactly and in the eikonal approximation. The solid line is the exact calculation the dashed line is the eikonal approximation.

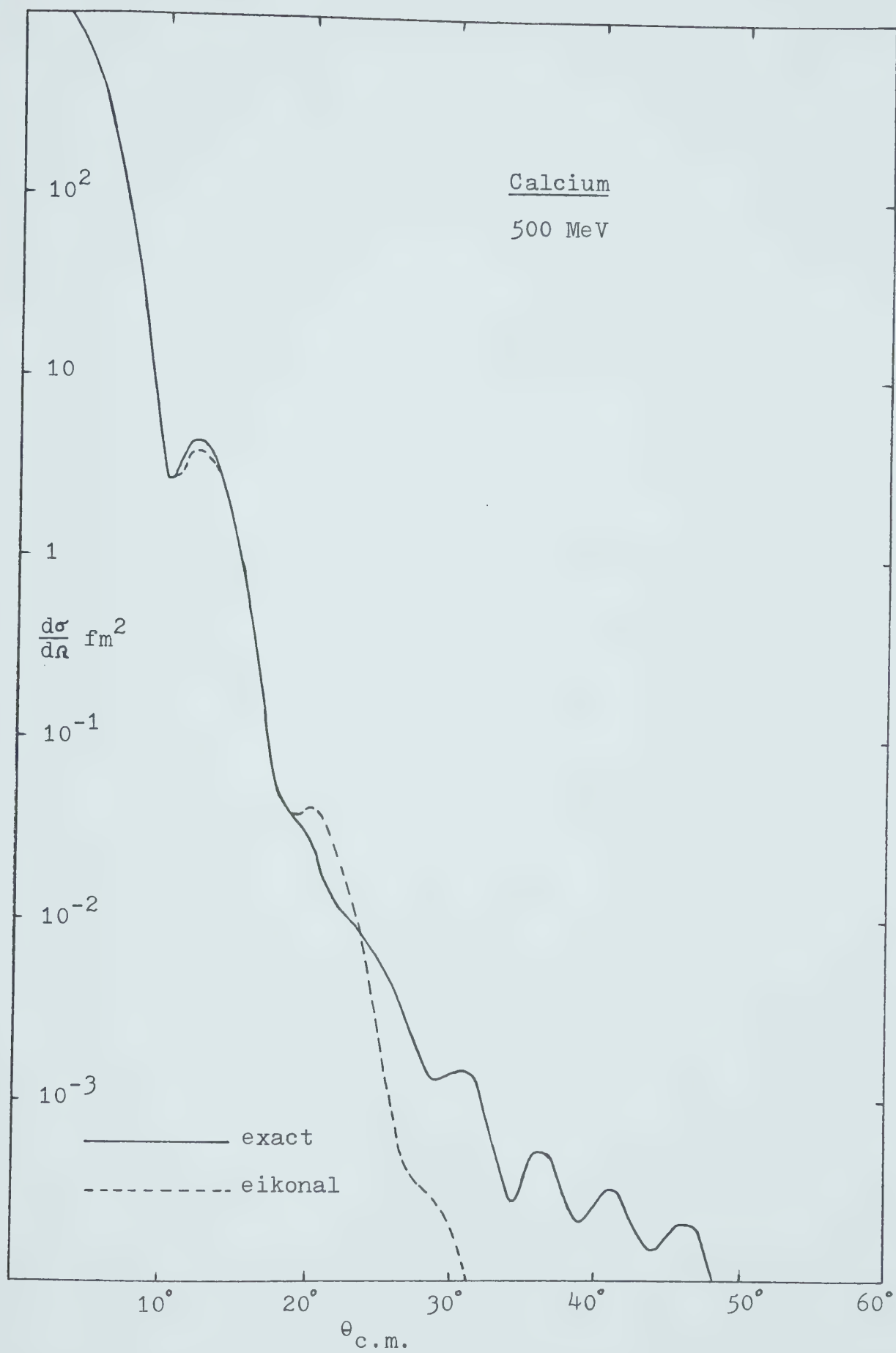


fig 16

The differential cross-section for calcium at 1044 Mev, calculated exactly and in the eikonal approximation. The solid line is the exact calculation, the dashed line is the eikonal approximation.

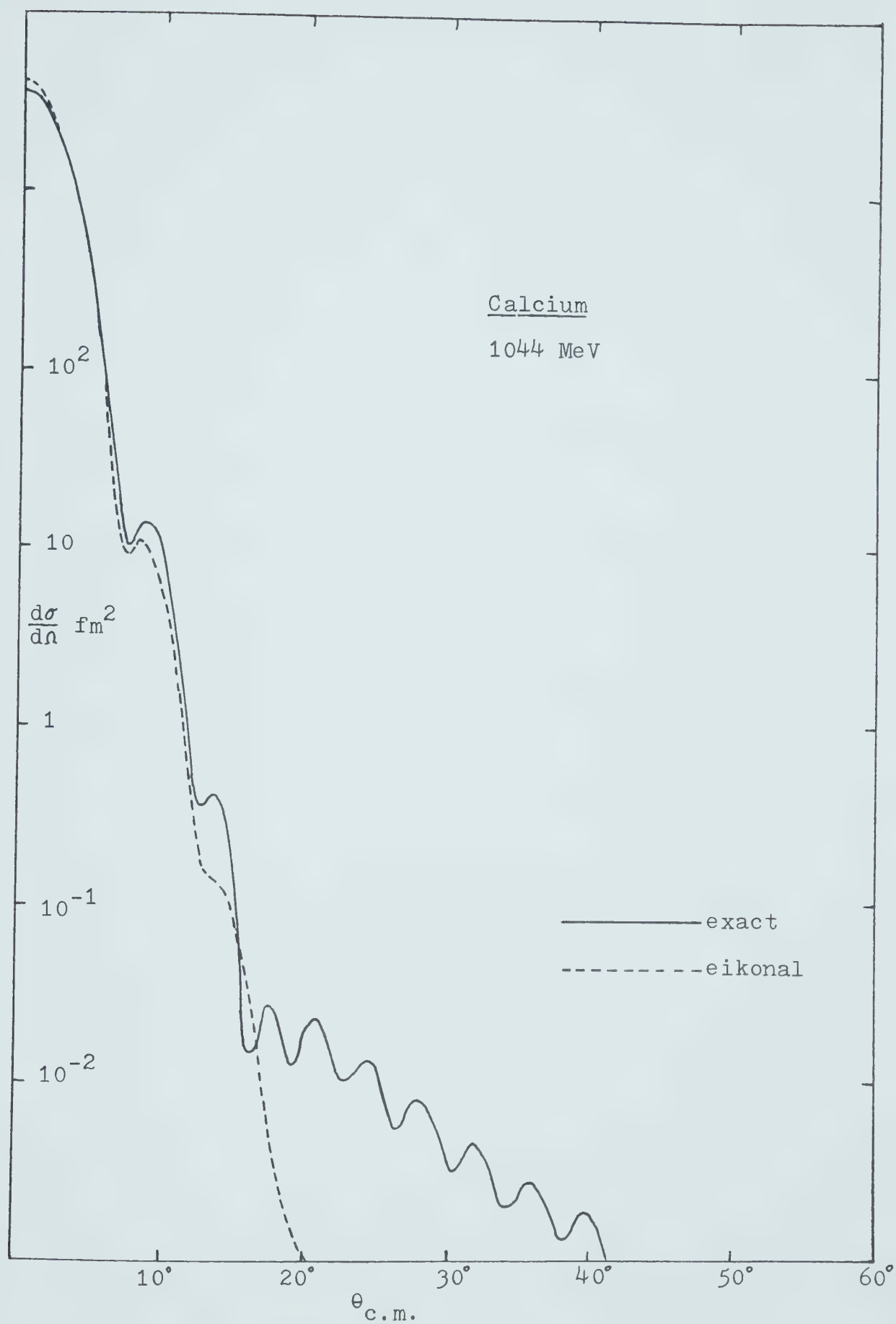


fig 17

The polarisation for calcium at 155 Mev, 500 Mev and 1044 Mev, calculated exactly and in the eikonal approximation. The solid line is the exact calculation, the dashed line is the eikonal approximation. The graphs are plotted as a function of momentum transfer.

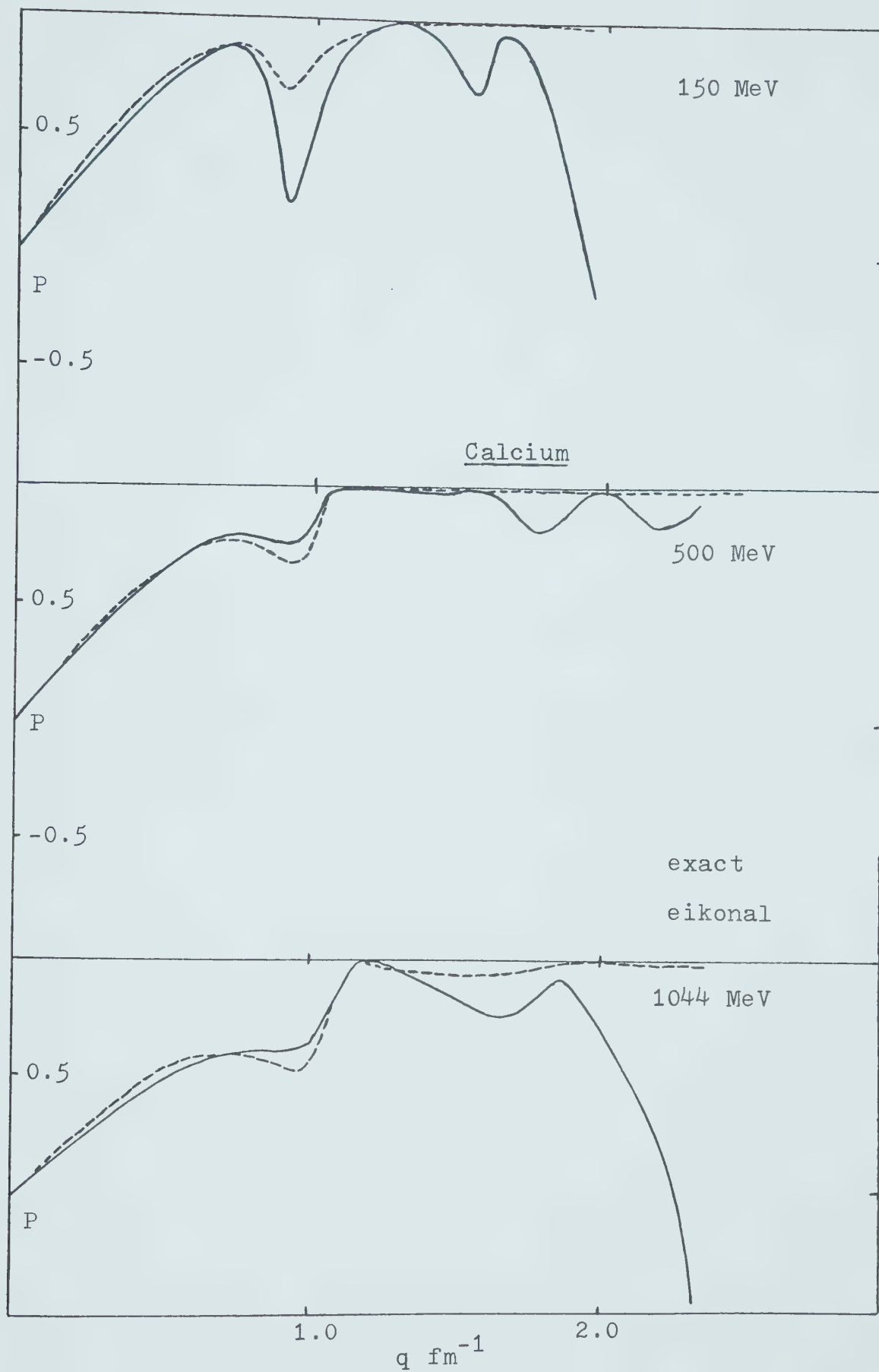


fig 18

The P.T.C. for calcium at 155 Mev, 500 Mev and 1044 Mev calculated exactly and in the eikonal approximation. The solid line is the exact calculation, the dashed line is the eikonal approximation. The graphs are plotted as a function of momentum transfer.

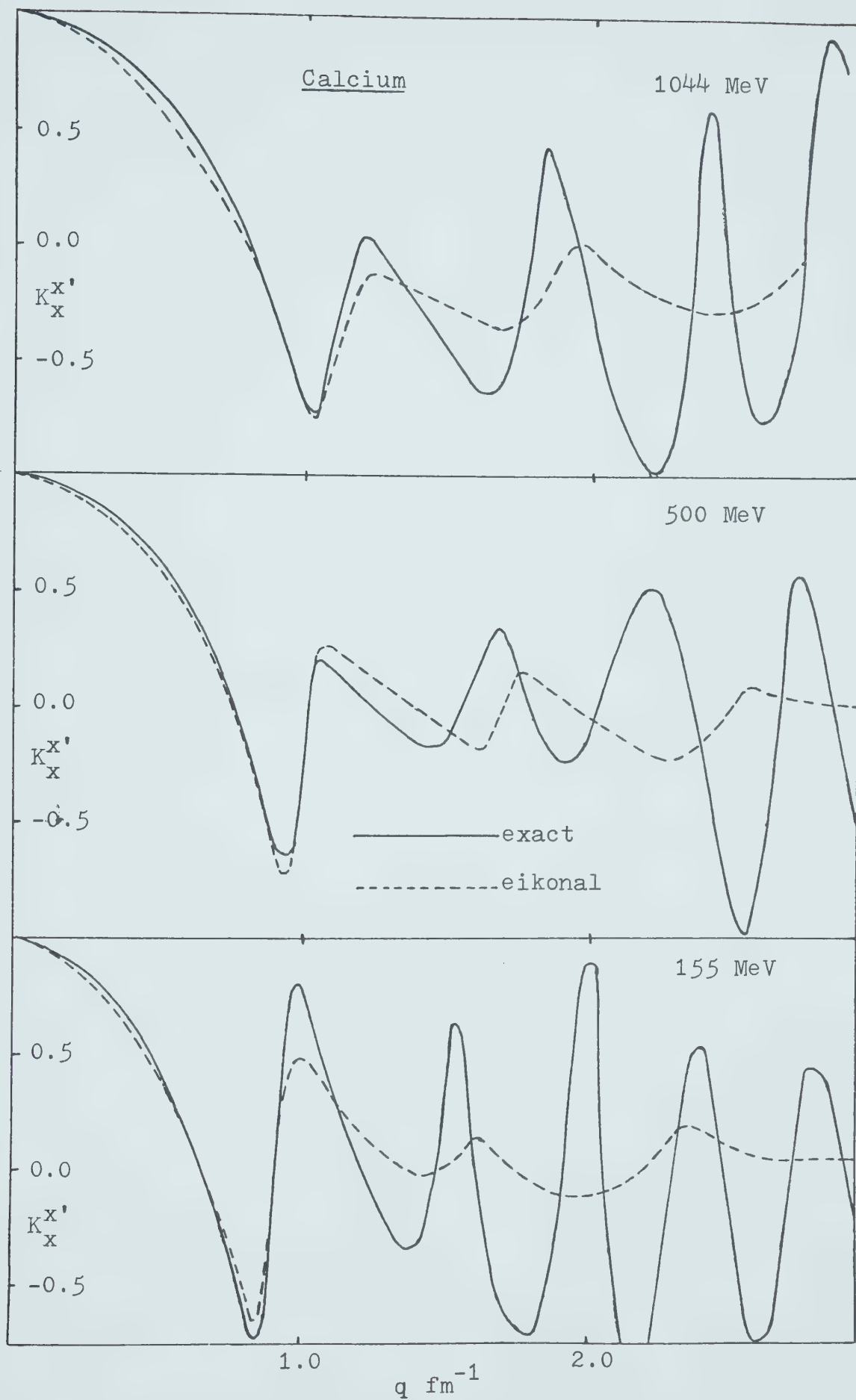


fig 19

The differential cross-section for lead at 155 Mev, calculated exactly and in the eikonal approximation. The solid line is the exact calculation, the dashed line is the eikonal approximation.

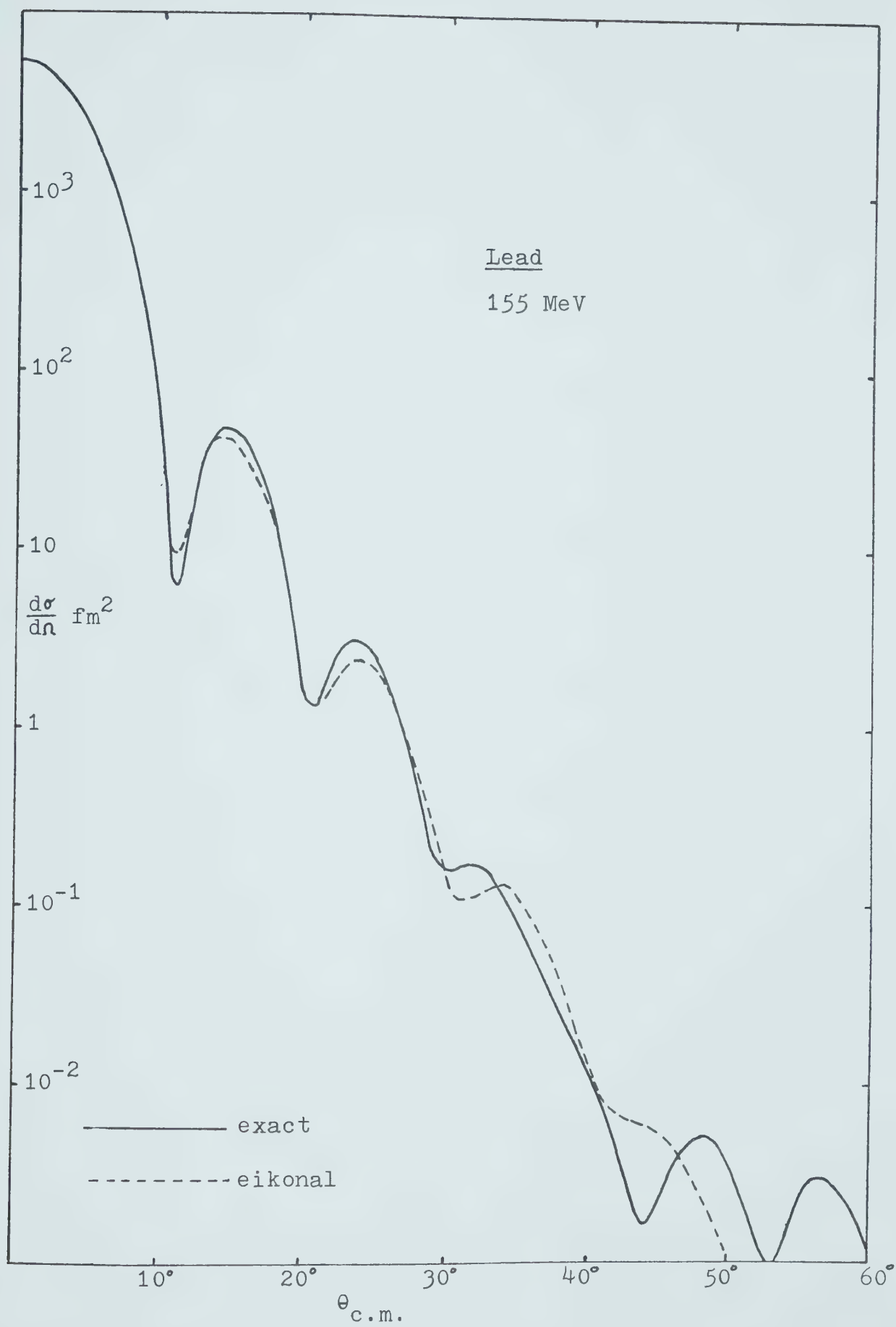


fig 20

The differential cross-section for lead at 500 Mev, calculated exactly and in the eikonal approximation. The solid line is the exact calculation, the dashed line is the eikonal approximation.

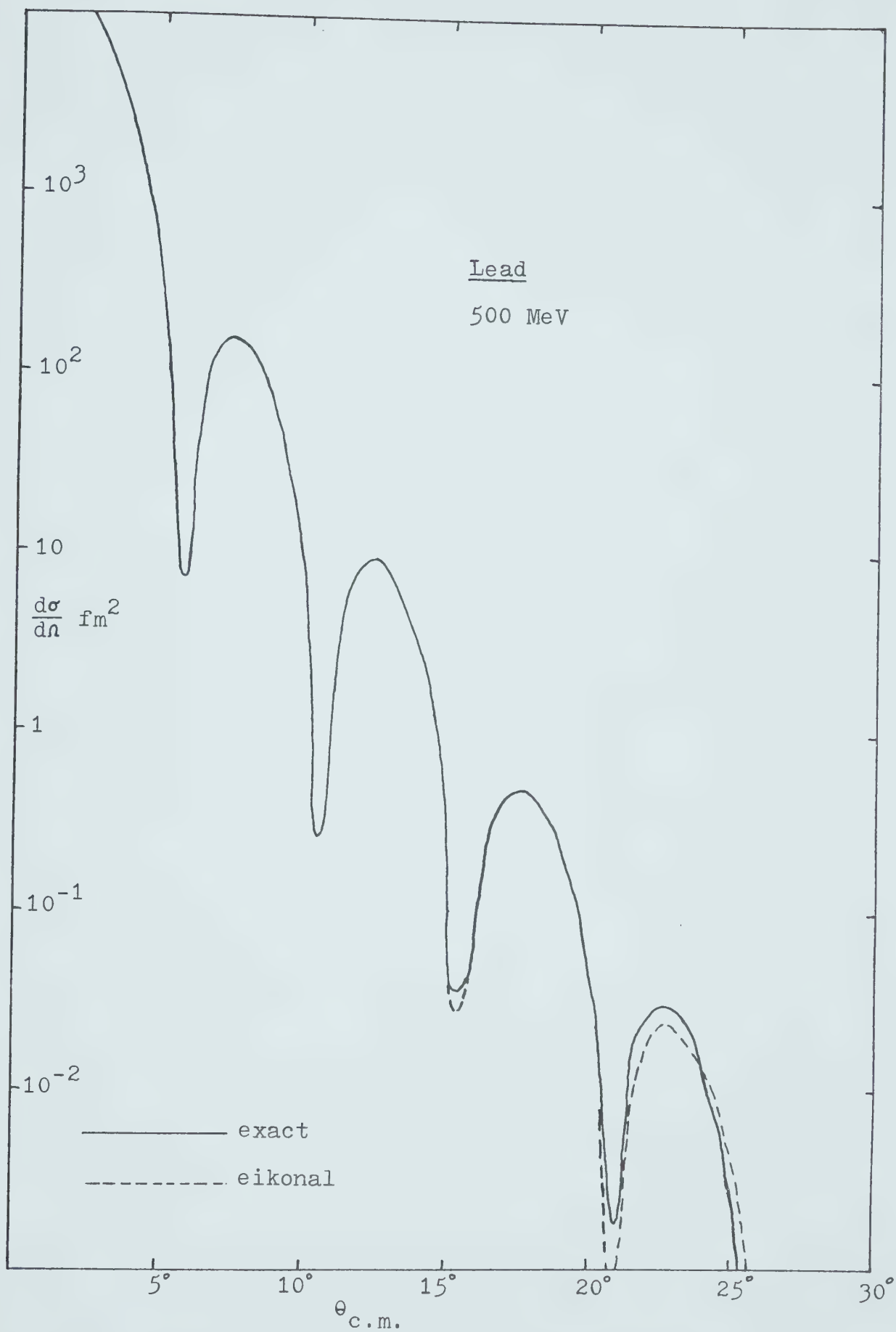


fig 21

The differential cross-section for lead at 1044 Mev, calculated exactly and in the eikonal approximation. The solid line is the exact calculation, the dashed line is the eikonal approximation.

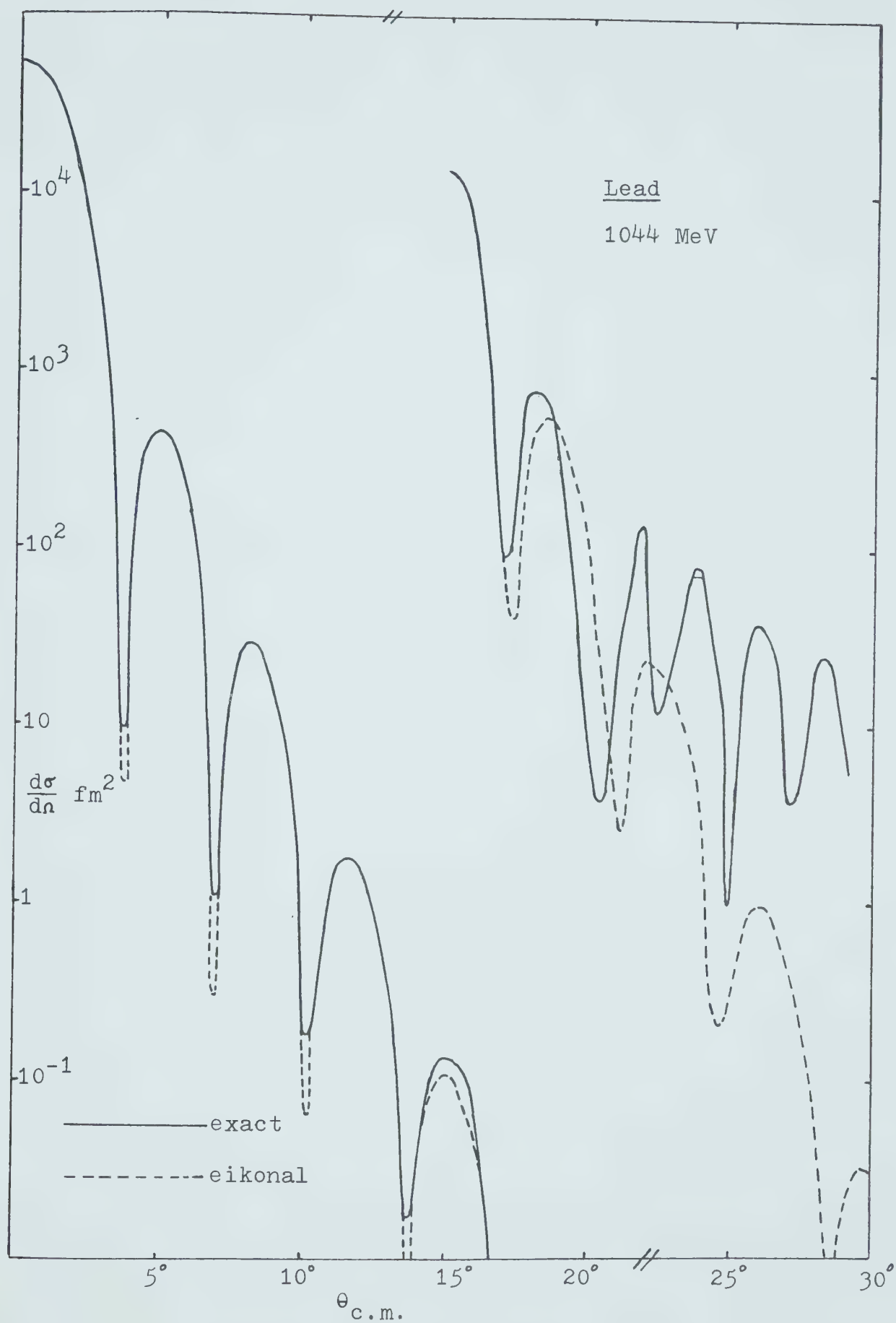


fig 22

The polarisation for lead at 155 Mev, 500 Mev and 1044 Mev, calculated exactly and in the eikonal approximation. The solid line is the exact calculation, the dashed line is the eikonal approximation. The graphs are plotted as a function of momentum transfer.

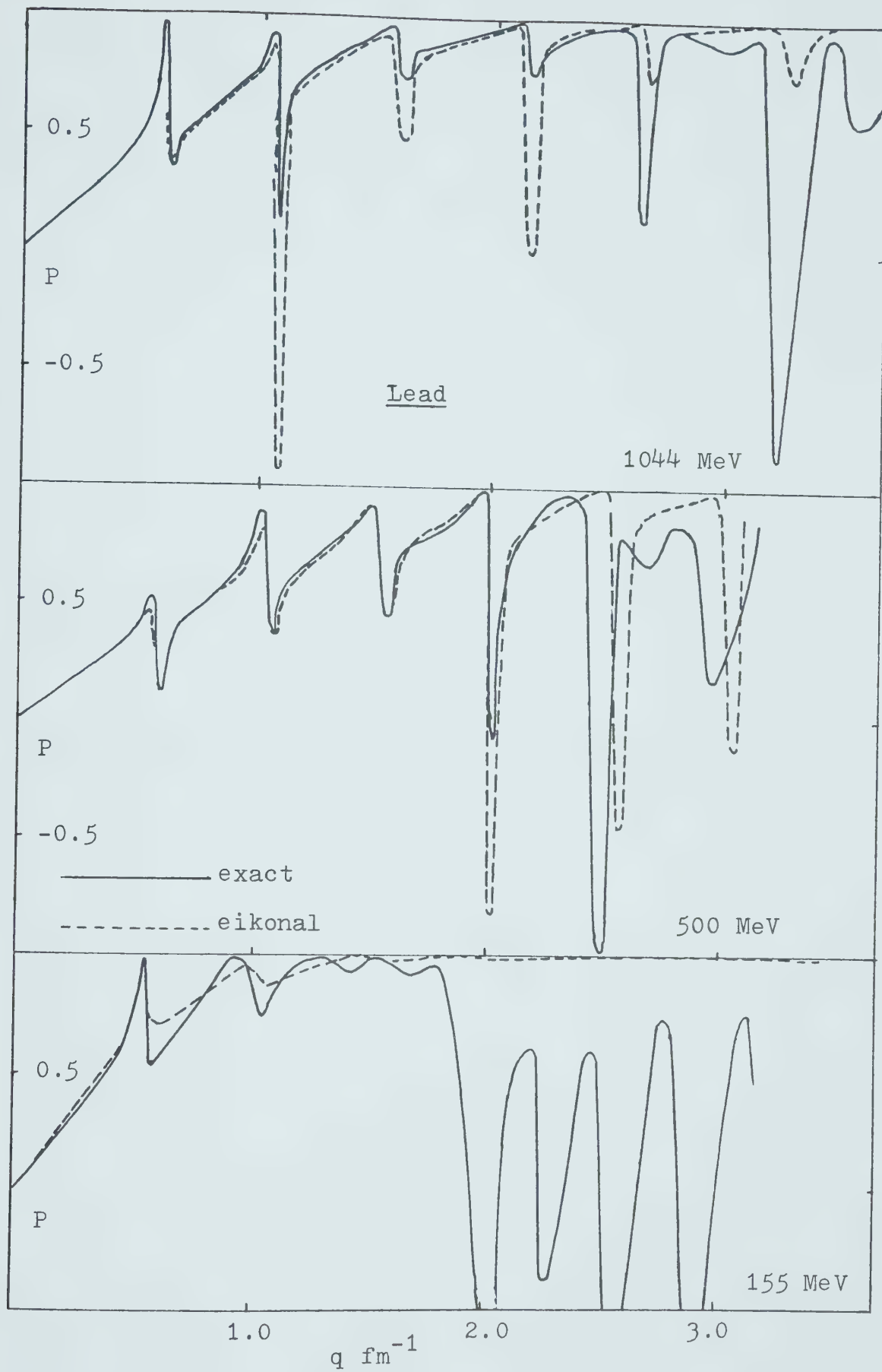
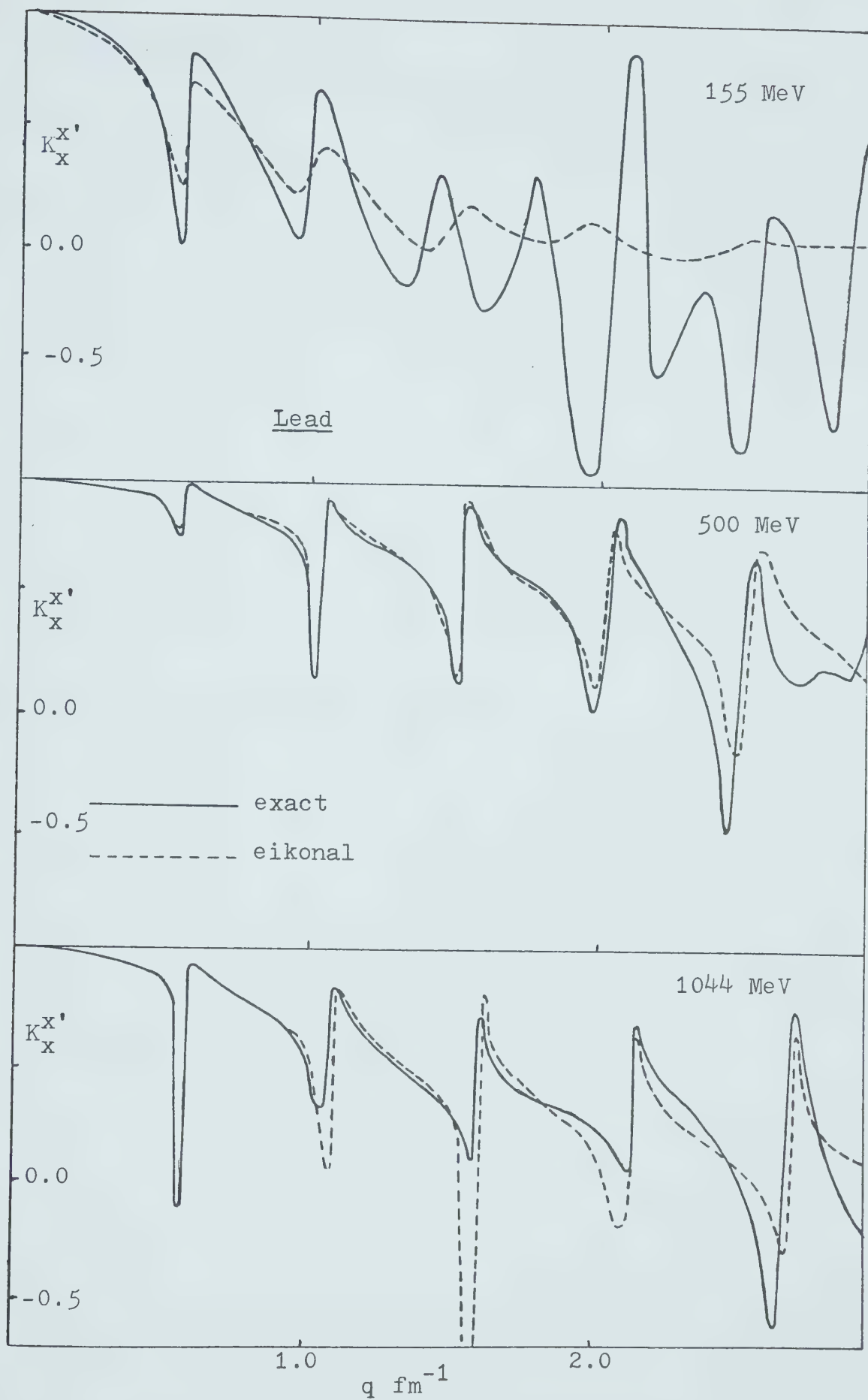


fig 23

The P.T.C. for lead at 155 Mev, 500 Mev and 1044 Mev, calculated exactly and in the eikonal approximation. The solid line is the exact calculation, the dashed line is the eikonal approximation. The graphs are plotted as a function of momentum transfer.



Comment on the amplitudes

It is observed (see figs 24 - 27) that in the replication of an amplitude by the Glauber eikonal approximation, the relative error is usually greater for the smaller of the real and imaginary parts. This may be explained in terms of the Born-series analogy; if the actual error in each term is about the same, then the relative error in the result will of course be larger if the series converges, through cancellations, to a relatively small value.

The effect of the greater relative error in the small part of the amplitude explains why the cross-section is reproduced more accurately than the polarisation or the P.T.C., which are sensitive to the individual phase of each amplitude.

The effect of the $\cos \theta/2$ factor

The effect of this factor is seen to be quite small. In the example given (fig 29) the factor is seen to improve the reproduction of the polarisation, but worsen the reproduction of the P.T.C. In other cases tested a similar sort of "random" amelioration/deterioration was observed, making it difficult to say anything about a practical reason for retaining or discarding the factor.

Table IV

The exact and eikonal non-spin-flip amplitudes tabulated for helium at 100 Mev as a function of both centre of mass scattering angle and momentum transfer. The units are fm.

TABLE OF EXACT AND EIKONAL
NON-SPIN-FLIP AMPLITUDES

taken from helium at 100 MeV

(The exponents of the numbers are shown in parentheses.)

$\theta_{\text{c.m.}}$	q fm^{-1}	Re(f) exact	Re(f) Glauber	Im(f) exact	Im(f) Glauber
0	0.00	8.070(-2)	1.243(-1)	1.946(0)	1.813(0)
5	0.15	7.916(-2)	1.226(-1)	1.925(0)	1.795(0)
10	0.31	7.474(-2)	1.175(-1)	1.862(0)	1.741(0)
15	0.46	6.797(-2)	1.094(-1)	1.762(0)	1.665(0)
20	0.61	5.966(-2)	9.900(-2)	1.629(0)	1.541(0)
25	0.77	5.079(-2)	8.694(-2)	1.471(0)	1.406(0)
30	0.92	4.238(-2)	7.406(-2)	1.297(0)	1.255(0)
35	1.06	3.535(-2)	6.112(-2)	1.113(0)	1.096(0)
40	1.21	3.045(-2)	4.883(-2)	9.290(-1)	9.347(-1)
45	1.35	2.813(-2)	3.773(-2)	7.508(-1)	7.771(-1)
50	1.50	2.854(-2)	2.820(-2)	5.847(-1)	6.295(-1)
55	1.63	3.155(-2)	2.046(-2)	4.348(-1)	4.935(-1)
60	1.77	3.675(-2)	1.455(-2)	3.040(-1)	3.723(-1)
65	1.90	4.351(-2)	1.039(-2)	1.937(-1)	2.670(-1)
70	2.03	5.113(-2)	7.415(-3)	1.040(-1)	1.779(-1)
75	2.15	5.883(-2)	6.463(-3)	3.392(-2)	1.044(-1)
80	2.28	6.591(-2)	6.180(-3)	-1.821(-2)	4.537(-2)
85	2.39	7.174(-2)	6.648(-3)	-5.463(-2)	-6.796(-4)
90	2.50	7.586(-2)	7.615(-3)	-7.785(-2)	-3.548(-2)

Table V

The exact and eikonal spin-flip amplitudes tabulated for helium at 100 Mev as a function of both centre of mass scattering angle and momentum transfer. The units are fm.

TABLE OF EXACT AND EIKONAL
SPIN-FLIP AMPLITUDES

taken from helium at 100 Mev

(The exponents of the numbers are shown in parentheses).

$\theta_{\text{c.m.}}$	$q_{\text{fm}^{-1}}$	Re(g) exact	Re(g) Glauber	Im(g) exact	Im(g) Glauber
0	0.0	0.0	0.0	0.0	0.0
5	0.15	-7.714(-2)	-5.091(-2)	1.241(-1)	1.183(-1)
10	0.31	-1.498(-1)	-9.884(-2)	2.400(-1)	2.290(-1)
15	0.46	-2.138(-1)	-1.411(-1)	3.405(-1)	3.255(-1)
20	0.61	-2.660(-1)	-1.756(-1)	4.199(-1)	4.025(-1)
25	0.77	-3.039(-1)	-2.010(-1)	4.745(-1)	4.566(-1)
30	0.92	-3.265(-1)	-2.165(-1)	5.031(-1)	4.864(-1)
35	1.06	-3.338(-1)	-2.223(-1)	5.067(-1)	4.928(-1)
40	1.21	-3.270(-1)	-2.194(-1)	4.880(-1)	4.782(-1)
45	1.35	-3.078(-1)	-2.091(-1)	4.513(-1)	4.463(-1)
50	1.50	-2.789(-1)	-1.930(-1)	4.016(-1)	4.017(-1)
55	1.63	-2.431(-1)	-1.730(-1)	3.441(-1)	3.488(-1)
60	1.77	-2.032(-1)	-1.507(-1)	2.836(-1)	2.922(-1)
65	1.90	-1.618(-1)	-1.277(-1)	2.244(-1)	2.356(-1)
70	2.03	-1.212(-1)	-1.053(-1)	1.696(-1)	1.821(-1)
75	2.15	-8.335(-2)	-8.433(-2)	1.215(-1)	1.336(-1)
80	2.28	-4.949(-2)	-6.553(-2)	8.130(-2)	9.166(-2)
85	2.39	-2.052(-2)	-4.921(-2)	4.937(-2)	5.668(-2)
90	2.50	3.142(-3)	-3.548(-2)	2.540(-2)	2.862(-2)

Table VI

The exact and eikonal non-spin-flip amplitudes tabulated for calcium at 500 Mev as a function of both centre of mass scattering angle and momentum transfer. The units are fm.

TABLE OF EXACT AND EIKONAL
NON-SPIN-FLIP AMPLITUDES

taken from calcium at 500 Mev

(The exponents of the numbers are shown in parentheses.)

$\theta_{\text{c.m.}}$	q fm^{-1}	Re(f) exact	Re(f) Glauber	Im(f) exact	Im(f) Glauber
0	0.00	-1.290(-1)	-1.310(1)	3.976(1)	4.101(1)
5	0.46	-5.328(0)	-5.158(0)	1.992(1)	1.990(1)
10	0.93	8.063(-1)	6.557(-1)	-1.856(-2)	-7.133(-2)
15	1.39	-1.377(-2)	-3.363(-2)	-7.210(-1)	-7.785(-1)
20	1.85	-8.837(-2)	-9.011(-2)	4.587(-2)	1.107(-1)
25	2.30	-8.697(-3)	1.794(-2)	5.670(-2)	2.514(-2)
30	2.75	1.816(-2)	3.546(-3)	-2.620(-2)	-9.922(-3)
35	3.20	-8.638(-3)	-1.506(-3)	1.273(-2)	-7.809(-4)
40	3.64	5.626(-3)	-1.029(-4)	-1.061(-2)	5.642(-4)
45	4.07	-4.805(-3)	9.660(-5)	8.871(-3)	7.646(-6)
50	4.50	4.099(-3)	4.172(-6)	7.609(-3)	3.170(-5)

Table VII

The exact and eikonal spin-flip amplitudes tabulated for calcium at 500 Mev as a function of both centre of mass scattering angle and momentum transfer. The units are fm.

TABLE OF EXACT AND EIKONAL
SPIN-FLIP AMPLITUDES

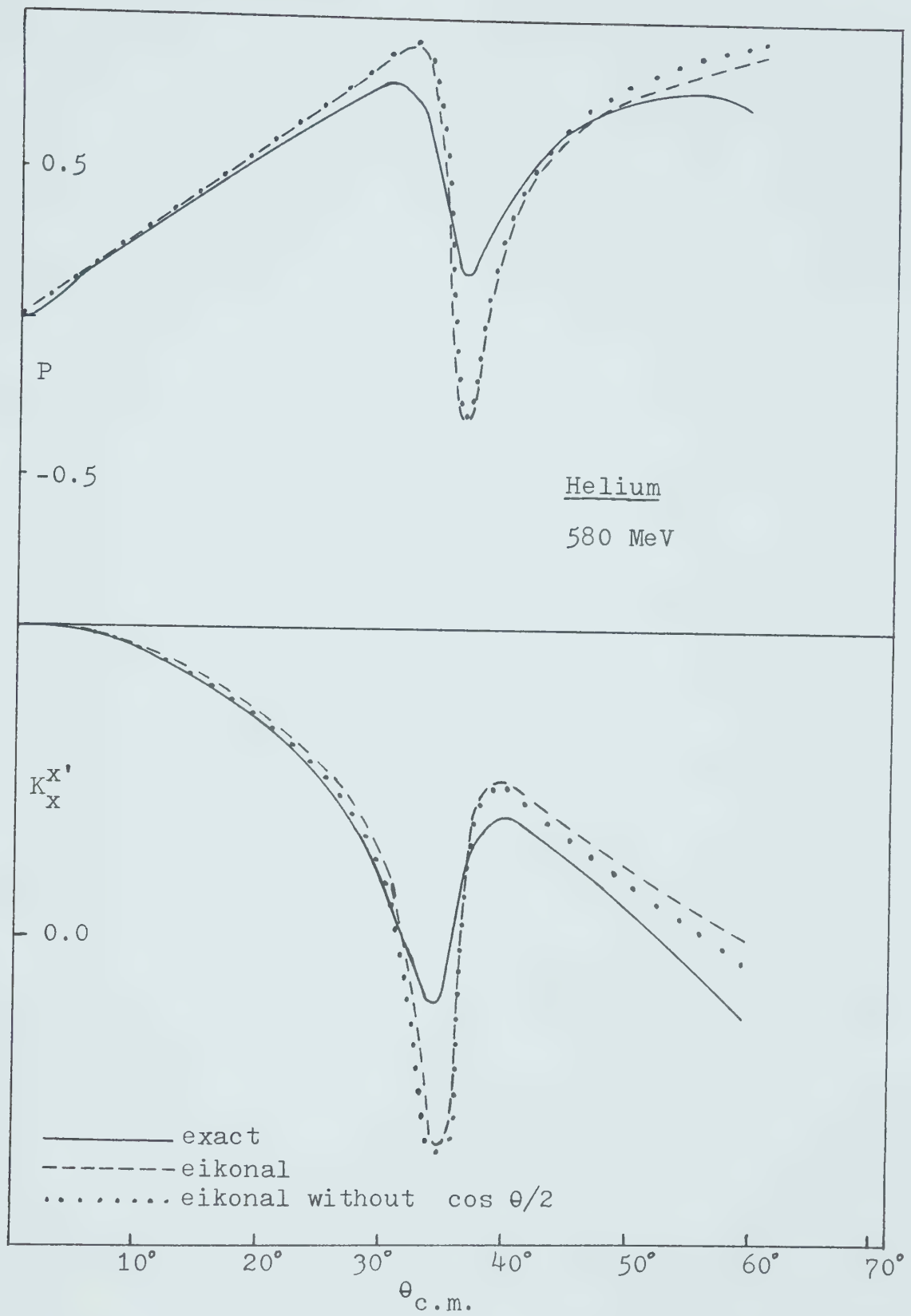
taken from calcium at 500 Mev

(The exponents of the numbers are shown in parentheses.)

$\theta_{\text{c.m.}}$	q	Re(g) exact	Re(g) Glauber	Im(g) exact	Im(g) Glauber
0	0.00	0.0	0.0	0.0	0.0
5	0.46	4.027(0)	4.344(0)	9.174(0)	9.447(0)
10	0.93	1.548(0)	1.465(0)	5.035(0)	4.231(0)
15	1.39	-9.575(-2)	-1.673(-1)	-8.724(-1)	-8.230(-1)
20	1.85	-9.667(-2)	-6.769(-2)	1.054(-1)	1.259(-1)
25	2.30	1.057(-2)	1.759(-2)	5.161(-2)	3.231(-2)
30	2.75	5.186(-3)	3.301(-3)	-2.220(-2)	-9.826(-3)
35	3.20	1.608(-3)	-1.411(-3)	1.263(-2)	-5.785(-4)
40	3.64	-2.284(-3)	-1.175(-4)	-1.117(-2)	5.621(-4)
45	4.07	1.335(-3)	8.691(-5)	8.890(-3)	4.444(-6)
50	4.50	-7.672(-4)	2.871(-6)	-6.337(-3)	-2.872(-5)

fig 28

The polarisation and P.T.C. curves calculated exactly and in the eikonal approximation, showing the effect of the $\cos \theta/2$ factor. The calculations are made for helium at 580 Mev.



CHAPTER V
CONCLUSION

The Glauber eikonal approximation has been studied at intermediate energies i.e. (0.1 Gev to 1.0 Gev). The study has been undertaken using a modified Gaussian potential rather than the more conventional Woods-Saxon potential. The former is chosen for its simplicity.

Most earlier analyses were done using only central real potentials. In this study we use a more realistic complex potential with the added important feature of including the rather inevitable spin-orbit interaction. This enables us to study the behaviour of spin dependant observables such as polarisation and polarisation transfer coefficients. From the results of the study we may tentatively draw some conclusions.

It seems that the performance of the approximation does not significantly improve as one increases the energy from the 500 Mev range to the 1000 Mev range. The optical potentials used in this study mimic realistic optical potentials in being weaker at the lower energy, this may explain the low energy success.

Generally one finds that the approximation fails at a smaller momentum transfer in the 100 Mev region than for the higher energy regions studied.

On average the polarisation and polarisation transfer coefficient reproduction were much the same, the approximation tending to break down at momentum transfer very roughly around 60% of that at which the reproduction of the cross-

section fails, but this varies considerably from case to case.

It bears repeating at this point that what constitutes a failing of the approximation is a subjective matter. Nevertheless a table where the significant deviations set in is given in Chapter IV (table III). From the table the following trends emerge. It is seen that for a specific nucleus, increasing the energy tends to decrease the angular range of the approximation, but increases the amount of momentum transfer reproduced. The lowest points of failure found in this study are at 10 and 0.5 fm^{-1} for the centre of mass scattering angle and momentum transfer respectively.

An extra factor was found multiplying the spin-flip amplitude, which was not present in previous works. Formally the presence of this factor ($\cos \theta/2$) is desirable since it leads to the expected reduction from Glauber to Born approximations in the limit of very weak potential strengths and a vanishing polarisation at 180° . The effect of the factor on the accuracy of the approximation was found to be small, it's presence neither consistently worsening nor improving the approximation.

For scattering off helium the results of (DY77) that the eikonal approximation produces diffraction minima which are too deep are reproduced. Their study also uses the profile functions from the multiple scattering to obtain an optical potential on which an exact calculation gives a good fit to the data. This indicates that the simple eikonal

approximation is not doing too well in the intermediate energy region for helium. However as shown in (GI74), the eikonal approximation does well in this region with the Wallace corrections.

For calcium this study has shown one may trust the eikonal approximation only as far as the first minimum if one considers polarisation, but the cross-section alone is generally reproduced up to the second minimum.

For lead the approximation seems to be doing surprisingly well, reproducing four minima of cross-section, polarisation and polarisation transfer coefficient fail early for the lower energy but are reproduced well for the higher energies -- spectacularly so at 500 Mev.

Thus we may conclude that the Glauber eikonal approximation must be used with caution at intermediate energies, especially where the observable in question fluctuates rapidly since the approximation has difficulty in reproducing minima.

Whether one should use the simple eikonal approximation or use corrections to it for a certain case is an open question. The accuracy in the case of helium is significantly improved by the Wallace corrections or by means of an intermediate optical potential, however much simplicity is lost; and so the final decision must be made by the requirements of accuracy imposed upon the approximation.

REFERENCES

- AB64 M. Abramowitz and I.A. Stigun. Handbook of Mathematical Functions. U.S. National Bureau of Standards. (1964)
- AD65 T. Adachi and T. Kotani. Supp. Prog. T. Phys. S.I.65 (1965) 316.
- AL76 Saclay Group. (G.D. Alkhazov et al.) Nucl. Phys. A262 (1976) 443.
- AS76 Saclay Group. (Aslanides et al.)(private communication) (1976)
- AU76 J.P. Auger, J. Gillespie and R.J. Lombard. Nucl. Phys. A262 (1976) 372
- BA73 A. Baker. Phys. Rev. D8 (1973) 1937
- BE73 R. Bertini et al. Phys. Lett. 45B (1973) 119
- BL61 R. Blankenbecler and M.L. Goldberger. Phys. Rev. 126 (1961) 766.
- BL76 M. Bleszynski and T. Jaroszewich. Nucl. Phys. A256 (1976) 429.
- B072 Berkeley Group. (E.T. Boshitz et al.) Phys. Rev. C6 (1972) 457.
- BR75 I. Brissaud, L. Bimbot, Y. LeBornec, B. Tatischeff and N. Willis. Phys. Rev. C8 (1975) 1537.
- BY73 F.W. Byron, C.J. Joachain and E.H. Mund. Phys. Rev. D8 (1973) 2622.
- DE74 A. Deshalit and H. Feshbach. Nuclear Structure. John Wiley and Sons (1974)
- DY77 R. Dymarz and A. Malecki. Phys. Lett. 66B#5 (1977) 413.
- FR67 R.F. Frosh, J.S. McCarthy, R.E. Rand and M.R. Yearian. Phys. Rev. 160 (1967) 874.
- GI75 J. Gillespie, C. Gustafsson and R.J. Lombard. Nucl. Phys. A242 (1975) 481.
- GL55 R.J. Glauber. Phys. Rev. 100 (1955) 242.
- GL59 R.J. Glauber. Lect. Theo. Phys. 1 ed. W.C. Brittin, Wiley Interscience (195()) 315

- GL70 R.J. Glauber and G. Matthiae. Nucl. Phys. B21 (1970) 135.
- G068 Berkeley Group. (K. Gotow et al.) Phys. Rev. Lett. 21 (1968) 1816.
- HA69 Y. Hahn. Phys. Rev. 184 (1969) 1022.
- HA70 Y. Hahn. Phys. Rev. C3 (1970) 775.
- HA73 Y. Hahn. Phys. Rev. C5 (1973) 1672.
- H063 P.E. Hodgson. The Optical Model of Elastic Scattering. Oxford University Press (1963).
- IN73 A. Ingermarsson, E. Hagberg and H.S. Sherif. Nucl. Phys. A216 (1973) 271.
- JA70 D. Jackson. Nuclear Reactions. Methuen and Co. Ltd. (1970)
- KA72 A.N. Kamal. Can. J. Phys. 50 (1972) 1862.
- MA54 J.M. Malenka. Phys. Rev. 95 (1954) 522.
- MO47 G. Moliere Z. Fur Naturf. 2A (1947) 133.
- OE76 A.E. Van Oers, H. Haw and N.E. Davison. Phys. Rev. C10 (1975) 207.
- OH72 G.G. Ohlsen. Rep. Prog. Phys. 35 (1972) 717.
- OS70 T. Osborn. Ann. Phys. 58 (1970) 417.
- RA71 M. Razavy. Can. J. Phys. 49 (1971) 1885.
- RA74 M. Razavy and R. Teshima. Nucl. Phys. A235 (1974) 278.
- RA76 M. Razavy and F.C. Salevsky. Nuove Cim. 33B (1976).
- RO67 L. Rodberg and R.M. Thaler. Introduction to the Quantum Theory of Scattering. Academic Press (1967).
- RO69 P. Robson. The Theory of Polarisation Phenomina. Oxford University Press (1969).

- SA57 D.S. Saxon and L.I. Schiff. Nuove Cim. 6 (957)
614
- SC56 L.I. Schiff. Phys. Rev. 103 (1956) 443.
- SE47 R. Serber. Phys. Rev. 72 (1947) 1008.
- SH68 H.S. Sherif. Thesis (Washington University) (1968).
- SU69 R.L. Sugar and R. Blankenbecler. Phys. Rev. 183
(1969) 1387.
- WA53 K.M. Watson. Phys Rev. 89 (1953) 575.
- WA70 S.J. Wallace. Thesis (Washington University) (1970).
- WA71 S.J. Wallace. Phys. Rev. Lett. 27 (1971) 622.
- WA77 S.J. Wallace and Y. Alexander. (To be published).
- WH68 A.D. Wheelon. Tables of Summable Series and
Integrals involving Bessel Functions. Holden Day
Advanced Physics Monographs (1968).

APPENDIX A

Total Cross Sections

In this appendix are calculated the total cross section, the scattering cross section and the reaction cross section. The physical interpretation of these quantities is well known and is expounded upon in great length in almost any book on quantum theory -- for example (R067).

A brief summary of the quantities is given. A particle is said to have been scattered during a process, if its state after the process is different from that before the process. Here the word state refers to both the internal state of the particle and also the momentum state of the centre of mass of the particle. A particle is said to have been elastically scattered if it has been scattered and its energy is the same in the final state as in the initial state.

The total cross section is defined as the ratio of the number of particles scattered per target particle to the number of incident particles per unit area. It is denoted by σ_T

The elastic scattering cross section is defined as the number of particles elastically scattered per target particle to the number of incident particles per unit area. It is denoted by σ_{SC} .

The reaction cross section is defined as the ratio of the number of particles scattered, by processes other than elastic scattering, per nucleus, to the number of incident particles per unit area. It is denoted by σ_R .

The above definitions imply the following relationship

$$\sigma_T = \sigma_R + \sigma_{SC} \quad (226)$$

The total cross section gives a measure of the number of particles deflected from their forward motion and is therefore related to the forward scattering amplitude. The relationship is the Optical Theorem (RO67).

$$\sigma_T = \frac{4\pi \operatorname{Im}}{k(2s+1)} (\operatorname{tr} M) \quad (227)$$

where \underline{k} is the wavevector of the particle and s is the spin of the particle.

$$\sigma_T = \frac{4\pi}{k} \operatorname{Im} f(0) \quad . \quad (228)$$

The scattering cross section is obtained by summing the probability of scattering into a certain angle over all angles.

The probability density of elastic scattering at angle θ from spin state μ to spin state ν is given by

$$|M_{\mu\nu}(\theta)|^2 \quad (229)$$

Thus to get the total probability of elastic scattering, we must average over the initial states and sum over the final states.

$$\sigma_{SC} = \frac{1}{2} \sum_{\mu=1}^2 \sum_{\nu=1}^2 \int_0^{2\pi} \int_0^{\pi} |M_{\mu\nu}(\theta)|^2 d\Omega \quad (230)$$

$$\sigma_{SC} = \frac{1}{2} \int \left\{ |f(\theta)|^2 + |ig(\theta)|^2 + |-ig(\theta)|^2 + |f(\theta)|^2 \right\} d\Omega \quad (231)$$

$$\sigma_{SC} = \int (|f(\theta)|^2 + |g(\theta)|^2) d\Omega \quad (232)$$

where $d\Omega$ is $\sin \theta d\theta d\phi$.

σ_R is most easily calculated by subtracting the above expression for σ_{SC} from σ_T .

The exact calculation of cross sections

We obtain the total cross section from unitarity. Specifically using the Optical Theorem

$$\sigma_T = \frac{4\pi}{k} \text{Im } f(\theta) \quad (233)$$

on our amplitudes

$$f(\theta) = \frac{1}{k} \sum_{l=0}^{\infty} \left\{ (l+1) e^{i\delta_l^+} \sin \delta_l^+ + l e^{i\delta_l^-} \sin \delta_l^- \right\} P_l(\cos \theta) \quad (234)$$

$$g(\theta) = \frac{1}{2k} \sum_{l=0}^{\infty} \left\{ e^{2i\delta_l^+} - e^{2i\delta_l^-} \right\} P_l^1(\cos \theta) \quad (235)$$

which gives

(236)

$$\sigma_T = \frac{4\pi}{k^2} \sum_{l=0}^{\infty} \text{Im} \left\{ (l+1) e^{i\delta_l^+} \sin \delta_l^+ + l e^{i\delta_l^-} \sin \delta_l^- \right\}.$$

It must be remembered that in optical model analyses a complex potential is employed, which gives rise to phase shifts which in turn will be complex.

To obtain the scattering cross-section we use equa-

tion (232). Splitting this into two parts and using the expression for $f(\theta)$ and $g(\theta)$, we get

$$\sigma_{SC}^f = \int |f|^2 d\Omega \quad (237)$$

$$= \frac{1}{k^2} \sum_{l=0}^{\infty} \sum_{l'=0}^{\infty} \left\{ (l+1) e^{i\delta_l^+} \sin \delta_l^+ + l e^{i\delta_l^-} \sin \delta_l^- \right\} \\ \left\{ (l'+1) e^{i\delta_{l'}^+} \sin \delta_{l'}^+ + l' e^{i\delta_{l'}^-} \sin \delta_{l'}^- \right\} \quad (238)$$

$$\iint_{\phi=0}^{2\pi} P_l(\cos \theta) P_{l'}(\cos \theta) \sin \theta d\theta d\phi .$$

The integral gives $\frac{4\pi \delta_{ll'}}{2l+1}$. Therefore

$$\sigma_{SC}^f = \frac{4\pi}{k^2} \sum_{l=0}^{\infty} \frac{|(l+1) e^{i\delta_l^+} \sin \delta_l^+ + l e^{i\delta_l^-} \sin \delta_l^-|^2}{2l+1} \quad (239)$$

$$\sigma_{SC}^g = \int |g|^2 d\Omega \quad (240)$$

$$= \frac{1}{(2k)^2} \sum_{l=0}^{\infty} \sum_{l'=0}^{\infty} \left(e^{2i\delta_l^+} - e^{2i\delta_l^-} \right) \left(e^{-2i\delta_{l'}^+} - e^{-2i\delta_{l'}^-} \right) \quad (241)$$

$$\iint_{\phi=0}^{2\pi} P_l^1(\cos \theta) P_{l'}^1(\cos \theta) \sin \theta d\theta d\phi .$$

The integral gives $4\pi \frac{l(l+1)}{2l+1} \delta_{ll'}$. Therefore

$$\sigma_{SC}^g = \frac{\pi}{k^2} \sum_{l=0}^{\infty} \frac{l(l+1)}{2l+1} |e^{2i\delta_l^+} - e^{2i\delta_l^-}|^2 . \quad (242)$$

Now we use the identity

$$e^{2i\delta_l^+} - e^{2i\delta_l^-} = 2i \left\{ e^{i\delta_l^+} \sin \delta_l^+ - e^{i\delta_l^-} \sin \delta_l^- \right\} \quad (243)$$

and obtain

$$\sigma_{SC} = \sigma_{SC}^f + \sigma_{SC}^g = \frac{4\pi}{k^2} \sum_{l=0}^{\infty} \frac{1}{(2l+1)} \chi_l \quad (244)$$

$$\begin{aligned} \text{where } \chi_l = & |(l+1)e^{i\delta_l^+} \sin\delta_l^+ + l e^{i\delta_l^-} \sin\delta_l^-|^2 \\ & + l(l+1)|e^{i\delta_l^+} \sin\delta_l^+ - e^{i\delta_l^-} \sin\delta_l^-|^2. \end{aligned} \quad (245)$$

The expression for χ_l may be simplified, getting

$$\sigma_{SC} = \frac{4\pi}{k^2} \sum_{l=0}^{\infty} \left[(l+1) |e^{i\delta_l^+} \sin\delta_l^+|^2 + l |e^{i\delta_l^-} \sin\delta_l^-|^2 \right]. \quad (246)$$

The Glauber Approximation

The scattering cross-section

We evaluate the expression

$$\int (|f(\theta)|^2 + |g(\theta)|^2) d\Omega \quad (247)$$

in the eikonal approximation.

Evaluating the expression

$$\sigma^f \equiv \int |f(\theta)|^2 d\Omega = \int f(\theta) f^*(\theta) d\Omega \quad (248)$$

and using the expression

$$f(\theta) = \frac{ik}{2\pi} \int e^{i\mathbf{q} \cdot \mathbf{b}} \Gamma_c(\mathbf{b}) d^2b \quad (249)$$

we get

$$\sigma^f = \int d\Omega' \left(\frac{ik}{2\pi} e^{i\mathbf{q} \cdot \mathbf{b}} \Gamma_c(\mathbf{b}) d^2b \right) \left(-\frac{ik}{2\pi} \int e^{-i\mathbf{q} \cdot \mathbf{b}'} \Gamma_c^*(\mathbf{b}') d^2b' \right) \quad (250)$$

$$= \frac{k^2}{4\pi^2} \iint \Gamma_c(\mathbf{b}) \Gamma_c^*(\mathbf{b}') d^2b d^2b' \left[\int_{\text{sphere}} e^{i\mathbf{q} \cdot (\mathbf{b} - \mathbf{b}')} d\Omega_f \right]. \quad (251)$$

The term in the brackets may be evaluated using an approximation. The integration is of course carried out over the angle made by the final wave-vector, which means \underline{k}_i is effectively a constant for this integration. The brackets become

$$e^{i\underline{k}_i \cdot (\underline{b} - \underline{b}')} \int_{\text{sphere}} e^{-i\underline{k}_f \cdot (\underline{b} - \underline{b}')} d\Omega_f \quad (252)$$

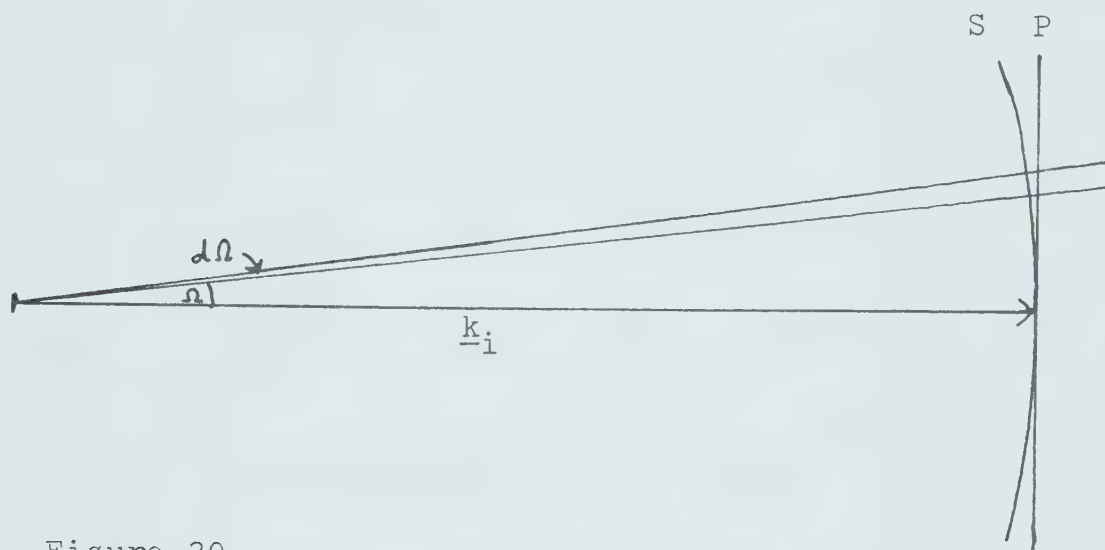


Figure 30

We are integrating over the sphere S at present, but for small angle scattering integration over S is approximately the same as integration over the plane P . Since in the eikonal approximation we always assume small angles, then we may make the replacement, obtaining, for the bracketed term;

$$e^{i\underline{k}_i \cdot (\underline{b} - \underline{b}')} \int e^{-i\underline{k}_f \cdot (\underline{b} - \underline{b}')} \frac{d^2 k_f}{|\underline{k}_i|^2} \cdot \quad (253)$$

(The volume element in the plane is $d^2 k_f$, on the sphere it is $|\underline{k}_i|^2 d\Omega_f$.)

We can simplify to obtain

$$\frac{e^{i\mathbf{k}_i \cdot (\mathbf{b}-\mathbf{b}')}}{k^2} (2\pi)^2 \delta(\mathbf{b}-\mathbf{b}') = \frac{4\pi^2}{k^2} (\mathbf{b}-\mathbf{b}'). \quad (254)$$

Substituting this back into (251) gives

$$\sigma^f = \int |\Gamma_c(\mathbf{b})|^2 d^2b. \quad (255)$$

Evaluating the expression

$$\sigma^g \equiv \int |g(\theta)|^2 d\Omega. \quad (256)$$

using the expression for g

$$g(\theta) = -\frac{k}{2\pi} \int e^{i\mathbf{q} \cdot \mathbf{b}} \sin \phi \Gamma_s(\mathbf{b}) d^2b, \quad (257)$$

which comes from equation (111), we get

$$\sigma^g = \int_{\text{sphere}} \left(-\frac{k}{2\pi} \int e^{i\mathbf{q} \cdot \mathbf{b}} \Gamma_s(\mathbf{b}) \sin \phi d^2b \right) \quad (258)$$

$$\left(-\frac{k}{2\pi} \int e^{-i\mathbf{q} \cdot \mathbf{b}'} \Gamma_s^*(\mathbf{b}') \sin \phi' d^2b' \right) d\Omega_f \quad (259)$$

$$= \frac{k^2}{4\pi^2} \int \Gamma_s(\mathbf{b}) \Gamma_s^*(\mathbf{b}') \sin \phi \sin \phi' d^2b d^2b' \left\{ \int_{\text{sphere}} e^{i\mathbf{q} \cdot (\mathbf{b}-\mathbf{b}')} d\Omega_f \right\}$$

Now, using the same approximation as before for the term in the brackets, we get

$$\sigma^g = \int \Gamma_s(\mathbf{b}) \Gamma_s^*(\mathbf{b}') \sin \phi \sin \phi' d^2b d^2b' \delta(\mathbf{b}-\mathbf{b}') \quad (260)$$

$$\sigma^g = \int |\Gamma_s(\mathbf{b})|^2 \sin^2 \phi d^2b. \quad (261)$$

The optical theorem (228) gives

$$\sigma_T = \frac{4\pi}{k} \operatorname{Im} \left[\frac{ik}{2\pi} \int e^{i\mathbf{q} \cdot \underline{b}} \Gamma_c(\underline{b}) d^2b \right] \quad (262)$$

$$\sigma_T = \int [2\operatorname{Re} \Gamma_c(\underline{b})] d^2b . \quad (263)$$

Adding (255) and (261) we obtain

$$\sigma_{SC} = \int (|\Gamma_c(\underline{b})|^2 + |\Gamma_s(\underline{b})|^2 \sin^2\phi) d^2b . \quad (264)$$

The reaction cross-section is obtained by subtracting equation (264) from (263) to obtain

$$\sigma_R = \int (2\operatorname{Re} \Gamma_c(\underline{b}) - |\Gamma_c(\underline{b})|^2 - |\Gamma_s(\underline{b})|^2 \sin^2\phi) d^2b \quad (265)$$

$$= \int (\Gamma_c(\underline{b}) + \Gamma_c^*(\underline{b}) - \Gamma_c(\underline{b})\Gamma_c^*(\underline{b}) - |\Gamma_s(\underline{b})|^2 \sin^2\phi) d^2b \quad (266)$$

$$= \int \left(1 - |1 - \Gamma_c(\underline{b})|^2 - |\Gamma_s(\underline{b})|^2 \sin^2\phi \right) d^2b . \quad (267)$$

Equations (263), (264), and (265) give the eikonal results for cross-sections. They may each be evaluated in a similar manner, and so only the result for σ_R is obtained here.

The other two results are quoted.

Reaction Cross-Section

Making the assumption of azimuthal symmetry for the potential in equation (267), and using equations (102) and (103), we obtain

$$\sigma_R = \int_0^{2\pi} \int_0^\infty \left\{ 1 - |e^{i\chi_c(b)} \cos(kb\chi_s(b))|^2 - |e^{i\chi_c(b)} \sin(kb\chi_s(b))|^2 \sin^2\phi \right\} b db d\phi \quad (268)$$

$$= 2\pi \int \left\{ 1 - |e^{i\chi_c(b)} \cos(kb\chi_s(b))|^2 - \frac{1}{2} |e^{i\chi_c(b)} \sin(kb\chi_s(b))|^2 \right\} b db . \quad (269)$$

Now, using equations (155a) and (155b) this becomes

$$\sigma_R = 2\pi \int_0^\infty \left(1 - e^{A_c} e^{-\alpha b^2} \cdot e^{A_c^*} e^{-\alpha b^2} \left\{ |\cos(bA_s e^{-\alpha b^2})|^2 + \frac{1}{2} |\sin(bA_s e^{-\alpha b^2})|^2 \right\} \right) b \, db \quad (270)$$

$$= 2\pi \int_0^\infty b \, db \left(1 - e^{A_c} e^{-\alpha b^2} e^{A_c^*} e^{-\alpha b^2} \left\{ \cos(bA_s e^{-\alpha b^2}) \cos(bA_s^* e^{-\alpha b^2}) + \frac{1}{2} \sin(bA_s e^{-\alpha b^2}) \sin(bA_s^* e^{-\alpha b^2}) \right\} \right) \quad (271)$$

$$\sigma_R = \pi \int b \, db \left(2 - e^{(A_c + A_c^*)} e^{-\alpha b^2} \left\{ \cos(b(A_s + A_s^*) e^{-\alpha b^2}) + \cos(b(A_s - A_s^*) e^{-\alpha b^2}) + \frac{1}{2} \cos(b(A_s - A_s^*) e^{-\alpha b^2}) - \frac{1}{2} \cos(b(A_s + A_s^*) e^{-\alpha b^2}) \right\} \right) \quad (272)$$

Introduce

$$\sigma_R = \sigma_R(A_s) + \sigma_R(-A_s). \quad (273)$$

$$\sigma_R(A_s) = \frac{\pi}{2} \int_0^\infty b \, db \left(2 - \frac{3}{2} e^{[(A_c + A_c^*) + ib(A_s - A_s^*)]} e^{-\alpha b^2} - \frac{1}{2} e^{[(A_c + A_c^*) + ib(A_s + A_s^*)]} e^{-\alpha b^2} \right) \quad (274)$$

$$= \pi \int_0^\infty b \, db \sum_{r=1}^\infty \left(-\frac{3}{4r!} [(A_c + A_c^*) + ib(A_s - A_s^*)]^r e^{-\alpha r b^2} - \frac{1}{4r!} [(A_c + A_c^*) + ib(A_s + A_s^*)]^r e^{-\alpha r b^2} \right) \quad (275)$$

Since the integral couldn't have been done analytically, we had to expand. The series is uniformly convergent for all $0 \leq b \leq \infty$, thus we may interchange sum and integral to obtain

an expression which still defies analytic integration, however upon further expansion the integrals may be performed to obtain the expression for σ_R .

$$\sigma_R = -\frac{\pi}{4} \sum_{r=1}^{\infty} \sum_{s=0}^{\left[\frac{r}{2}\right]} \frac{(A_c + A_c^*)^{r-2s} (-1)^s s!}{(2s)! (r-2s)! (\alpha r)^{s+1}} \left\{ 3(A_s - A_s^*)^{2s} + (A_s + A_s^*)^{2s} \right\}. \quad (276)$$

The total and scattering cross-sections may be evaluated in a similar manner to obtain the results

$$\begin{aligned} \sigma_{SC} = \frac{\pi}{4} \sum_{r=1}^{\infty} \sum_{k=0}^{\frac{r}{2}} \frac{(-1)^k k!}{(2k)! (r-2k)! (\alpha r)^{k+1}} & \left\{ (A_c + A_c^*)^{r-2k} ((A_s + A_s^*)^{2k} \right. \\ & \left. + 3(A_s - A_s^*)^{2k}) - 8\text{Re}[(A_c)^{r-2k} A_s^{2k}] \right\} \end{aligned} \quad (277)$$

and

$$\sigma_T = -2\pi \sum_{r=1}^{\infty} \sum_{k=0}^{\left[\frac{r}{2}\right]} \frac{(-1)^k k! \text{Re}[(A_c)^{r-2k} A_s^{2k}]}{(2k)! (r-2k)! (\alpha r)^{k+1}}. \quad (278)$$

APPENDIX B

Matching Woods-Saxon Potentials to Gaussian Potentials

We attempt here to give a prescription whereby, given a Woods-Saxon potential, we match it with a Gaussian potential so that it will have similar scattering properties.

There are several physical characteristics that one may wish to equate. They are

- (i) the volume integral,
- (ii) the r.m.s. radius,
- (iii) the potential gradients at the nuclear surface
- (iv) the depth,
- (v) the strength at the nuclear surface.

The analytic forms of the potentials matched are:

$$(v_o + iw_o)e^{-\alpha r^2}(1 + \rho r^2) + (v_{s.o.} + iw_{s.o.})e^{-\alpha r^2}(1 + \rho r^2) \quad \underline{\sigma.L}$$

and

$$\frac{(v_o + iw_o)}{1 + e^{r-R/a}} + (v_{s.o.} + iw_{s.o.}) \frac{1}{r} \frac{d}{dr} \frac{1}{1 + e^{r-R/a}} \quad \underline{\sigma.L}.$$

Often only expressions for $\rho = 0$ will be given; however, all formulae that are used in this study are given.

(i) The Volume Integral

Woods-Saxon

$$J_{WS} = \int \frac{v}{1 + e^{r-R/a}} d^3r = \frac{4\pi}{3} v \left[R(R^2 + \pi^2 a^2) - 6a^3 \sum_{r=1}^{\infty} \frac{(-)^r}{r^3} e^{-rR/a} \right]$$

Gaussian

$$J_G = \int v e^{-\alpha r^2} d^3r = \frac{4\pi v}{4\alpha} \sqrt{\frac{\pi}{\alpha}}$$

Woods-Saxon Spin-Orbit

$$J_{SWS} = \int v_{s.o.} \frac{1}{r} \frac{d}{dr} \left(\frac{1}{1 + e^{r-R/a}} \right) d^3r = -4\pi v_{s.o.} (R + a \ln(1 + e^{-R/a}))$$

Gaussian Spin-Orbit

$$J_{SG} = \int v_{s.o.} \frac{1}{r} \frac{d}{dr} (e^{-\alpha r^2}) d^3r = -4\pi v_{s.o.} \sqrt{\frac{\pi}{\alpha}}$$

Modified Gaussian

$$J_{MG} = \int v (1 + \rho r^2) e^{-\alpha r^2} d^3r = \frac{4\pi v}{8\alpha^2} \sqrt{\frac{\pi}{\alpha}} (2\alpha + 3\rho)$$

Modified Woods-Saxon

$$J_{MWS} = \int \frac{v (1 + \rho r^2)}{1 + e^{r-R/a}} d^3r = \frac{4\pi v}{3} \left[R(R^2 + \pi^2 a^2) - 6a^3 \sum_{r=1}^{\infty} \frac{(-)^r e^{-rR/a}}{r^3} \right] \\ + \frac{4\pi \rho v}{15} \left[R(3R^4 + 10\pi^2 a^2 R^2 + 7\pi^4 a^4) - 360a^5 \sum_{r=1}^{\infty} \frac{(-)^r}{r^5} e^{-rR/a} \right]$$

(ii) The R.M.S. RadiusWoods-Saxon

$$\langle r^2 \rangle^{\frac{1}{2}} = J_{WS}^{-1} \frac{4\pi v}{15} \left[R(3R^4 + 10\pi^2 a^2 R^2 + 7\pi^4 a^4) - 360a^5 \sum_{r=1}^{\infty} \frac{(-)^r}{r^5} e^{-rR/a} \right]$$

Gaussian

$$\langle r^2 \rangle^{\frac{1}{2}} = J_G^{-1} 4\pi v \frac{3}{8\alpha^2} \sqrt{\frac{\pi}{\alpha}}$$

Modified Gaussian

$$\langle r^2 \rangle^{\frac{1}{2}} = 4\pi v \frac{3}{16\alpha^3} \sqrt{\frac{\pi}{\alpha}} (2\alpha + 5\rho) J_{MG}^{-1}$$

(iii) Potential Gradients at the Nuclear SurfaceWoods-Saxon

$$\left. \frac{d}{dr} \left(\frac{v}{1 + e^{r-R/a}} \right) \right|_{r=R} = -\frac{v}{4a}$$

Modified Woods-Saxon

$$\left. \frac{d}{dr} \left(\frac{v (1 + \rho r^2)}{1 + e^{r-R/a}} \right) \right|_{r=R} = \frac{1}{4a} (\rho R (4a - R) - 1)$$

Gaussian

$$\left. \frac{d}{dr} \left(v e^{-\alpha r^2} \right) \right|_{r=R} = -2\alpha R v e^{-\alpha R^2}$$

Modified Gaussian

$$\left. \frac{d}{dr} \left(v (1 + \rho r^2) e^{-\alpha r^2} \right) \right|_{r=R} = -2v e^{-\alpha R^2} R (\alpha + \rho (\alpha R^2 - 1))$$

(iv) and (v) The Depths and Strengths at Nuclear Surfaces

These are found by evaluating the potential function at $r = 0$ and $r = R$ respectively.

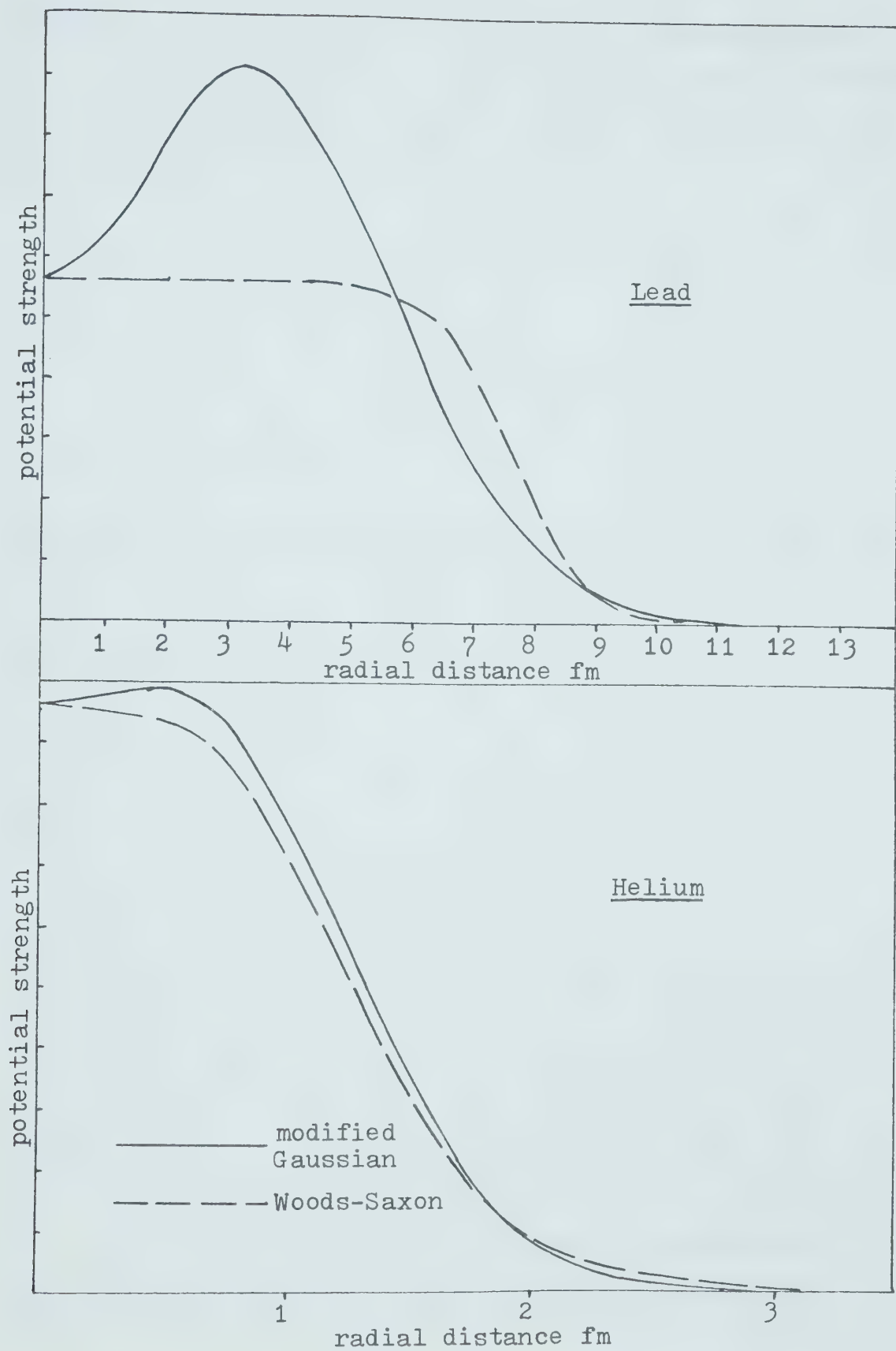
General

It was found during the study that matching potentials was satisfactory for light nuclei. The criteria for a Woods-Saxon potential to be well matched by a (modified) Gaussian is that R/a should be small. The critical value of this parameter is around 6 above which the match is unsatisfac-

tory, For example, consider the best matches obtained for helium ($R/a = 3.6$) and lead ($R/a = 12$):

fig 29

The successes and failures of matching short and long range Woods-Saxon potentials by a modified Gaussian potential. The solid and dashed lines are the modified Gaussian and Woods-Saxon potentials respectively.



APPENDIX C

Summary of Tests Performed on the Calculation and Program

Three separate checks were performed, each to calculate the scattering amplitudes from a different potential. The potentials were

$$(i) (v_0 + iw_0)e^{-\alpha r^2} + (v_{s.o.} + iw_{s.o.})e^{-\alpha r^2} \underline{\sigma} \cdot \underline{L} ,$$

$$(ii) (v_0 + iw_0)e^{-\alpha r^2} (1 + \rho r^2) .$$

$$+ (v_{s.o.} + iw_{s.o.})e^{-\alpha r^2} (1 + \rho r^2) \underline{\sigma} \cdot \underline{L} ,$$

$$(iii) v_0 e^{-\alpha r^2} (1 + \rho r^2) .$$

These give rise to expressions for five scattering amplitudes:

$$f_1(\theta), \quad f_2(\theta), \quad f_3(\theta), \quad g_1(\theta), \quad \text{and} \quad g_2(\theta).$$

The following reductions are found:

$$f_2 \rightarrow f_1 \quad \text{as} \quad \rho \rightarrow 0 ,$$

$$f_3 \rightarrow f_1 \quad \text{as} \quad \rho \rightarrow 0 ,$$

$$g_2 \rightarrow g_1 \quad \text{as} \quad \rho \rightarrow 0 ,$$

$$f_2 \rightarrow f_3 \quad \text{as} \quad v_{s.o.} + iw_{s.o.} \rightarrow 0 ,$$

$$f_1 \rightarrow f_3 \leftrightarrow f_2 \quad \text{as} \quad (\rho; v_{s.o.}; iw_{s.o.}) \rightarrow 0 .$$

Three separate Born approximations were performed, and the results compared to the first term ($r = 1$) in the series for f_1 , f_2 , f_3 , g_1 , and g_2 . Providing one keeps the $\cos \theta/2$ factor in the g terms, then it was found that the $r = 1$ term was identical to the first term in the Born series.

In his thesis (WA70) Wallace gives the expression for the scattering amplitude from a potential of the form

$$V_0 e^{-\alpha r^2}$$

This expression is reproduced by;

$$\begin{aligned} f_1 & \text{ if } w_0, v_{s.o.}, w_{s.o.} \rightarrow 0 \\ f_2 & \text{ if } w_0, v_{s.o.}, w_{s.o.}, \rho \rightarrow 0 \\ f_3 & \text{ if } \rho \rightarrow 0 \end{aligned}$$

From each of the three separate calculations three computer programs were constructed, and tests were performed upon the numerical results obtained from them.

Under the reductions described in the previous section of this appendix, the programs produced identical results.

For each of the programs the first (and simplest) term was evaluated. This number tallied exactly with the results obtained from a hand calculation using the first Born approximation. The calculation was repeated for angles from 0° to 180° in steps of 5° and the tally between results was still found to be exact.

For the first program the third and fifth terms were evaluated by hand, these, too, tallied with those obtained from the program.

If one chooses to match a Gaussian potential by a Woods-Saxon potential, this may be done very closely (as opposed to the other way round!) and upon using the section of the first program to compute exact scattering amplitudes, then the amplitudes were found to be close.

It was found that in the high energy limit, and for small angles, that the Born and eikonal results were close, as they should be.

Wallace's (WA72) results of comparison of exact and eikonal calculations appear to be reproduced, although Wallace only gives a graph, there is no visible deviation between the two sets of results.

Y. Hahn in a series of three papers (HA69) (HA70) (HA73) has done fairly extensive tests of the eikonal approximation, and has numerical results tabulated for the scattering amplitude obtained from a potential of the form

$$V_c e^{-\alpha r^2} (1 + \rho r^2).$$

His eikonal approximation results are reproduced by programs (ii) and (iii), his exact calculations are almost reproduced, the small difference between exact calculations being thought to stem from a small error in his calculation, possible (but not checked) taking too few phase shifts.

So far the tests have always been on the non-spin-flip scattering amplitude. No references found seem to give numerical results for the spin-flip amplitudes, except (BR75) which uses a Woods-Saxon potential.

We discuss next a test performed to check the spin-flip amplitude.

Relation between the two scattering amplitudes

For a spherically symmetric potential

$$f(\theta) = ik \int_0^{\infty} J_0(qb) (1 - e^{i(v_c + iw_c) \Lambda(b)} \cos(kb(v_s + iw_s) \Lambda(b))) b \, db$$

$$g(\theta) = ik \int_0^{\infty} J_1(qb) e^{i(v_c + iw_c) \Lambda(b)} \sin(kb(v_s + iw_s) \Lambda(b)) b \, db .$$

$\Lambda(b)$ is the eikonal phase function, defined by

$$\Lambda(b) = - \frac{1}{\hbar v} \int_{-\infty}^{\infty} \frac{\pi}{\alpha} e^{-\alpha b^2} .$$

We require here of course, that the functional form of the central spin-orbit potentials be the same, in fact they must be linear multiples of one another.

$$\frac{\partial f}{\partial \theta} = - ik \frac{\partial q}{\partial \theta} \int_0^{\infty} b J_1(qb) (1 - e^{i(v_c + iw_c) \Lambda(b)} \cos(kb(v_s + iw_s) \Lambda(b))) b \, db$$

$$\frac{\partial}{\partial v_c} \left(\frac{\partial f}{\partial \theta} \right) = -2ik^2 \int_0^{\infty} \frac{\partial(\sin \theta/2)}{\partial \theta} b^2 J_1(qb) (-i \Lambda(b) e^{i(v_c + iw_c) \Lambda(b)} \cos(kb(v_s + iw_s) \Lambda(b))) b \, db$$

$$= -k^2 \cos \theta/2 \int_0^{\infty} J_1(qb) \Lambda(b) e^{i(v_c + iw_c) \Lambda(b)} \cos(kb(v_s + iw_s) \Lambda(b)) b^2 \, db$$

$$= -i \frac{\partial}{\partial w_c} \left(\frac{\partial f}{\partial \theta} \right) .$$

Similarly

$$\frac{\partial g}{\partial v_s} = ik^2 \int_0^{\infty} J_1(qb) \Lambda(b) e^{i(v_c + iw_c) \Lambda(b)} \cos(kb(v_s + iw_s) \Lambda(b)) b^2 \, db$$

$$= -i \frac{\partial g}{\partial w_s} .$$

Therefore

$$\frac{\partial^2 f}{\partial v_c \partial \theta} = -i \frac{\partial^2 f}{\partial w_c \partial \theta} = i \cos \theta/2 \frac{\partial g(\theta)}{\partial v_s} = \cos \theta/2 \frac{\partial g(\theta)}{\partial w_s} .$$

Note that if one has used the definition of the $g(\theta)$ with the $\cos \theta/2$ factor, these formulae would take a more natural, simpler form

$$\frac{\partial^2 f(\theta)}{\partial v_c \partial \theta} = -i \frac{\partial^2 f}{\partial w_c \partial \theta} = i \frac{\partial g(\theta)}{\partial v_s} = \frac{\partial g(\theta)}{\partial w_s} .$$

This is yet another argument (albeit weak) for the presence of the $\cos \theta/2$ factor.

These relations were tested numerically and found to hold. This is comforting, but shows only that $g(\theta)$ is being calculated correctly within an additive function of all the variables except v_s and w_s !

B30181